博士論文

Study on the utilization of bio-crystals for bio-sensing

生体計測のための生物由来結晶利用法の研究

Dilipkumar Mootha Archana

広島大学大学院先端物質科学研究科

2021 年 3 月

目 次

1. 主論文

Study on the utilization of bio-crystals for bio-sensing

（生体計測のための生物由来結晶利用法の研究）

Dilipkumar Mootha Archana

2. 公表論文

(1) Quenching of light flickering in synthetic guanine crystals in aqueous solutions under strong static magnetic fields

Mootha A, Takanezawa Y, Iwasaka M.

AIP Advances 8(5),1-6(2018).

(2) Guanine Vesicle Hybrid Particles for Bio-Reflector-Based Bio-Imaging

Mootha A, Suzuki K, Asada H, Iwasaka M.

IEEE Transactions on Magnetics 99,1-4 (2018).

(3) Refinement of synthetic guanine crystals for fast diamagnetic rotation

Mootha A, Suzuki K, Kimura T, Kurahashi M, Muneyama E, Iwasaka M, Asada H.

AIP Advances 9, 1-4(2019).

主　論　文

(Main Thesis)

Table of Contents

1. Introduction

1.1 Background and Research Objective

Medical research is one of the most rapidly evolving technology and highly demanding areas of expertise. The need for novel, reliable, and rapid diagnostic techniques have been on the rise from the day diagnostic technology was applied in clinical practice. Diagnostic techniques can be either invasive, i.e., a biopsy, or, non-invasive, i.e., radiograph or taking a saliva sample. The importance of collection of bodily fluids as a sample is due to the presence of functional and biological markers which guide the clinician to arrive at a suitable diagnosis and track the patient's prognosis. Innovation in diagnostic technology has a huge influence upon a myriad of aspects in medicine and dentistry. A biosensor is an analytical tool which aids instant diagnostic results with a usually high sensitivity [1]. Among other tools, a photon is an excellent mode of diagnosis employed in photonic biosensing. Several optical based technologies using fluorescence were introduced for early detection of dental caries, assessment of surface deposits such as plaque and calculus and its bacterial biofilm on tooth surfaces[2], [3].

To understand the dynamics and operation of naturally occurring optical systems, naturally occurring optical crystal present on skin of aquatic creatures has been extensively investigated by several researchers. Guanine is an anhydrous crystal with unique optical anisotropic properties that has long been utilized by the cosmetic industry as esthetic enhancing agents. It is present on skin of many aquatic creatures and demonstrates diamagnetic properties under weak and strong magnetic fields [4] – [9]. Additional to natural photonic crystals, past literature proves that other biological molecules also demonstrated diamagnetism

[10] – [18]. However, the effect of magnetic exposure on synthesized guanine particles is still unclear. Our goal was to utilize the previously established theory of diamagnetic susceptibility of biogenic guanine crystals for analyzing the potential role of guanine for applicability in biological research and possible clinical works in the future. Additionally, our aim was to clarify the magnetic anisotropy of synthesized guanine particles due to diamagnetic orientation under exposure of 0.3~ 0.5 T using a permanent Neodymium magnet. The magnetic orientation of commercially available synthesized guanine particles was assessed in this study.

Biological molecules have been reported to display structural colors by light interference phenomena [19] , [20]. In the case of photonic crystals, the crystals occur in cells or sacs called chromatophores, and form multilayered stacks which is responsible for the strong light interference from the skin of fish [21]. To mimic this natural light-interference device, water dispersed with biogenic guanine was mixed with lipid dried films and hydrated. It was seen that some guanine crystals were trapped inside the vesicle during formation. The rotation and light reflection dynamics of the hybrid complex of guanine and lipid vesicle under Magnetic Field (MF) and external light was further assessed to understand and mimic the optical mechanism employed by chromatophores.

As guanine crystals are biogenic, its procurement from fish skin is time consuming and the amount of crystals obtained at any given time depends on the number of fishes. An effort to artificially form guanine crystal to replicate the physical and chemical properties of biogenic guanine was undertaken. Characteristics requirements of an ideal synthetic crystals are compatibility, acceptable stability

at room temperature, insoluble in water, light weight, thin, along with crystals with a definite shape and reflective property will assist to closely resemble naturally occurring biogenic crystals. Here, we demonstrate a protocol for developing synthetic guanine crystals by solubilizing guanine particles.

Biogenic guanine is routinely incorporated in beautifying products for their light weight, biological source, and luminous effect. Here, a novel hypothesis was presented to enhance the esthetic value of dental acrylic resin cements that are used as dental filling materials. Biogenic guanine was purified to remove impurities or pigments and frozen to remove any residual water. After de-freezing the guanine pellet, it was dispersed in organic solvents of dental cements to assess its solubility and dispersibility.

1.2 Chapter Summaries

Chapter 1 briefly states the research objective of this thesis study. Background information regarding the diamagnetic susceptibility of guanine, light interference and light anisotropy are discussed in *Chapter 2*. The aim of this doctoral thesis study is to analyze the possibility of utilization of guanine crystals for Bio-sensing. In this doctoral study we performed the following assessments,

i) Analysis of quenching of flickering of biologic guanine crystals under magnetic fields of 0.5T,

ii) Recrystallization of synthetic guanine particles for artificial micro-mirror fabrication for biological use,

iii) An in-vitro vesicle model for analyzing interaction of guanine molecule with organic compounds.

Chapter 3 focusses on discussing the assessment of the dynamic behavior of synthetic guanine particles under a static magnetic field (MF) at ~ 0.5T and ~5 T. Flickering light intensities of guanine particles was inhibited under MF, and further analysis revealed a change in the flickering frequency under MF of 300-500 mT (milli-tesla). Applying magnetic forces of ~500 mT caused particle vibrational entrainment at 20Hz. This quenching phenomenon of the guanine particles could serve as a micro-mirror for detection of bacteria in the surrounding aqueous medium.

To reduce procurement of biogenic Guanine Crystals (GC) from fish, we considered it to be fascinating to fabricate a GC with external properties of a specific suitable shape to be identifiable as similar to biogenic guanine, along with a magnetic

orientation and light reflective properties will be beneficial to develop a photo-optical reflective system. *Chapter 4* discusses guanine powder recrystallization by Ostwald ripening, slow recrystallization and rapid recrystallization methods. Microscopic analysis of recrystallized guanine indicated that they showed strong light reflective properties, with an average size of several tens of micrometers; and belonged to the same classification system of GC.

Skin of aquatic creatures consists of guanine crystals enclosed in transparent thin bi-layered sacs (iridosome) that allows light to enter and be freely reflected from inside, thus allowing structural light reflection from mammalian skin. We presumed that vesicles could serve as in-vitro iridosome models for our analysis. *Chapter 5* discusses interaction with guanine crystals derived from Japanese koi-fish with biological lipid molecules, primarily to understand its interaction of guanine with biological molecules. Results showed GC interacted with vesicles in an interesting manner, indicating its affinity to biological molecules. These findings prompt further research into application of GC as a potential candidate for photonic bio-imaging. Further we demonstrate the possibility of dispersing GC without clumps in organic solutions like methyl methacrylate (MMA) solution, while maintaining their reflective property.

Lastly, *Chapter 6* explains the future potentials uses of findings from these studies and scope for future development and applications.

References for Chapter 1

[1] P. Mehrotra, “Biosensors and their applications - A review”, *J Oral Biol Craniofac Res.*, vol. 2, pp. 153-159, 2016.

[2] H. Tassery , B. Levallois, E. Terrer, D. J. Manton, M. Otsuki, S. Koubi, N. Gugnani, I. Panayotov, B. Jacquot, F. Cuisinier and P. Rechmann, “Use of new minimum intervention dentistry technologies in caries management”, Aust Dent J., vol. 58, pp. 40-59, 2013.

[3] Y.K. Lee., “Fluorescence properties of human teeth and dental calculus for clinical applications”, J Biomed Opt., vol. 20, pp. 1-8, 2015.

[4] K. Takahashi, H. Yamamoto, A. Onoda, M. Doi, T. Inaba, M. Chiba, A. Kobayashi, T. Taguchi, T. Okamura, and N. Ueyama, “Highly oriented aragonite nanocrystal biopolymer composites in an aragonite brick of the nacreous layer of Pinctada fucata,” Chem. Commun., no. 8, pp. 996–997, 2004.

[5] E. Nakamura, S. Yoshioka, and S. Kinoshita, “Structural color of rock dove's neck feather,” J. Phys. Soc. Jpn., vol. 77, Art. no. 124801, 2008.

[6] C. W. Mason, “Structural colors in insects. II,” J. Phys. Chem., vol. 31, pp. 321−354, 1927.

[7] H. Ghiradella, “Structure of iridescent lepidopteran scales: variations on several themes,” Ann. Entomol. Soc. Am., vol. 77, pp. 637–645, 1984.

[8] S. Yoshioka, E. Nakamura, and S. Kinoshita, “Origin of Two-Color Iridescence in Rock Dove's Feather,” J. Phys. Soc. Jpn., vol. 76, Art. no. 013801, 2007.

[9] S. Yoshioka, and S. Kinoshita, “Effect of Macroscopic Structure in Iridescent Color of the Peacock Feathers,” Forma, vol. 17, pp. 169–181, 2002. M. Fujiwara, T. Chidiwa, and Y. Tanimoto, “Magnetic Orientation under Gravity: Biphenyl and Naphthalene Crystals,” J. Phys. Chem. B, vol. 104, pp. 8075–8079, 2000.

[10] J. Torbet, “Fibrin assembly in human plasma and fibrinogen/albumin mixtures,” Biochemistry, vol. 25, pp. 5309–5314, 1986.

[11] A. Yamagishi, T. Takeuchi, T. Higashi, and M. Date, “Magnetic field effect on the polymerization of fibrin fibers,” Physica B., vol. 164, pp. 222−228, 1990.

[12] H. Yokomichi, H. Sakima, M. Ichihara, F. Sakai, K. Itoh, and N. Kishimoto, “Effects of high magnetic field on the morphology of carbon nanotubes and selective synthesis of fullerenes,” Appl. Phys. Lett., vol. 74, pp. 1827–1829, 1999.

[13] J. Torbet, J. M. Freyssinet, and G. Hudry-Clergeon, “Oriented fibrin gels formed by polymerization in strong magnetic fields,” Nature, vol. 289, pp. 91−93, 1981.

[14] N. Morii, and H. Morii, “DNA as functional material with one-dimensionally oriented molecular chains,” J. Biol. Macromol., vol. 9, pp. 3−12, 2009.

[15] M. Iwasaka, S. Ueno, and H. Tsuda, “Effects of magnetic fields on fibrinolysis,” J. Appl. Phys., vol. 75, pp. 7162–7164, 1994.

[16] T. Takeuchi, T. Mizuno, T. Higashi, A. Yamagishi, and M. Date, “High field magnetic orientation of red blood cells,” Physica B., vol. 201, pp. 601−605, 1994.

[17] J. Torbet, “Solution behavior of DNA studied with magnetically induced birefringence,” Methods Enzymol., vol. 211, pp. 518–532, 1992.

[18] K. Suzuki, T. Toyota, K. Sato, M. Iwasaka, S. Ueno, and T. Sugawara, “Characteristic curved structure derived from collagen-containing tubular giant vesicles under static magnetic field,” Chem. Phys. Lett., vol. 440, pp. 286–290, 2007.

[19] M. Iwasaka and S. Ueno: "Polarized light transmission of smooth muscle cells during magnetic field exposures" Journal of Applied Physics., vol. 93, pp. 1-7,
2003.

[20] A. L. Lior, B. Pokroy, B. L. Sivan, L. Leiserowitz, S. Weiner and L. Addadi, “Biogenic Guanine Crystals from the Skin of Fish May Be Designed to Enhance Light Reflectance,” Cryst. Growth Des., vol. 8, pp. 507-511, 2009.

[21] E. Kreit, L. M. Mäthger, R. T. Hanlon, P. B. Dennis, R. R. Naik, E. Forsythe, and J. Heikenfeld, “Biological versus electronic adaptive coloration: how can one inform the other?”, J R Soc Interface., vol. 19, pp. 1-13, 2013.

2. General Background

2.1 Guanine

2.1.1 Introduction to Guanine

Frequently observable colorful surface of the skin of aquatic creatures is mostly due to underlying reflecting particles beneath the color-forming structure [1] – [3]. Guanine is a photonic microcrystal that is found in the skin of many aquatic creatures. The word guanine was derived from the word “’guano” which means excreta of seabirds, from where it was first extracted in the form of guanine. It is the primary component of naturally occurring optical light and color controlling systems that transcends the principles seen in any other synthetically developed systems. Each guanine crystal is an elongated hexagonal plate that has a length of 20 µm, width of 5 µm and a thickness of approximately 80 nm [4]. Past evidence reports that guanine crystals are found on the surface of skin of many aquatic creatures and it is responsible for the bright luminous appearance and luster of their skin. These creatures are said to synthesize guanine crystals naturally to utilize the phenomenon of light reflection and light scatter [5] – [6].

Biogenic guanine appears in nature as two physical forms, such as block-like crystals and plate-like crystals. The block-form of guanine is said to mainly scatter most of the light and produce a white appearance [7]; whereas the plate form has a very unique property to reflect light and cause structural light interference [8] , [9] thereby acting as minute biological light manipulating micro-mirrors. Guanine crystals are stacked in a uniform multilayered fashion inside chromatophores cells on the surface of fish, which are responsible for the luminous bright colors displayed from their skin [10], [11]. These natural micro sized light controllable

systems exhibit dynamic magnetic orientation pertaining to their inherent nature of anisotropy and diamagnetism [12]. Guanine crystals rotate in a two direction plane under external magnetic field of intensity ~5T, and they were able also emit reflected light from a very narrow window at two crystal planes (i.e., (012) and (012)) [13]. Additionally, under an external magnetic field of ~5T, a cooperative light reflection phenomenon was observed when the micro-particles floating in water rotated together. This cooperative light reflection was noted when a peak in the intensity of the reflected light was noted [14]. These published findings show that guanine platelets can act as biological micro-mirrors and can be fine-tuned to control their movement and flickering using external forces like magnetic fields similar to other biological molecules [15].

References for Chapter 2.1

[1] J. Teyssier, S. V. Saenko, D. V. D. Marel, and M. C. Milinkovitch, "Photonic crystals cause active color change in chameleons," Nature Commun., vol. 6, pp. 1-7, 2015.

[2] T. M. Jordan, J. C. Partridge, N. W. Roberts, “Non-polarizing broadband multilayer reflectors in fish,” Nat. Photonics., vol. 6, pp. 759–763, 2012.

[3] P. J. Herring, “Reflective systems in aquatic animals,” Comp. Biochem. Physiol., vol. 109, pp. 513–546, 1994.

[4] Y. Mizukawa, and M. Iwasaka, “Magnetic control of the inclination of biogenic guanine crystals fixed on a substrate,” Journal of Applied Physics., vol. 117, pp. 1-4, 2015.

[5] B. A. Palmer, D. Gur, S. Weiner, L. Addadi, and D. Oron, “The Organic Crystalline Materials of Vision: Structure–Function Considerations from the Nanometer to the Millimeter Scale,” Adv. Mater., vol. 30, pp. 1-6, 2018.

[6] D. Gur, B. A. Palmer, S. Weiner, and L. Addadi, “Light Manipulation by Guanine Crystals in Organisms: Biogenic Scatterers, Mirrors, Multilayer Reflectors and Photonic Crystals,” Adv. Funct. Mater., vol. 27, pp. 1-14, 2017.

[7] A. L. Lior, E. Shimoni, O. Schwartz, E. G. Regev, D. Oron, G. Oxford, S. Weiner, and L. Addadi, “Guanine-Based Biogenic Photonic-Crystal Arrays in Fish and Spiders,” Adv. Funct. Mater., vol. 20, pp. 320-329 , 2010.

[8] T. M. Jordan, J. C. Partridge, and M. W. Roberts, “Non-polarizing broadband multilayer reflectors in fish,” Nat. Photonics., vol. 6, pp. 1-12, 2012.

[9] D. Gur, B. Leshem, D. Oron, S. Weiner, and L. Addadi, “The Structural Basis for Enhanced Silver Reflectance in Koi Fish Scale and Skin,” J. Am. Chem. Soc., vol. 136, pp. 1-7, 2014.

[10] E. J. Denton, and M. F. Land, “Mechanism of Reflexion in Silvery Layers of Fish and Cephalopods,” Proc. Roy. Soc. London. A., vol. 178, pp. 43–61, 1971.

[11] R. T. Hanlon, “The functional organization of chromatophores and iridescent cells in the body patterning of Loligo plei (Cephalopoda: Myopsida),” Malacologia., vol. 23, pp. 89–119, 1982.

[12] T. Higashi, A. Yamagishi, T. Takeuchi, N. Kawaguchi, S. Sagawa, S. Onishi, and m. Date, “Orientation of erythrocytes in a strong static magnetic field,” Blood., vol. 82, pp. 1328–1334, 1993.

[13] T. Chikashige, and M. Iwasaka, “Magnetically-assembled micro/mesopixels exhibiting light intensity enhancement in the (012) planes of fish guanine crystals,” AIP Advances., vol. 8, pp. 1-5, 2018.

[14] K. Baba and M. Iwasaka, “Intense light scattering by cooperative relaxation of magnetically-aligned organic crystal particles,” AIP Advances., vol. 9, pp. 1-5, 2019.

[15] J. Torbet and M. C. Ronziere: “Magnetic alignment of collagen during self-assembly,” Biochem. J., vol. 219, pp. 1057–1059, 1984.

2.2 Diamagnetic Susceptibility, Light Interference and Light anisotropy

2.2.1 Diamagnetism

Diamagnetism was initially discovered and named by Michael Faraday in September 1845. It basically means that an object moves away from the magnetic field as they are magnetized in the opposite direction [1] , [2]. It is the weakest form of magnetism that occurs in the presence of an external magnetic field. Water droplets and lipid molecules also depict diamagnetic anisotropy, as they move towards a direction where the magnetic force is the weakest. Diamagnetism is found in all materials; however, since it is a very weak force, its presence can be identified only in the absence of other magnetic forces or magnetism such as para-magnetism or ferro-magnetism.

- *Origin of Diamagnetism*

Whenever two electrons are paired together in an orbit, or their total spin is 0, they are called as diamagnetic electrons. Atoms with these kinds of electrons are called as diamagnetic atoms. When these atoms are placed under an external magnetic field, there is a change in orbital motion of electrons of an atom. This induced magnetic moment is extremely small, and interestingly, it occurs in a direction opposite to the applied magnetic field. A diamagnetic object consists of atoms that have no unpaired electrons, i.e., there are completely balanced [3].

- *Movement of diamagnetic object under magnetic field*

When a diamagnetic object is placed in an external magnetic field, the object tends to move and align itself in a direction where the magnetic force has the weakest influence on the object [4]. The effect of diamagnetism is removed as soon as the

magnetic field is removed and is not permanent. A basic comparison between diamagnetism, para-magnetism and ferro-magnetism has been explained in Table 2.2.1.

Past studies on magnetic orientations of biological macromolecules made up of amino acids, nucleic acids, and lipids oriented perpendicular versus applied external magnetic fields of several tesla (T). In this work, the effect of magnetic field on synthesized guanine particles was analyzed, to understand the flickering dynamics of guanine from non-biological source.

Table 2.2.1 Table shows basic differences between Diamagnetism, Para magnetism and Ferromagnetism.

Characteristics	Diamagnetism	Para magnetism	Ferromagnetism
Magnetic attraction	Slightly repelled	Slightly attracted	Strongly attracted
Electrons	Paired	Unpaired	Unpaired
Magnetic susceptibility	Close to 0	~10^{-5} to 10^{-1}	++
Direction of induced MF	Against applied MF	Weakly towards MF	Strongly towards MF
Magnetism	No	Non retainable	Retained for a time
Affected by temperature	No	Decreases with temperature fall	Decreases with temperature rise
Example	Water, Bismuth, Zinc, Mercury, Sulphur, Iodine, Silica	Iron oxide (Fe_2O_3), and oxygen (O_2). Titanium and aluminum	iron-based magnets, rare earth magnets, cobalt, nickel

.

2.2.2. Light Interference

When there is a superimposition of two light waves, a phenomenon of light interference occurs. Interference may be constructive or destructive. Constructive light interference occurs, when the amplitude of the resultant wave is greater than the individual waves of light, whereas destructive light interference occurs when the final amplitude of the final wave is smaller than the combined initial waves. (Figure 2.3.1) This interference occurs when the electric field and MF of individual light waves are combined. The ability to manipulate light for tunable photonic devices has a high scope of application in optical devices using polymers, etc. [5]. Light interference occurs commonly among living creatures. The optical principles occurring in biological systems holds huge potential for replicating synthetical optical systems. It occurs due to the periodic arrangement of photonic crystals present near the skin. Animals are able to dynamically change the color of their skin by rearranging this structural arrangement, thus modulating the band gap or movement of crystals [6], [7].

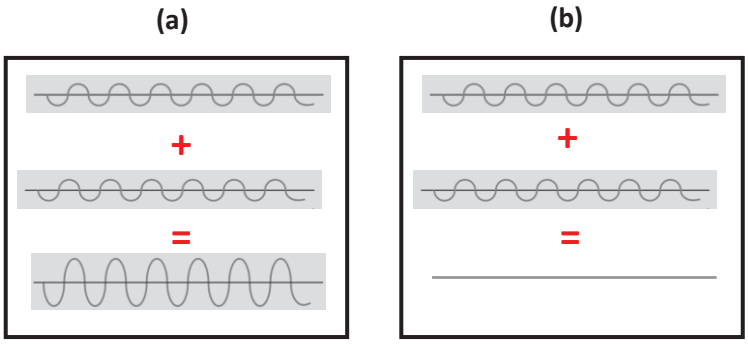

Figure 2.3.1 Figures representing the phenomenon of (a) constructive light interference and (b) destructive light interference.

- For light interference to occur:

a) The interfering object should occur consecutively at definite periodic intervals

   at a constant phase with respect to each object

b) The incoming light source should be monochromatic.

A recent study demonstrated experimentally that guanine crystal platelets of fishes' aid in efficiently controlling the enhancement of light intensity based on light interference between platelets floating in a micro-space inside an iridophore. Precisely, the structural color light interference occurs due to modifications in the geometry of the multilayered/ stacked guanine crystals in iridophore cells in fishes [8] - [11].

Similar to the mechanisms occurring in nature, light interference can be demonstrated by employing diamagnetic torque forces on guanine crystals in aqueous environment. Experimentally, when biogenic guanine crystals were aligned in definite patterns, it was possible to magnetically control aligned guanine crystals platelet (like a micro- mirror), and to increase the intensity of light by two-fold as shown in Figure 2.2.2 [12].

Cytoplasm
between crystals

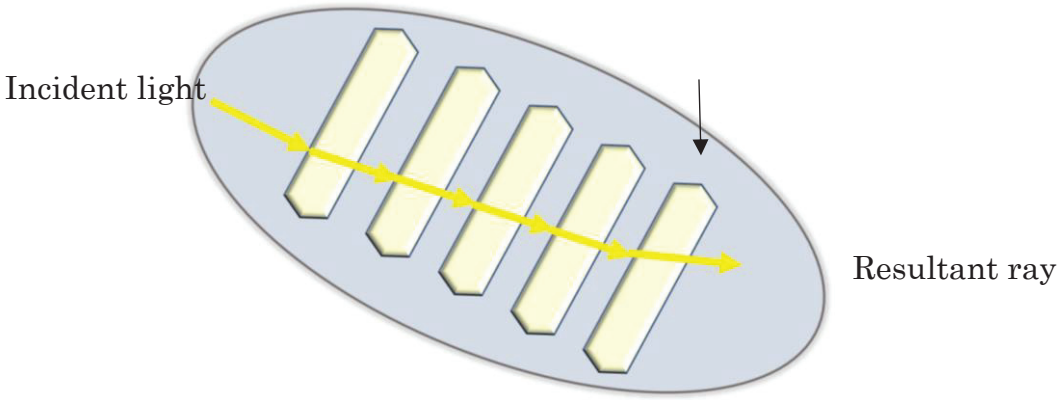

Figure 2.3.2 Diagrammatic representation of arranged of guanine crystals in a stacked fashion inside the iridophore. This facilitates light interference and structural color generation from the iridophore.

2.2.3 Light anisotropy:

When light is reflected on guanine crystals with variable incident angles, the guanine platelet may be visible as a dark or a bright platelet. This could be attributed to the anisotropy of refractive index of guanine crystals, i.e., the crystals exhibit a structural dependence on direction and the polarization state of the incident light. Guanine crystal platelets respond rapidly to a magnetic field due to their inherent diamagnetic property [13].

The reason for their strong diamagnetic anisotropy is due to the π electrons (pi - electrons) in the six-membered rings of the crystals. For this reason, the magnetic field amplitude essential for magnetic orientation of guanine platelets is quite small when compared to magnetic fields required for larger biological molecules such as fibrin and collagen [14] – [16].

Possible explanations of optical anisotropy could be a) Intrinsic anisotropy, which is due to atomic structure, (intrinsic birefringence is the difference between two

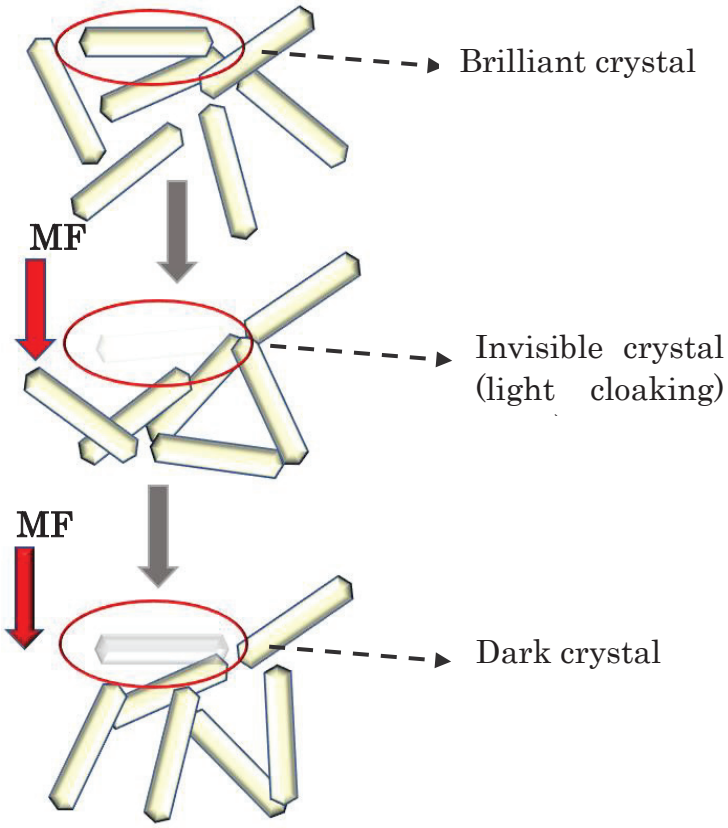

Figure 2.3.3 Schematic representation light reflection, cloaking of crystal and dark appearance of crystal under the influence of an external magnetic field.

refractive indices of a material); b) Form birefringence, which is an induced difference in the effective refractive indices of a material due to sub-wavelength periodic structure in that material [17] – [19], or c) Structural anisotropy, which can occur from anisotropic arrangements of scattering crystals and results in different optical responses due to different periodicities in different directions [20].

References for Chapter 2.2

[1] A. Sakaguchi, A. Hamasaki, and S. Ozeki, “Colloid and Interface Chemistry under Magnetic Fields,” Chem. Lett., vol. 41, pp. 342-348 , 2012.

[2] R. S. M. Rikken, R. J. M. Nolte, C. J. Maan, J. C. M. V. Hest, D. A. Wilson and P. C. M. Christianen, “Manipulation of micro- and nanostructure motion with magnetic fields,” Soft Matter., vol. 10, pp. 1295–1308, 2014.

[3] H. Sondheimer, and A. H. Wilson, “The Diamagnetism of Free Electrons,” Proc. Roy. Soc. London. A., vol. 210, pp. 173–190, 1951.

[4] R. S. M. Rikken, R. J. M. Nolte, J. C. Maan, J. C. M. Hest, D. A. Wilson, and P. C. M. Christianen, “Manipulation of micro- and nanostructure motion with magnetic fields,” Soft Matter., vol. 10, pp. 1295–1308, 2014.

[5] Y. Fang, Y. Ni, S. Y. Leo, C. Taylor, V. Basile, and P. Jiang, “Reconfigurable photonic crystals enabled by pressure-responsive shape-memory polymers,” Nat Commun., vol. 6, pp. 1-8, 2015.

[6] T. Jordan, J. Partridge, and N. Roberts, “Non-polarizing broadband multilayer reflectors in fish,” Nature Photon., vol. 6, pp. 759–763, 2012.

[7] E. J. Denton, “Review Lecture: On the organization of reflecting surfaces in some marine animals,” Philos. Trans. R. Soc. London Ser. B., vol. 258, pp. 285–313, 1970.

[8] S. Yoshioka, B. Matsuhana, S. Tanaka, Y. Inouye, N. Oshima and S. Kinoshita, “Mechanism of variable structural color in the neon tetra: quantitative evaluation of the Venetian blind model,” J. R. Soc. Interface., vol. 8, pp. 56–66, 2011.

[9] R. T. Hanlon, “The functional organization of chromatophores and iridescent cells in the body patterning of Loligo plei (Cephalopoda: Myopsida),” Malacologia., vol.23, pp. 89−119, 1982.

[10] J. N. Lyngsum, and J. Shand: “Changes in spectral reflexions from the iridophores of the Neon tetra,” J. Physiol., vol. 325, pp. 23−34, 1982.

[11] L. M. Mathger, M. F. Land, U. E. Siebeck, and N. J. Marshall, “Rapid color changes in multilayer reflecting stripes in the paradise whiptail, Pentapodus paradiseus,” J. Exp. Biol., vol. 206, pp. 3607–3613, 2003.

[12] M. Iwasaka, and H. Asada, “Floating photonic crystals utilizing magnetically aligned biogenic guanine platelets,” Sci Rep., vol. 8, pp. 1-11, 2018.

[13] M. Iwasaka, Y. Miyashita, Y. Mizukawa, K. Suzuki, Toyota T, and T. Sugawara, “Biaxial Alignment Control of Guanine Crystals by Diamagnetic Orientation,” Applied Appl. Phys. Express., vol. 6, pp. 1-4, 2013.

[14] J. Torbet, J. M. Freyssinet, and G. H. Clergeon, “Oriented fibrin gels formed by polymerization in strong magnetic fields,” Nature., vol. 289, pp. 91-93, 1981.

[15] J. Torbet, and M. C. Ronziere, “Magnetic alignment of collagen during self-assembly,” Biochem J., vol. 219, pp. 1057–1059, 1984.

[16] T. M. Jordan, J. C. Partridge, and N. W. Roberts, “Non-polarizing broadband multilayer reflectors in fish,” Nature Photon., vol. 260, pp. 759–763, 2012.

[17] M. Born, and E. Wolf, “Principles of optics: electromagnetic theory of propagation, interference and diffraction of light,” Cambridge University Press., vol. 77, pp. 837–840, 1999.

[18] Beche, and E. Gaviot, “Matrix formalism to enhance the concept of effective dielectric constant,” Opt. Commun., vol. 219, pp. 15–19, 2003.

[19] K. D. Feller, J. M. Thomas, D. Wilby, and N. W. Roberts, “Selection of the intrinsic polarization properties of animal optical materials creates enhanced structural reflectivity and camouflage,” Phil. Trans. R. Soc. B., vol. 372, pp. 1-9, 2017.

[20] T. M. Jordan, D. Wilby, T. H. Chiou, K. D. Feller, R. l. Caldwell, T. W. Cronin N. W. Roberts, “A shape-anisotropic reflective polarizer in a stomatopod crustacean,” Sci. Rep., vol. 6, pp. 1-8, 2016.

3. Quenching of light flickering in synthetic guanine crystals in aqueous solutions under strong static magnetic fields

3.1 Introduction

The demand for new functional biological markers for the biomedical industry has recently increased tremendously. Additionally, tools using modern technology and scientific innovations for faster and instant detection of bio-markers and bio-sensory are on huge demand. Conventional fluorescent markers, light-absorbing or light reflecting markers may be highly useful in today's medical and dental practice.

In the recent years, biomedical-technology has influenced a myriad of aspects in medicine and dentistry. Techniques like Fiber-Optic Trans illumination (FOTI), Digital Imaging Fiber-Optic Trans illumination (DIFOTI), Quantitative Light Induced Fluorescence (QLF), Fluorescence Spectroscopy, Laser Fluorescence etc. [1] – [5] were introduced for early detection of dental caries, assessment of surface deposits such as plaque and calculus and its bacterial biofilm on teeth surfaces [6] , [7]. As dental cavities and surface deposits on teeth harbor high bacterial load, diagnosing these areas with bio-sensing tools which might be missed by the human eye are indispensable. Dental caries is the scientific term used to address the condition that is caused by the harmful bacteria in the mouth that are not cleaned efficiently [8]. The resultant cavity formed on the tooth due to tooth destruction

which is caused by the bacteria is called as a “dental cavity” [9] , [10]. These techniques are highly sensitive, requiring short testing time and a small sample size. Caries and biofilms are detected by the capture of fluorescence of infrared light emitted from bacterial porphyrins and their metabolic compounds in the oral cavity. Excitation of biological molecules also releases fluorescence, which is used for diagnosis of neoplastic and non-neoplastic lesions as well [11]. Caries detection is also enhanced by QLF which detects the alteration of light scattered by molecules due to variation in mineral content of enamel. A similar principle is used by FOTI and the Digitized-FOTI for caries detection [12]. Use of such advanced technology has helped in early and minimally invasive diagnosis, clear quantification of disease with an overall decline in undetected cases. Under the wet conditions in which biological reactions take place, biogenic materials with high reflectivity offer an efficient way to enhance the signal to noise ratio for light detection in an aqueous medium.

In this work, we have examined the capabilities of applying and potential use of artificially synthesized guanine crystals for visualization or tracing of micrometer-sized spaces / particles in surrounding aqueous medium. Guanine is a kind of nucleic acid base and it is already known that the molecules form a hydrogen bonded network. An anhydrous guanine crystal has parallel stacked guanine

molecules.[13] In the previous literature, it was shown that biogenic guanine crystals showed a quick and spontaneous response to external magnetic fields where the crystal platelets oriented parallel to the magnetic field and distinctly switched the intensity of light reflection [14] – [18]. The present study focused on assessing the dynamic behavior of guanine by using synthetic guanine crystals under applied external magnetic field.

3.2 . Methodology

A digital microscope was built up with a 70mm room temperature bore superconducting magnet, and the light reflection properties of artificially synthesized guanine crystal particles were observed while varying the applied magnetic field between 0 T and 5 T as shown in Figure 3.2.1. Briefly, Synthetic guanine crystals (Wako Chemical, Tokyo, Japan) were dispersed with water to form a colloidal solution in a test tube. Then, 5µl of the solution was carried by an automated pipette and dropped over a clean cover slip under extremely sterile conditions. The colloidal solution was then pressed into a flat layer of even thickness with a second cover slip for visualizing under the microscope. Initially, the reflectivity and the flickering of the guanine crystals was checked by placing magnet in various positions corresponding to the position of the light source. Then we noticed that maximum intensity of light, and flickering of the nanoparticle was observed when the magnetic source was placed below the sample, which was directly opposite to the high speed vision camera. If a straight line was drawn connecting the camera and the magnetic source, the light source was placed at a 90° to this line.

The flickering and Brownian motion of the synthetic guanine crystals was observed with a CCD microscope and captured using a high - speed camera (IDT, Inc. U.S.A.). The flame rate of the high-speed camera was set to 100 fps to 500 fps. The video obtained from the high-speed vision camera was viewed first with the naked eye to check the overall flickering rate of guanine particles. Then, using the Area 61 Software, snapshots of the videos were extracted. Later the images series were isolated and viewed with Irfan Viewer Software, and a nanoparticle with

distinct clarity was observed and viewed in isolation. Finally, Image J Analysis Software was used to analyze the data in the images. Minimum, maximum, and mean variations in the intensity of the flickering of the nanoparticle along with delta 't' were analyzed as shown in Figure 3.2.2.

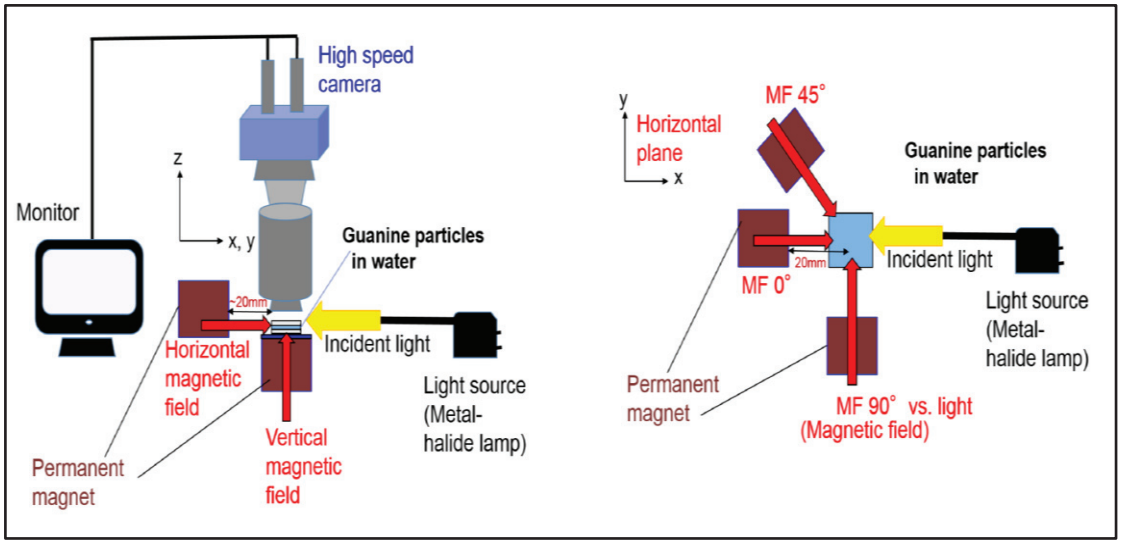

Figure 3.2.1 Configuration of high-speed camera measurements of analysis of flickering dynamics of synthesized guanine particles with magnetic fields and light source.

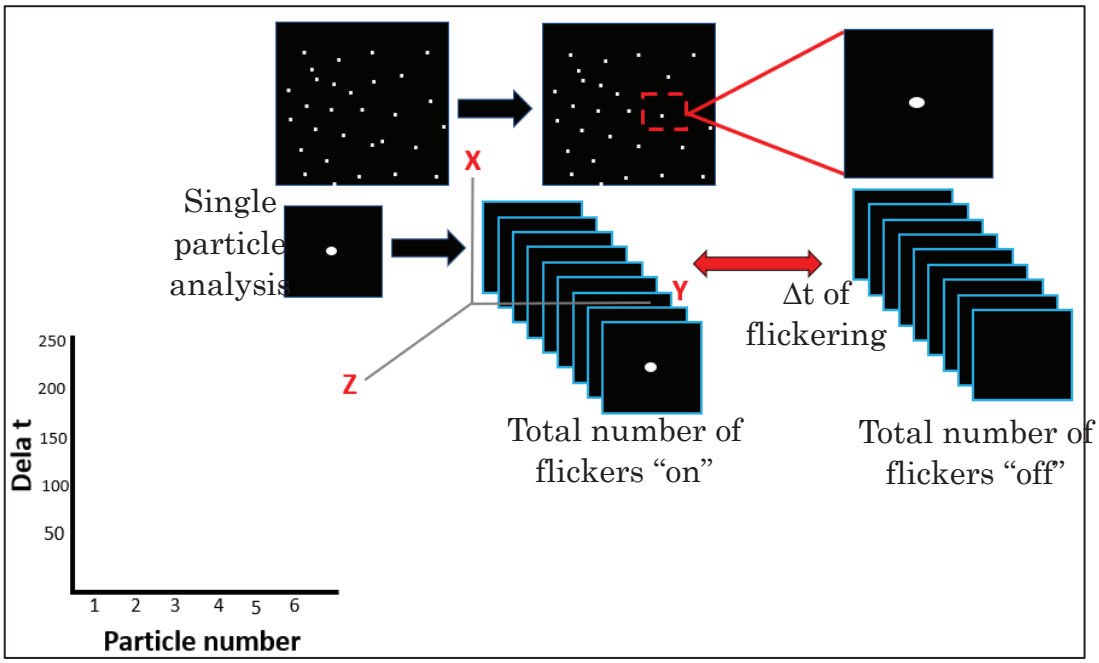

Figure 3.2.2 Data analysis of flickering of synthesized guanine particles.

3.3 Results and Discussion

The small particles under magnetic field exposure at 5 T showed slow fluctuation and darker surfaces while particles before the exposure showed active Brownian motions inducing strong flickering of light. The dynamics of the particle motion was analyzed using time-sequence of the images, as shown in Figure 3.3.2. (c) and (d).

The results show that the mean intensity of the individual synthetic guanine particles distinctly decreased at 5 T (Figure 3.3.1) , while the standard deviation of the intensity, i.e., the fluctuation in motion caused by Brownian motion, decreased but was not so distinct. Here, the observed quenching of light flickering in synthetic guanine particles might have originated due to decrease in Brownian motion, however other mechanisms, for example light cloaking effects inside guanine crystal, are required to completely explain the disturbance of light flickering (Figure 3.3.2). These phenomena occurred also in biogenic guanine crystals which were derived from fish scales.

The micro-particles of synthetic guanine are diamagnetic; however, guanine molecule has aromatic rings which can generate a large diamagnetic anisotropy under an external magnetic field. Both biogenic fish guanine crystal and the utilized synthetic guanine crystal are anhydrous crystals wherein guanine molecules are stacked in parallel. The structure provides enough diamagnetic energy for the micro-crystals under magnetic fields at 500 mT at room temperature. The experimental analysis indicated that the diamagnetic energy of guanine crystal in one micrometer scale was larger than thermal energy kT. An experiment using fiber optic measurements showed that the intensity of the light

reflected in the direction perpendicular to the magnetic field increased, while the intensity in the direction parallel to the field decreased. This behavior can be explained based on the diamagnetic orientations of the sub-micron scale crystals [5] – [7].

In addition, we carried out an observation of the nano/micro particle motion under magnetic field at 500 mT by utilizing a high-speed camera. Figure 3.3.3 and 3.3.4 shows flickering light intensity and time span (Δt) between maximum/minimum intensities, with and without a magnetic field at 500 mT which was generated by a permanent magnet. Under magnetic fields of 500 mT, the time spans of flickering ((Δt) in synthetic particles were shortened. It was conjectured that the motion of the synthetic guanine particles became faster, so the time duration providing the reflected light to vision became smaller. As a result, the vibration frequency of the particles caused an entrainment around 20 Hz.

The synthetic guanine particles maintain a rather constant delta T compared to without MF. Perhaps, a reasonable explanation is that it has a narrow span of Brownian motion leading to a short delta T compared to a haphazard flicker without magnetic exposure.

Figure 3.3.5 shows a flickering frequency analysis by utilizing the fiber optic light intensity measurement. The measurement was carried out by recording the dynamics of intensity fluctuation of refracted light in a time series. The guanine particles floating in water in a thin chamber (25 μl volume, 300 μm in thickness) exhibited an oscillation of refracted light intensity.

After recording the light intensity at 600nm of every 20 ms by a spectrophotometer

(Ocean Photonics HR2000+, U.S.A.), we analyzed the autocorrelation

$$G(\tau) = \sum I(t) \times I(t + \tau) \quad \ldots\ldots\ldots\ldots\ldots\ldots (1)$$

where I is the light intensity,

t is time, and

τ is the correlating time span.

By changing the time span (τ) at every 100 ms varying from 100 ms to 1000 ms, G(τ) for τ = 0.1 s to 1 s were obtained. Figure 3.3.5 (a) and (b) are examples of with and without magnetic fields of 500 mT, respectively. Figure 3.3.5 (c) is the averaged pattern of the (G (t)= 0.1 s ~1 s)). It is clearly shown that the maximum peaks without MF exposure appeared at 't' = 0.3 s and also at 0.8 s (Figure 3.3.5 (a)) and overall in this case, peaks appeared to be more scattered, whereas the maximum peaks at 500 mT appeared at 't' = 0.5 s (Figure 3.3.5 (b)), and the signs of G (t) with and without MF at t =1 s became opposite to each other. The measured intensities of the auto-correlation of water were only distinctly smaller than those with micro-particles. So, we considered that background fluctuations in the light source was negligible.

The observation of synthetic guanine crystals at 5 T provided an inhibition of light flickering by micro/nanoparticles and showed a slight decrease in Brownian motion (Figure 3.3.6, Table 3.3.1). On the contrary, the observation by high speed camera showed an enhanced behavior of vibrational speed of synthetic guanine particles in a particular fashion (Figure 3.3.7). The results of the flickering frequency analysis shown in Figure 3.3.5 (a) and (b) supports the explanation that there is an occurrence of shift in resonance frequencies of the vibration of the central axis of individual particles. During the vibration, the maximum tilting

angle of a particle may be affected by the thermal energy supplied to the particle. The possible competing of the provided diamagnetic anisotropic energy of guanine crystal with the thermal energy should modulate the resonance frequencies of the vibration. In this mechanism, the shift of resonance may result in an observable increase in vibration speed. A reasonable explanation to this could be that the span of vibration became narrower, resulting in a higher vibrational frequency.

We can infer that it is thus possible to use synthetic guanine crystals in the same manner as biogenic crystals to act as efficient fluidic tracers by obtaining their flickering/quenching signals with and without magnetic field exposure. In addition, we think that guanine crystal platelet is a promising material for a new tracer for dynamics of any objects in aqueous solution. The technique for the tracing is not established at this point. For the first approach to the biological tracing (imaging), we are expecting that dental cavities can be the first model where guanine crystal platelets can be proved as “biological tracers” for bacterial viability.

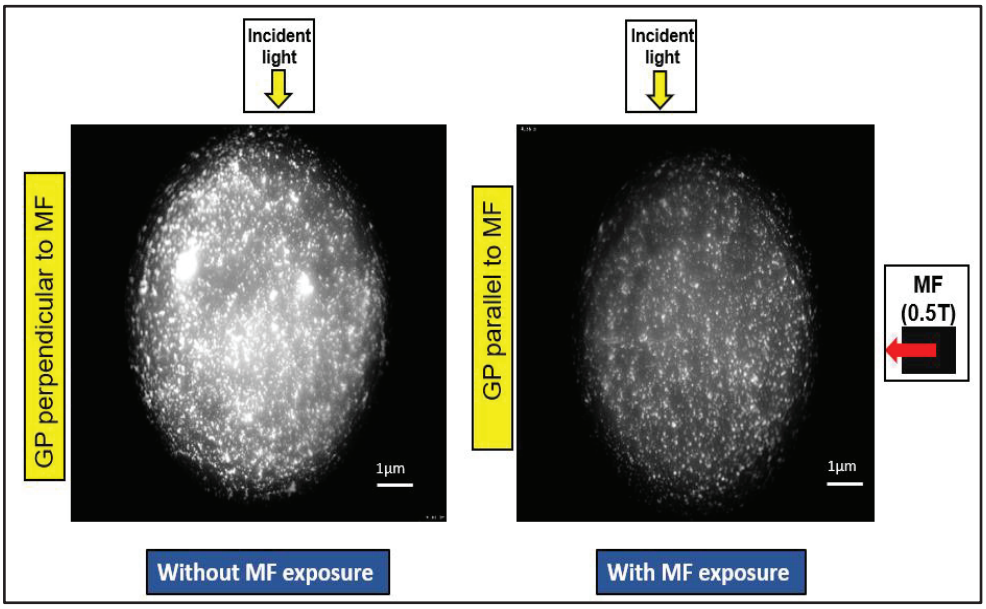

Figure 3.3.1 Left: Bright flickering of guanine particles under external light. Right: Quenching of flickering of guanine particles under external light and applied magnetic field (~ 0.5T).

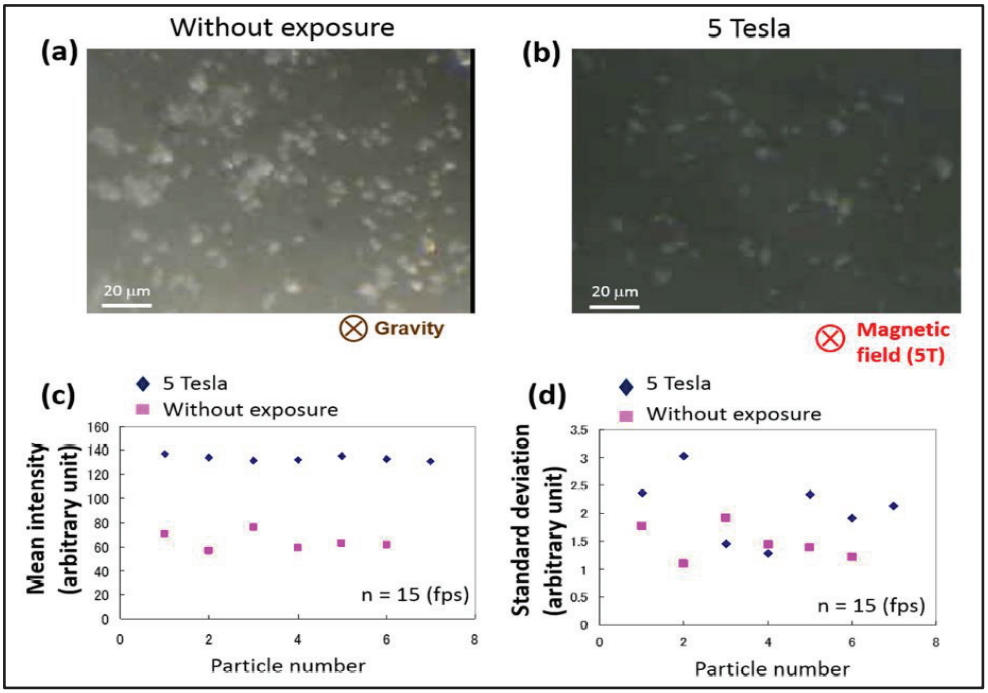

Figure 3.3.2 Quenching of light flickering in a synthetic guanine crystal particle by magnetic field exposure at 5 T. (a) Synthetic guanine crystal particle without magnetic field exposures, (b) Particles under 5 T, (c) Mean intensity of flickering light. (d) Standard deviation of the flickering light intensity per one second (15 frames).

(a)

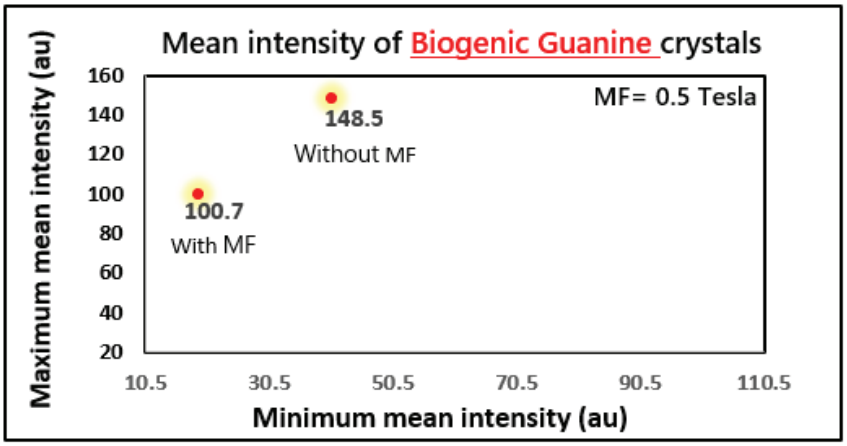

(b)

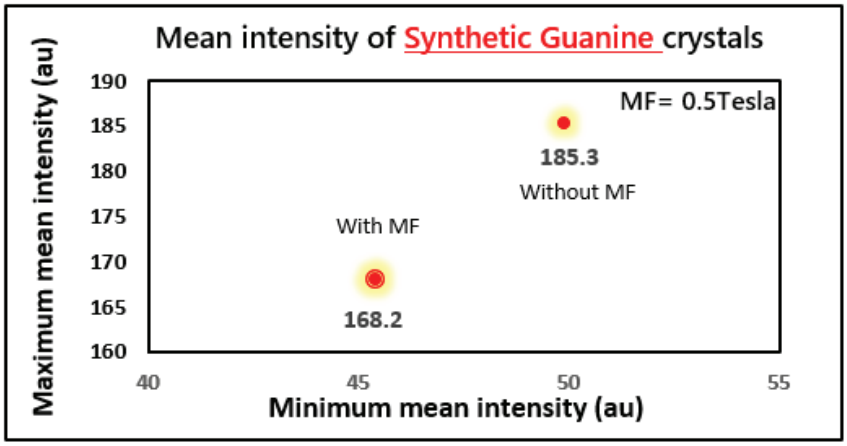

Figure 3.3.3 Plot of maximum and minimum intensity of (a) biogenic guanine crystals and (b) synthetic guanine particle under magnetic field.

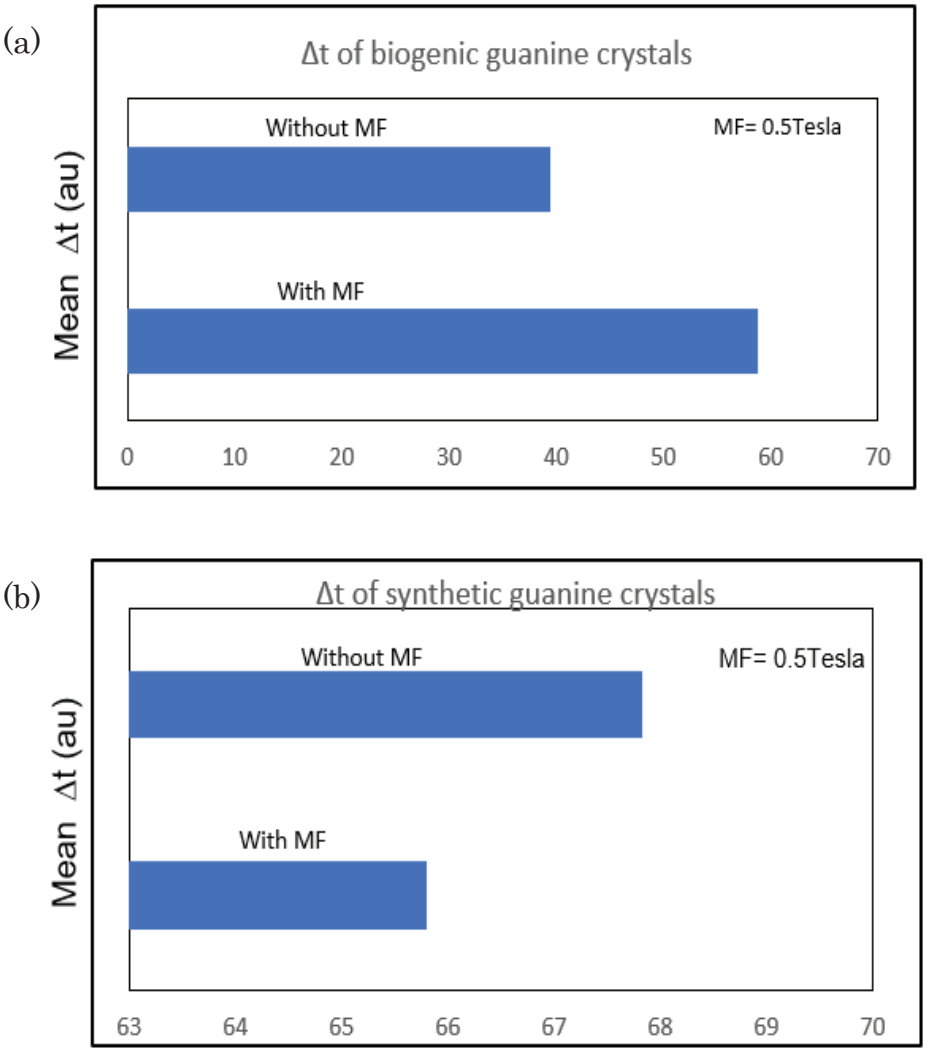

Figure 3.3.4 Mean Δt of (a) biogenic guanine crystals and (b) synthesized guanine particles with and without magnetic fields at 500 mT, which is perpendicular to the incident light and parallel to the vision. Graphs show the value in the x-axis when the flickering was first noticed ('n' th second).

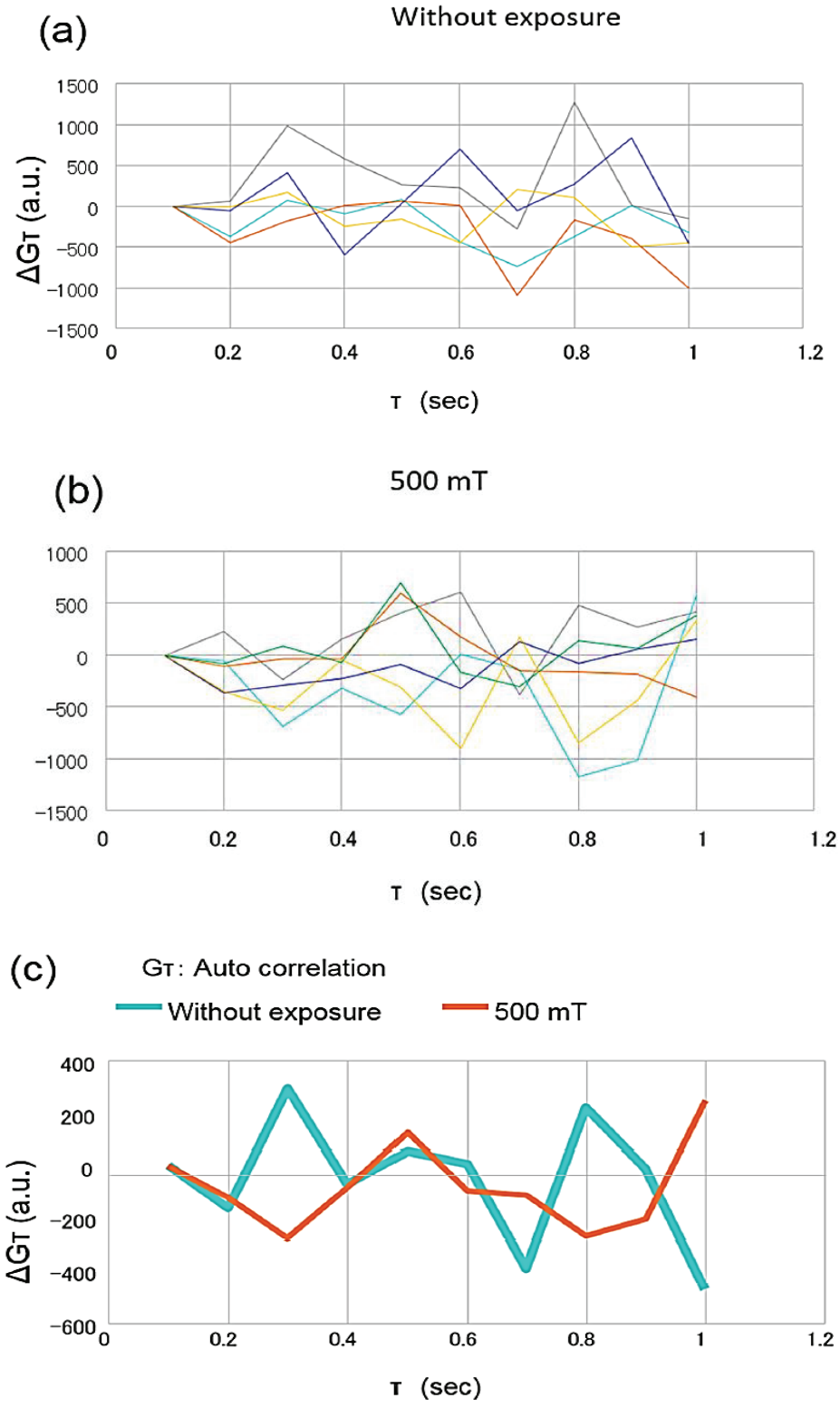

Figure 3.3.5 Effects of 500 mT magnetic fields on the flickering frequencies of synthetic guanine crystal particles. (a) Autocorrelation without magnetic field exposures. (b) Auto-correlation with 500 mT (c) Average of spectra.

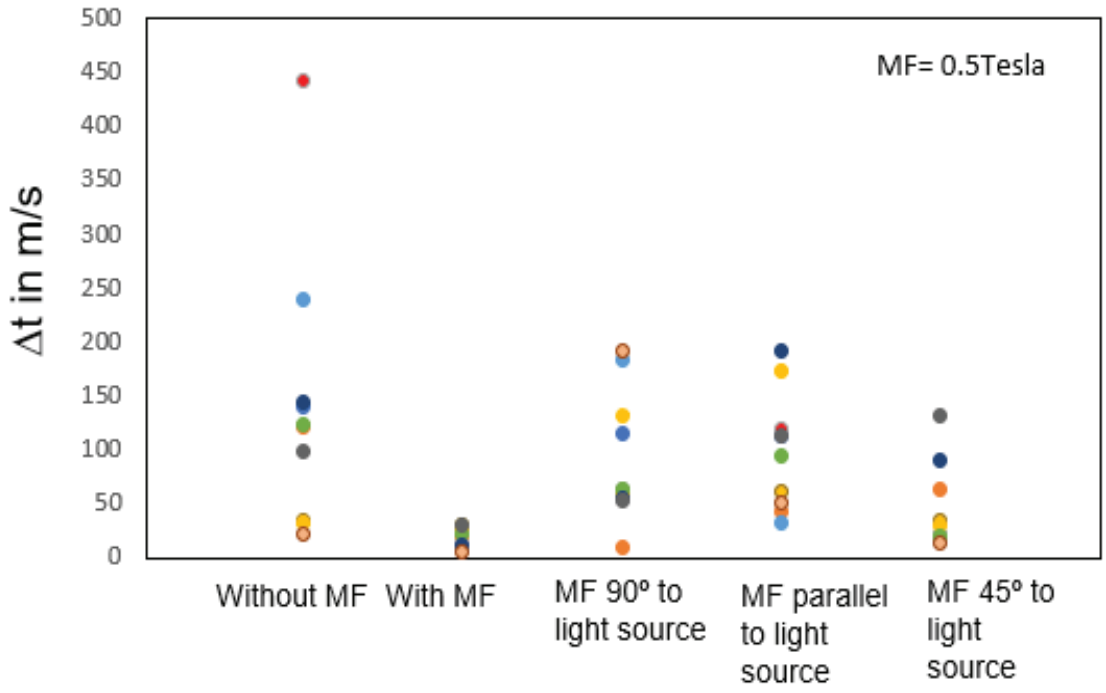

Figure 3.3.6 Scatter plot of Δt with various methods of light illumination angle versus magnetic field.

Without MF	With MF	MF 90° To Light Source	MF Parallel To Light Source	MF At 45° To Light Source
138	21	113	111	17
120	18	8	40	62
440	10	61	117	20
31	23	58	170	28
238	6	181	30	13
122	20	61	93	17
142	10	52	189	89
19	4	189	48	12
97	29	50	111	129
33	28	130	60	32

Table 3.3.1 Raw data of scatter plot of Δt with various methods of light illumination angle versus magnetic field.

(a)

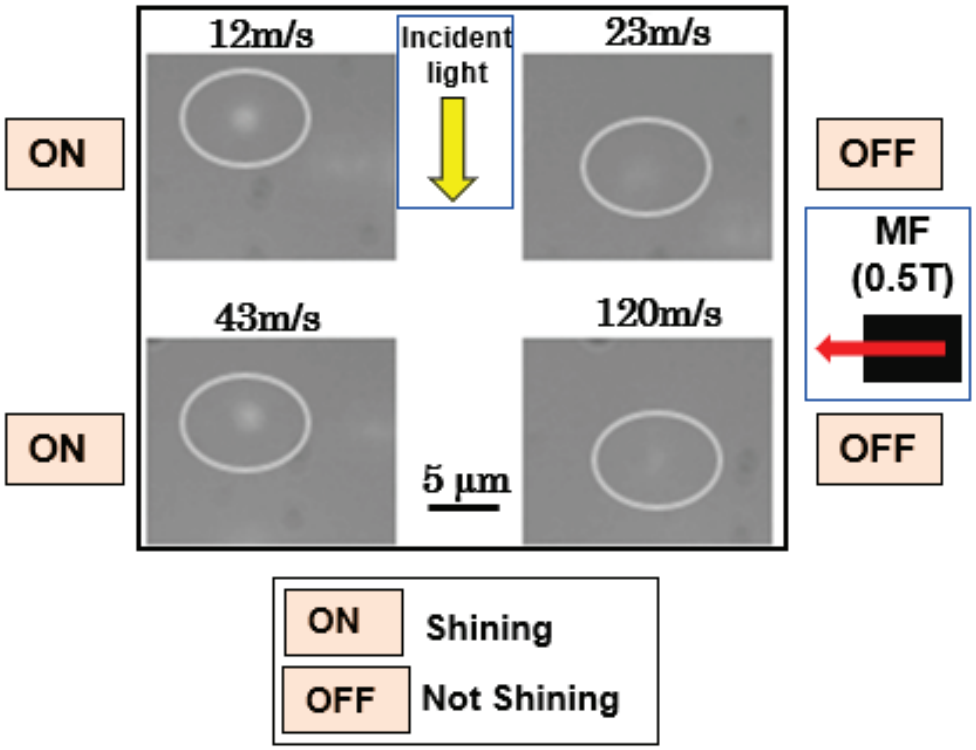

(b)

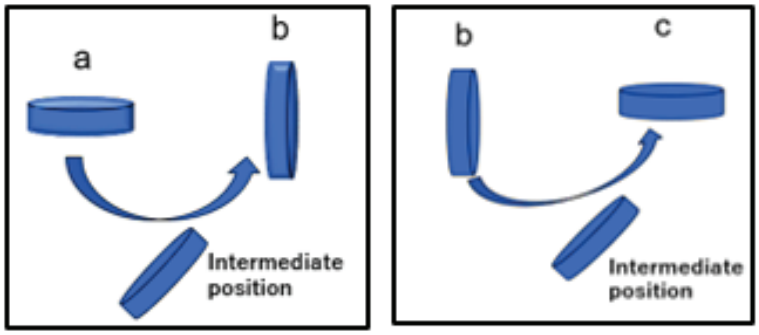

Figure 3.3.7 (a) Flickering on and off images, (b) Schematic representation of flickering pattern.

3.4 Summary

A static magnetic field at 5 T inhibited the flickering light intensities in synthetic guanine crystal particles. High speed camera analysis of the particle motion revealed a change in the flickering frequency with magnetic field exposures at 300-500 mT. The synthetic guanine particles without magnetic field exposures had a vibrational frequency of 1-10Hz. However, applying the magnetic fields at 500 mT caused an entrainment of the particle vibration at 20Hz.

References for Chapter 3

[1] H. E. Strassler, and M. L. Pitel, “Using fiber-optic transillumination as a diagnostic aid in dental practice,” Compend Contin Educ Dent., vol. 35, pp. 80-8, 2014.

[2] J. L. Yu, R. T. Tang, L. Feng, and Y. M. Dong, Digital imaging fiber optic transillumination (DIFOTI) method for determining the depth of cavity,” Beijing Da Xue Bao Yi Xue Ban., vol. 49, pp. 81-85, 2017.

[3] M. R. Alammari, P. W. Smith, J. E. de Josselin de, and S. M. Higham, “Quantitative light-induced fluorescence (QLF): a tool for early occlusal dental caries detection and supporting decision making in vivo,” J Dent., vol. 41, pp. 127-132, 2013.

[4] W. Buchalla, A. M. Lennon, and T. Attin, “Fluorescence spectroscopy of dental calculus,” J Periodontal Res., vol. 39, pp. 327-32, 2004.

[5] Z. Bahrololoomi, S. A. Musavi, and M. Kabudan, “In vitro evaluation of the efficacy of laser fluorescence (DIAGNOdent) to detect demineralization and remineralization of smooth enamel lesions,” J Conserv Dent., vol. 16, pp. 362-366, 2013.

[6] H. Tassery, B. Levallois, E. Terrer, D. J. Manton, M. Otsuki, S. Koubi, N. Gugnani, I. Panayotov, B. Jacquot, F. Cuisinier, and P. Rechmann, “Use of new minimum intervention dentistry technologies in caries management,” Aust Dent J., vol. 58, pp. 40-59, 2013.

[7] Y. k. Lee, “Translucency of human teeth and dental restorative materials and its clinical relevance,” J Biomed Opt., vol. 20, pp. 1-8, 2015.

[8] N. B. Pitts, D. T. Zero, P. D. Marsh, K. Ekstrand, J. A. Weintraub, F. R. Gomez, J Tagami, S. Twetman, G. Tsakos, and A. Ismail, “Dental caries,” Nat Rev Dis Primers., vol. 3, pp. 1-44 , 2017.

[9] C. Usha, and R. Sathyanarayanan, “Dental caries - A complete changeover (Part I),” J Conserv Dent., vol. 12, pp. 46-54, 2009.

[10] J. D. B. Featherstone, “Dental caries: a dynamic disease process,” Aus Dent J., vol. 53, pp. 286–291, 2008.

[11] W. Liu, X. H. Zhang, K. p. Liu, S. D. Zhang, and Y. X. Duan, “Laser-induced fluorescence: Progress and prospective for in vivo cancer diagnosis,” Chinese Science Bulletin., vol. 58, pp. 2003-2016, 2013.

[12] L. Karlsson, “Caries Detection Methods Based on Changes in Optical Properties between Healthy and Carious Tissue,” International Journal of Dentistry., vol. 2010, pp. 1-9, 2010.

[13] J. H. Davis, and J. R. Williamson, “Structure and dynamics of bacterial ribosome biogenesis,” Phil. Trans. R. Soc. B., vol. 372, pp. 1-9, 2017.

[14] A. L. Lior, B. Pokroy, B. L. Sivan, L. Leiserowitz, S. Weiner, and L. Addadi, “Biogenic Guanine Crystals from the Skin of Fish May Be Designed to Enhance Light Reflectance,” Cryst. Growth Des., vol. 8, pp. 507–511, 2008.

[15] M. Iwasaka, “Effects of static magnetic fields on light scattering in red chromatophore of goldfish scale,” J. Appl. Phys., vol. 107, pp. 1-3, 2010.

[16] M. Iwasaka, Y. Miyashita, M. Kudo, S. Kurita, and N. Owada, “Effect of 10-T magnetic fields on structural colors in guanine crystals of fish scales,” J Appl Phys., vol. 111, pp. 1-3, 2012.

[17] M. Iwasaka, and Y. Mizukawa, “Light Reflection Control in Biogenic Micro-Mirror by Diamagnetic Orientation,” Langmuir., vol. 29, pp. 4328–4334, 2013.

[18] M. Iwasaka, Y. Mizukawa, and Y. Miyashita, “Rapid magnetic wiper featuring biogenic guanine particles: Magnetic non-contact switching of opto-fluidic mirrors featuring biogenic guanine crystals,” Appl Phys Lett., vol. 104, pp. 1-4, 2014.

4. Guanine-vesicle hybrid particles for bio-reflector based bio-imaging

4.1 Introduction

Vesicles are spherical bi-layered sacs that enclose a fixed volume of liquid. Lipid vesicles (Liposomes) mimic natural cell membrane structures of humans and animals, as the cell membrane is abundant in lipids. Undeniably, these artificial cells serve as excellent laboratory models of biological membranes. Multiple applications including artificial cell synthesis, targeted drug delivery, study of cell biochemistry and others have already been scrutinized. It has a membrane thickness of a few nanometers in thickness of ~4nm [1] – [4] compared to its larger diameter in the case of giant vesicles and is almost impermeable to molecules [5]. Its fragile membrane makes them transparent and translucent, allowing light to enter freely. Consequently, it is logical to assume that if optical nanoparticles with a strong light reflective property is enclosed within vesicles, one can expect a strong light reflection or light scatter from the vesicle, observable under dark field microscopy. Additionally, impermeability of vesicles prevents spill-over of their contents in the extracellular space; allowing availability of endocytosed particle for a time-period that is proportional to the half-life of the vesicle.

Color changing animals have certain organic crystals in their skin serving as natural optical devices, transcending all current artificial optical systems. Guanine is one such organic crystal with the highest refractive index present in the skin of color reflecting members of the animal kingdom [6].

It lies enclosed within specialized cells resembling vesicles, called iridocytes that are responsible for their iridescent surface [7] and aligns parallel to applied

magnetic field [8]. Guanine crystal inside an iridocyte forms as “iridosome” in animals. The natural stacked arrangement of guanine crystals in iridocytes leads to a continuous internal light reflection, where the reflections from the different interfaces of stacked thin films results in a brilliant shine [9]. By this similar principle of chromatophore-based photonic ability with brilliant light reflective properties, it is possible to create artificial bio-reflectors akin to those in animals [10]. As synthetic GC behaved similar to biogenic [11], we used both biogenic and synthetic GC in this experiment. Our aim was to endocytose GC into liposomes, in order to fabricate an “artificial iridosome”; more appropriately a “hybrid-vesicle” for further application in bio-reflector based live cell imaging. An iridosome is a tissue-specific, membrane-bounded cytoplasmic organelle within which purines crystalize in reflective stacks.

4.2 Methodology

POPC (1-palmitoyl – 2 -oleoyl phosphatidylcholine) and POPG (1- palmitoyl-2-*sn*-glycero-3-phosphoglycerol sodium salt) was purchased from NOF Corporation (Japan); synthetic guanine crystals were obtained from Wako Chemicals, (Japan). All the materials were stored at -4°C and were warmed up to room temperature before use. Biogenic guanine crystals were extracted from the skin of Japanese Koi fish. Briefly, fish scales were picked from the skin of carp fish under sterile conditions. Then, each scale was disrupted to remove all GC from it. Then this extract was washed and subjected to a series of repetitive centrifugation cycles to remove maximum impurities from the sample. (Figure 4.2.1) The resultant supernatant was removed completely from the GC sediment and stored at 4°C with a disinfectant to prevent any bacterial growth for future use.

POPC and POPG were dissolved in chloroform to uniformly distribute these lipids in the solvent. For the fabrication of POPC/POPG hybrid vesicle, 1 pair of POPG stock solution was prepared, among which 1mg synthetic GC was added to one and biogenic GC was added to the other POPG stock. Vesicles with POPC (100%) and POPG/PC (1:3) concentration were prepared in aqueous solution as described below. Subsequently, dried thin film (Figure 4.2.2) containing phospholipids (mmol) was constructed on a surface of glassware by using manual rotatory evaporation method and then dried overnight *in vacuo* to remove remaining organic solvent as shown in Figure 4.2.3. [12] Resulting dried thin films of phospholipids were soaked by distilled water (1000µl) at room temperature and allowed to form vesicles on a magnetic hotplate (IKA® C-MAG HS7 Digital.) in a warm water bath with a temperature of ~22°C for ~2-3 hours. Eventually, 30µl of

dispersion of vesicles containing guanine crystals was dispensed into a chamber comprising of a frame-seal incubation chamber SLF (Bio-Rad, US) sandwiched between a pair of thin cover glasses and viewed under a phase contrast MS optical microscope. The specimens were exposed to a strong halogen light source and magnetic field from a permanent neodymium magnet with a magnetic flux density of ~0.5T. The optical microscope was connected to a high-speed vision camera (Motic Images Plus 2.3S. Japan.) for magnification and data recording.

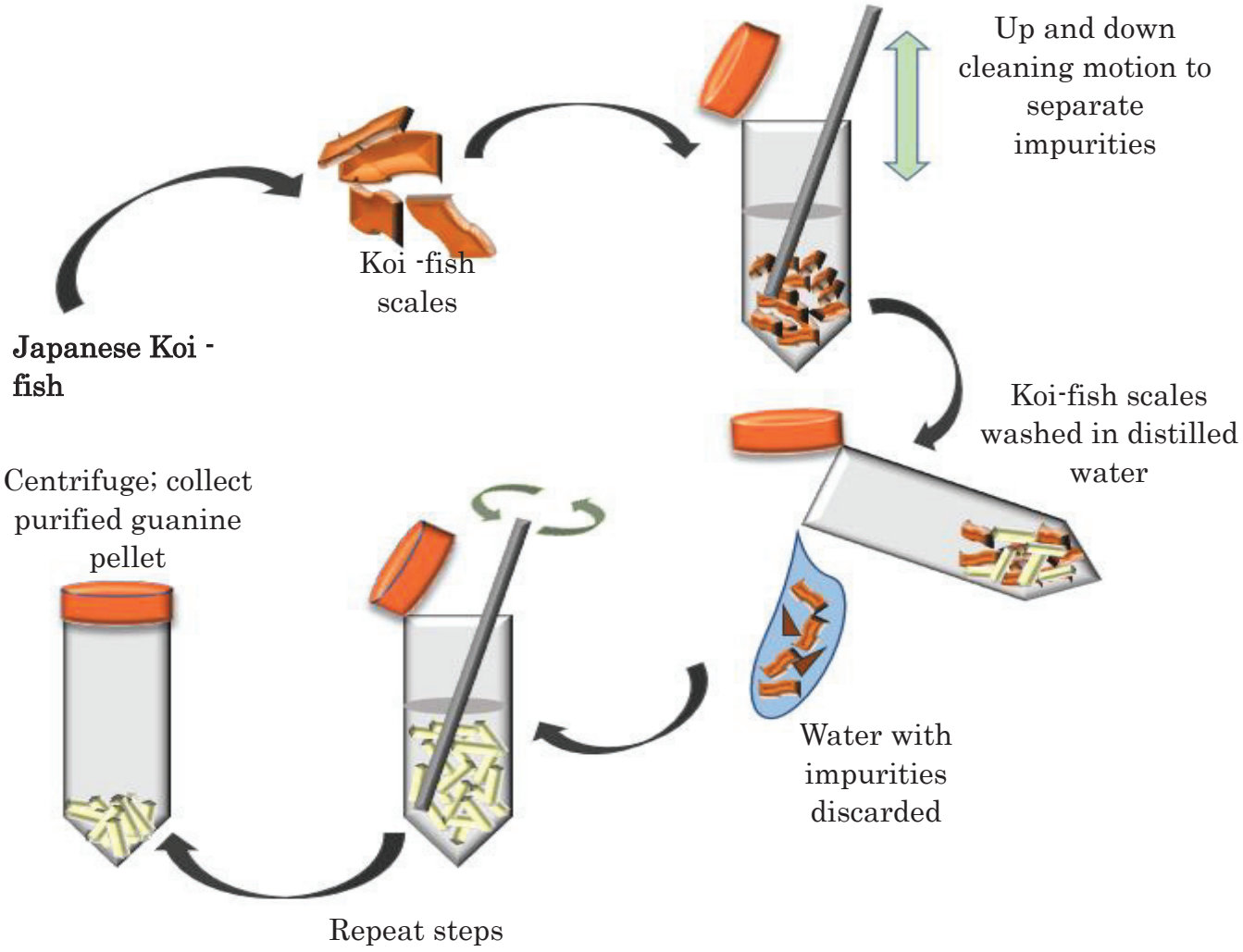

Figure 4.2.1 Steps for extraction of biogenic guanine crystals from Japanese Koi fish and its purification.

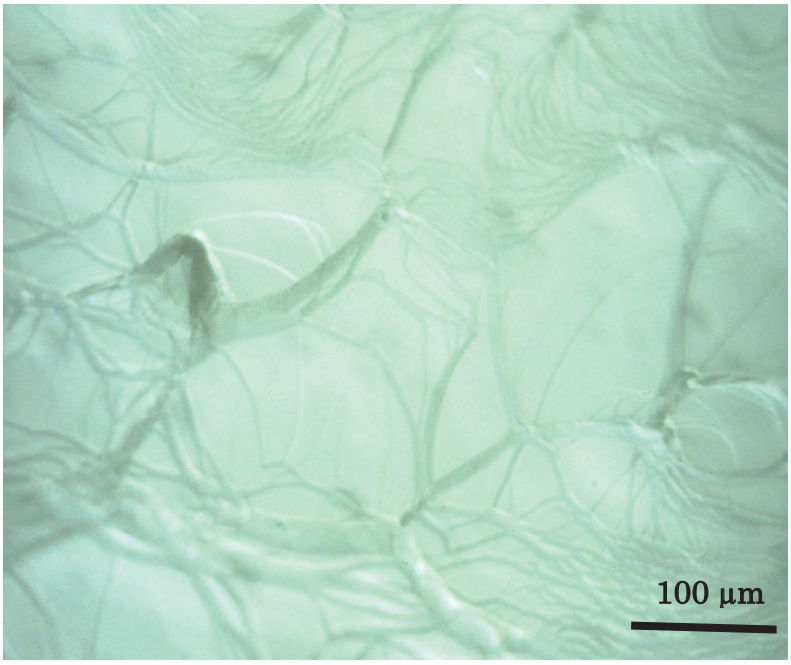

Figure 4.2.2 Dried lipid layer.

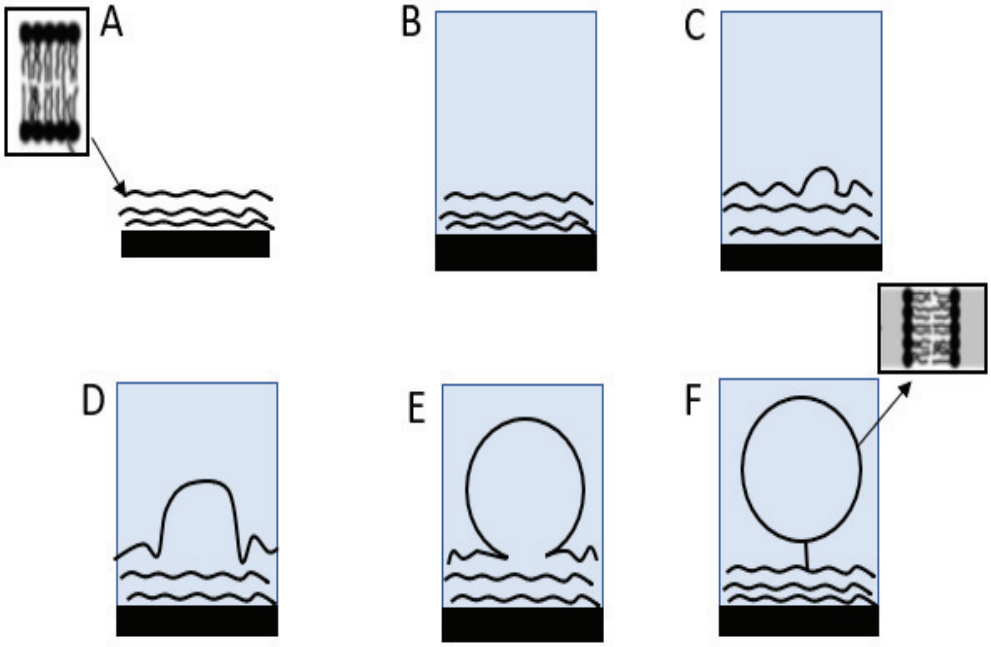

Figure 4.2.3 Formation of lipid vesicle.

4.3 Results and Discussion

4.3.1: Results

Optical light microscopic observation showed numerous floating vesicles (~10-50nm) with single/ multiple small particles present in the intravesicular space. Presence of guanine crystals inside vesicles were confirmed visually, leading to the formation of a "hybrid vesicle" complex. (Figure 4.3.1 and Figure 4.3.2) Dark field microscopy showed a luminous radiance from the intravesicular space with an observable illuminated outline of the vesicle. In addition, the trajectory of light reflected from the vesicle consistently corresponded to opposite to that of light source; and when light was exposed from different angles (Figure 4.3.3 (a)) directed towards GC with a strong light reflected from the hybrid-vesicle thus confirming the presence of intravesicular guanine crystal (Figure 4.3.3 (b)). The hybrid-vesicles suspended in a liquid with low viscosity oscillated continuously, occasionally shifted due to Brownian motion of distilled water. (Figure 4.3.4)

Further, we analyzed the response of hybrid-vesicle to magnetic field of a flux density of ~0.5T generated from a permanent Neodymium magnet. The magnetic field was exposed from a distance of about half a centimeter above the sample without disturbing it. During magnetic exposure, increased quivering of vesicle and motion was observed. (Figure 4.3.5, B) The enhanced vibration of vesicle was perhaps due to increased Brownian motion of suspension (distilled water) on exposure to magnetic field, provoking a visually distinct flickering sheen from the hybrid-vesicle. (Figure 5.3.18)

Additionally, the effulgent intravesicular guanine crystal caused illumination of hybrid-vesicle itself. (Figure 4.3.6) There were specific patterns of in-plane motion

and outward-inward motion of hybrid-vesicle under an applied MF. (Figure 4.3.7 and Figure 4.3.8)

The number of GC varied in different vesicles. When vesicles were exposed to a magnetic field and light source, they illuminated brilliantly. Some vesicles had a single GC, whereas a cluster of GCs was seen in some vesicles. The reason for this remains unknown. However, regardless of the number of intravesicular crystals present, the light trajectory was always opposite to the direction of the external applied light source. (Figure 4.3.3, B) The intensity of light reflected from the hybrid-vesicles varied at different points of time. There was increased light intensity reflected from the hybrid-vesicle for a period, followed by decrease in the same for a prolonged period of time (few seconds) before the light intensity increased in the next cycle. There was a constant minor change in intensity of light reflected as analyzed using Image J analysis software version 32.0., which was due to the vibration of the hybrid-vesicle corresponding to the Brownian motion. (Figure 4.3.6)

The time difference (Delta t) between two different intensities also varied periodically. (Figure 4.3.5, A) This again can be explained due to constant Brownian motion of water in which the hybrid-vesicles were suspended.

A diagrammatic representation of the hypothesis of the dynamics of rotation (Figure 4.3.7) mechanics of rotation of hybrid-vesicle (Figure 4.3.8) has been demonstrated. Figure 4.3.9 and Figure 4.3.10 shows a proposed model of rotation pattern and change in direction of hybrid-vesicle, with change in direction of light reflection path from the hybrid-vesicle under magnetic field when there is close interaction of vesicle and guanine as shown in Figure 4.3.11, and that the hybrid-

vesicle show a specific pattern of rotation (Figure 4.3.12). Analysis showed that grouped hybrid-vesicles always moved at the same vibration frequency and showed a same number of vibrations (Figure 4.3.13). Simulation of light reflection from “hybrid-vesicle” floating in water has been shows from Figures 4.3.14 to Figures 4.3.17, showing an arrangement suitable for light interference by guanine.

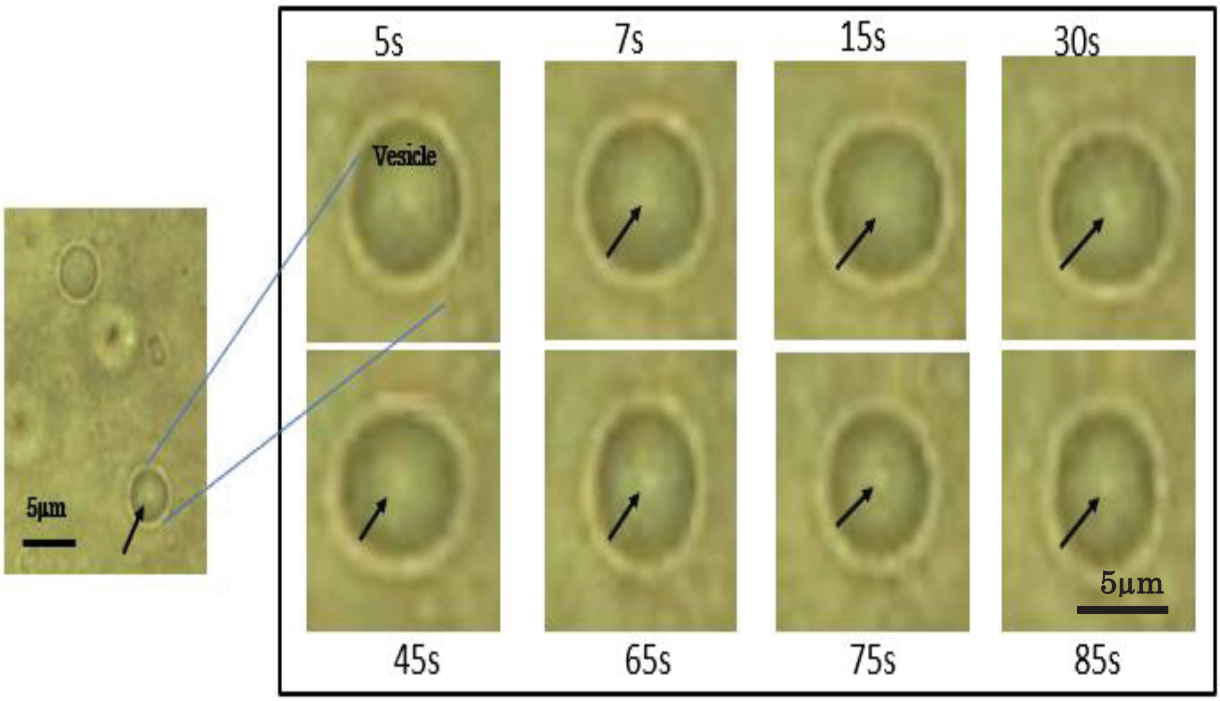

Figure 4.3.1 Vesicle showing encapsulated guanine (invisible here) in time series images.

(a) (b) (c)

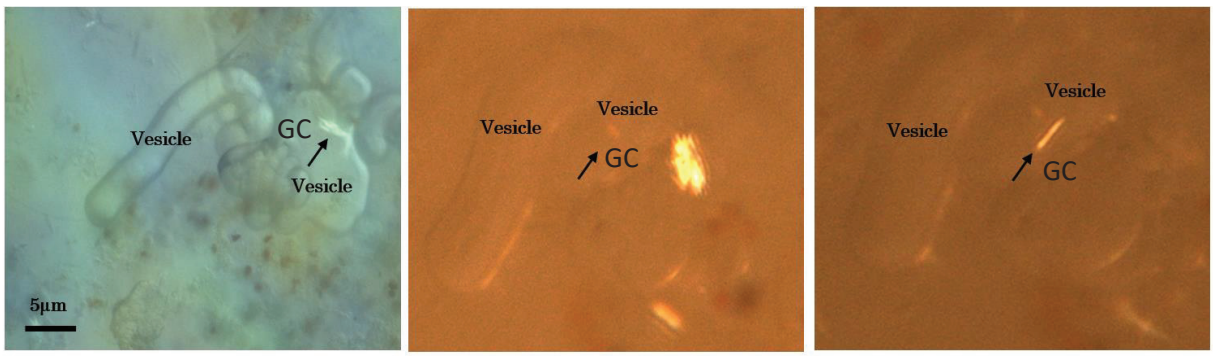

Figure 4.3.2 Hybrid-vesicle. (a) Guanine encapsulation and Guanine interaction with lipid vesicle, (b) Accumulated guanine near vesicle, (c) Freely floating guanine crystal inside vesicle (Arrows indicate guanine crystal platelets (GC).

(a)

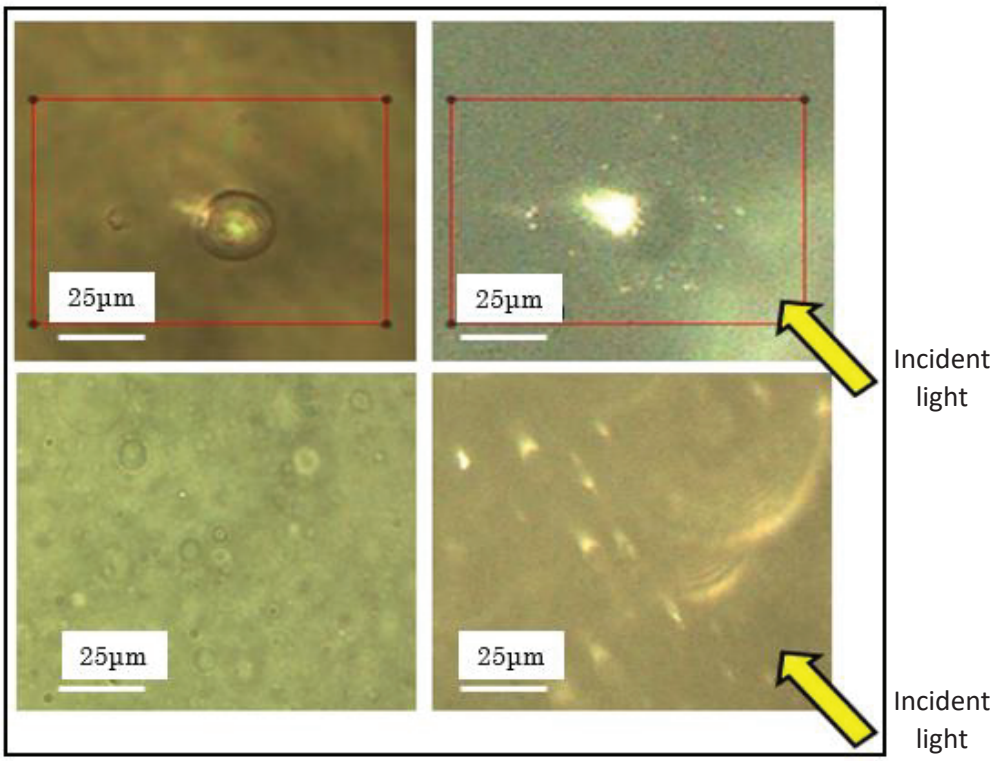

(b)

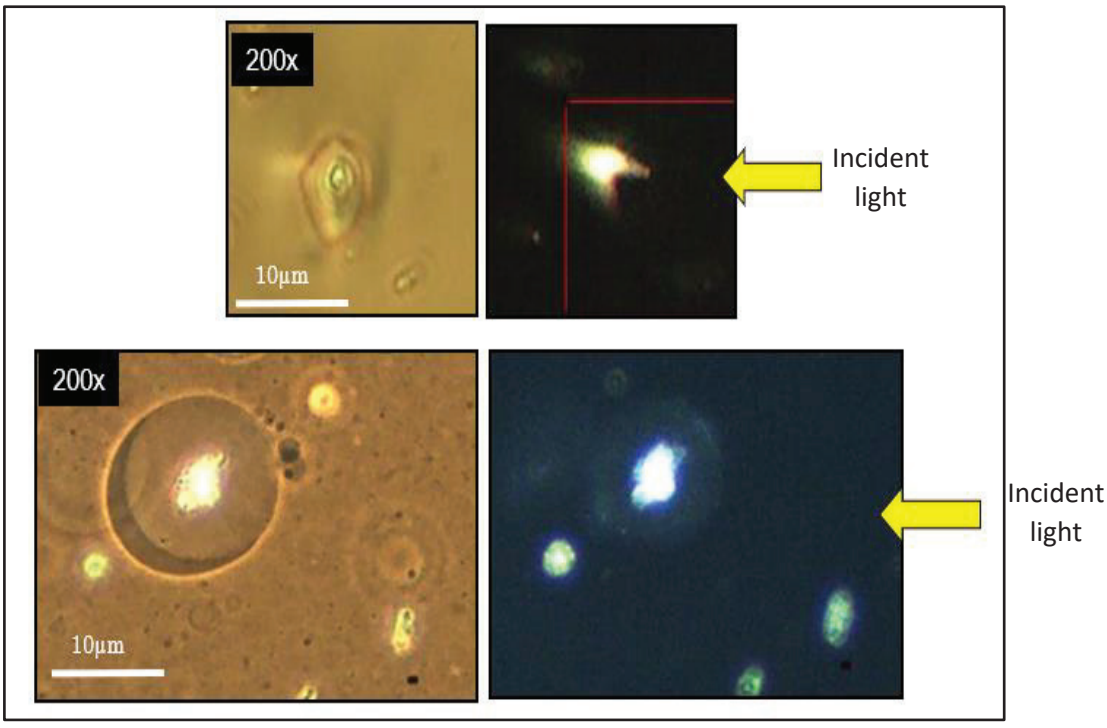

Figure 4.3.3 Vesicle under strong external light illumination.

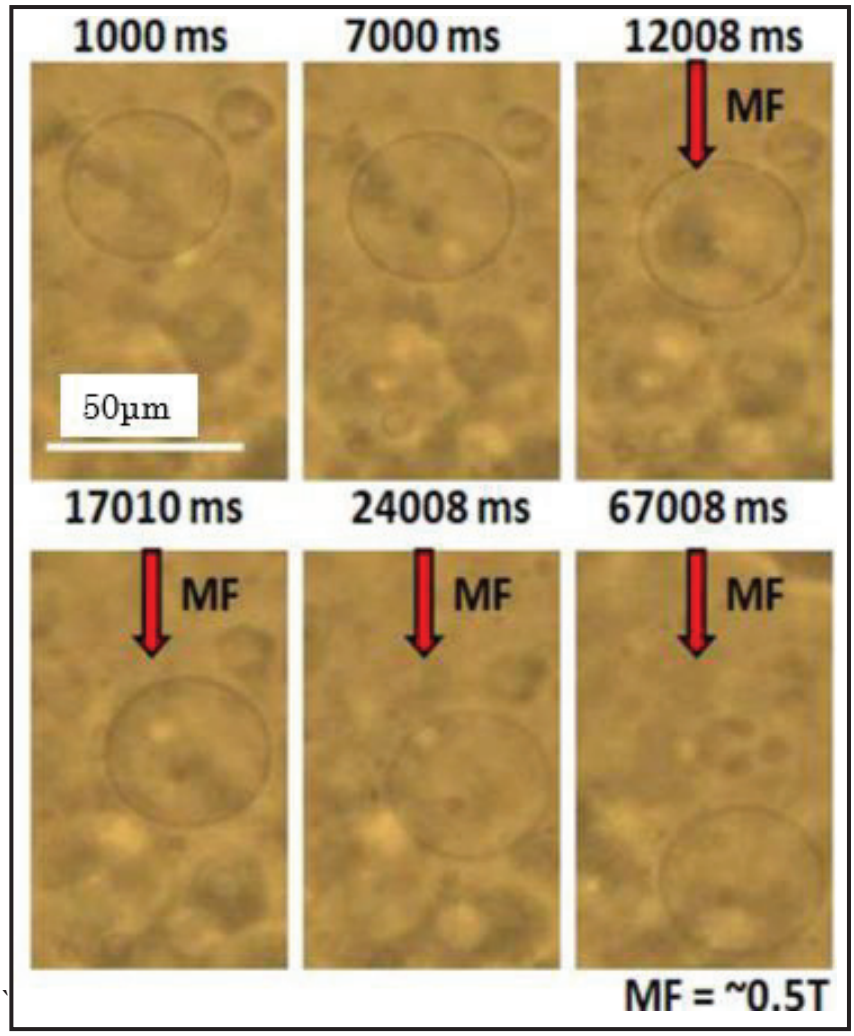

Figure 4.3.4 A time series image shows increased Brownian motion of hybrid-vesicles under magnetic exposure (~0.5T).

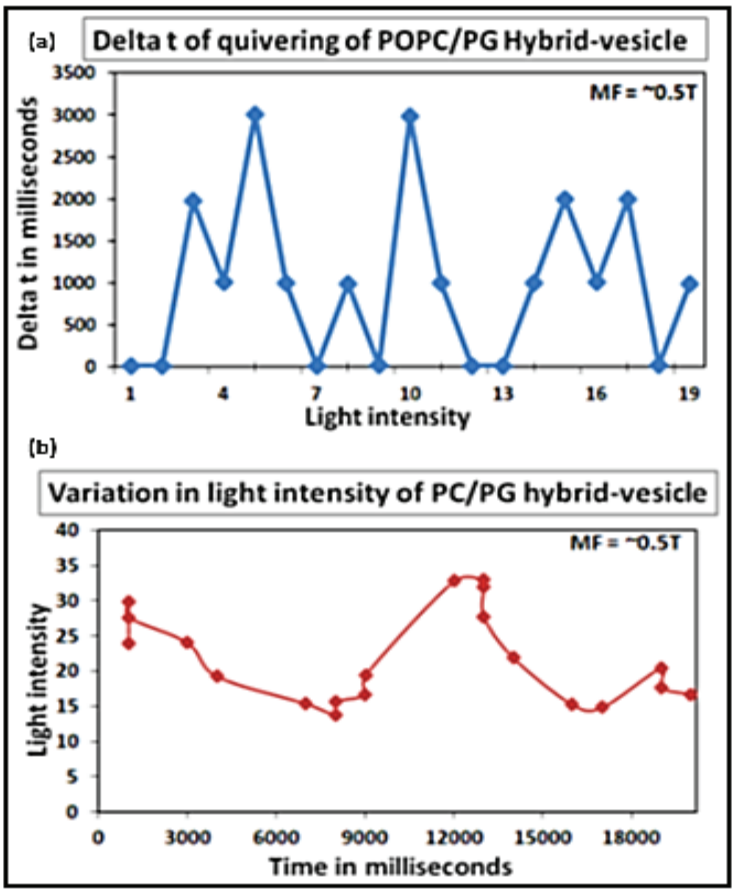

Figure 4.3.5 (a) Delta t of flickering of vesicle under magnetic field, and (b) Variation in light intensity reflected from the hybrid-vesicle.

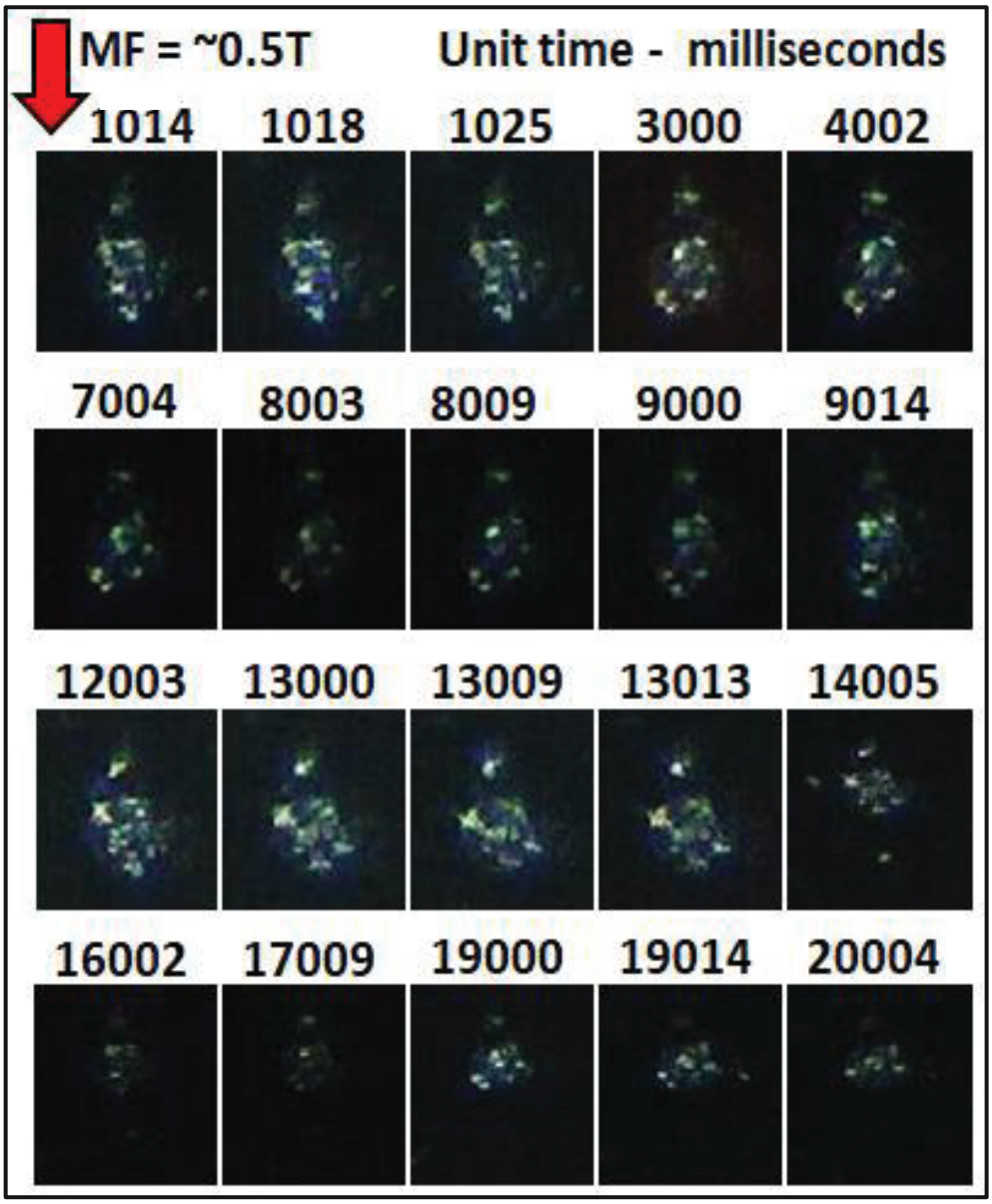

Figure 4.3.6 Positional change of hybrid-vesicle under external magnetic field.

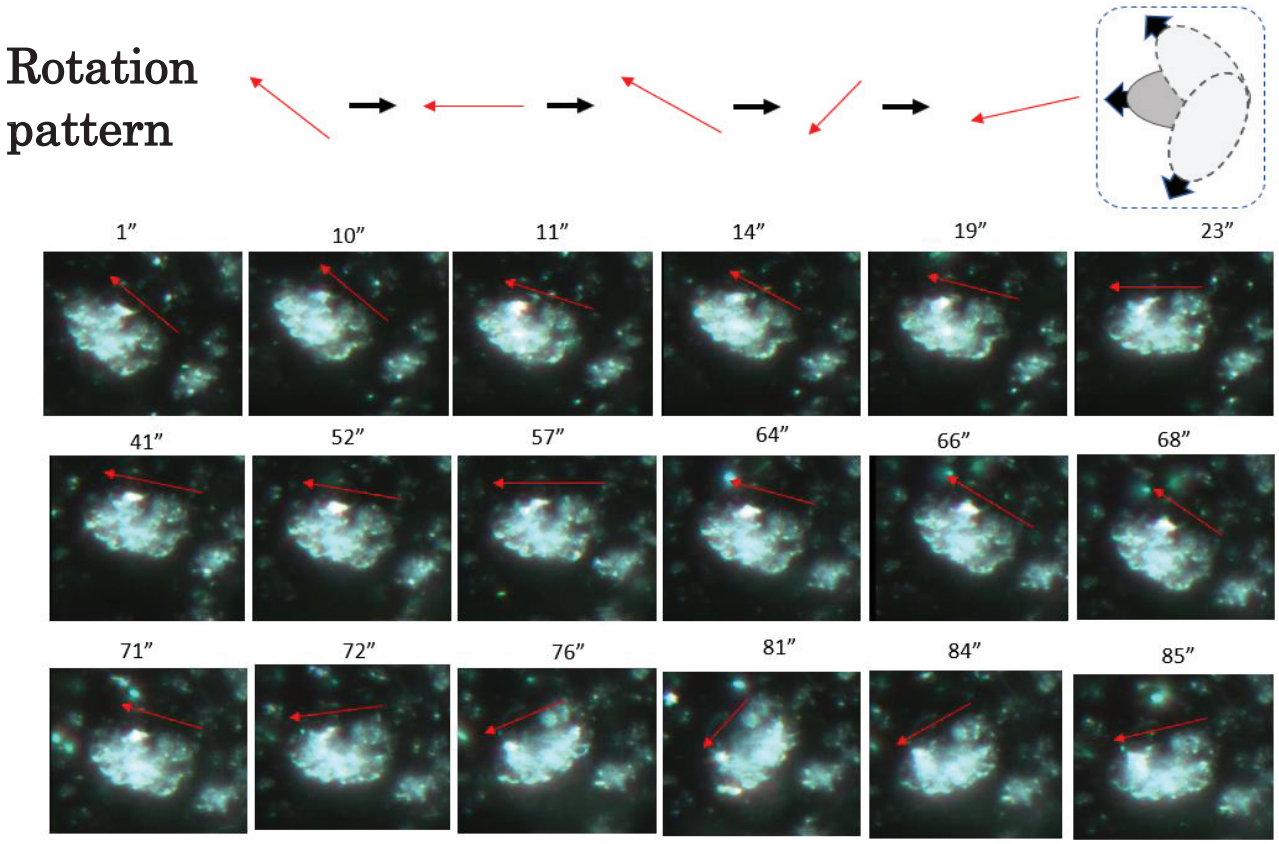

Figure 4.3.7 In plane rotation of hybrid-vesicle.

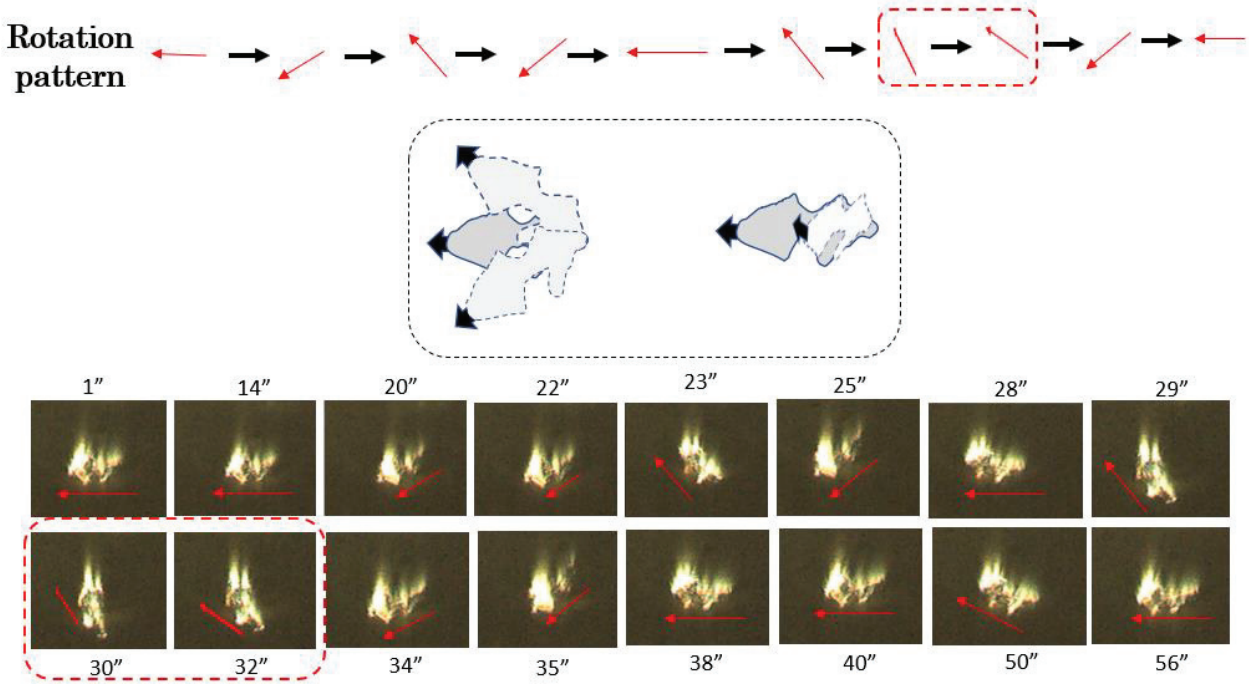

Figure 4.3.8 In-ward and out-ward movement of hybrid-vesicle.

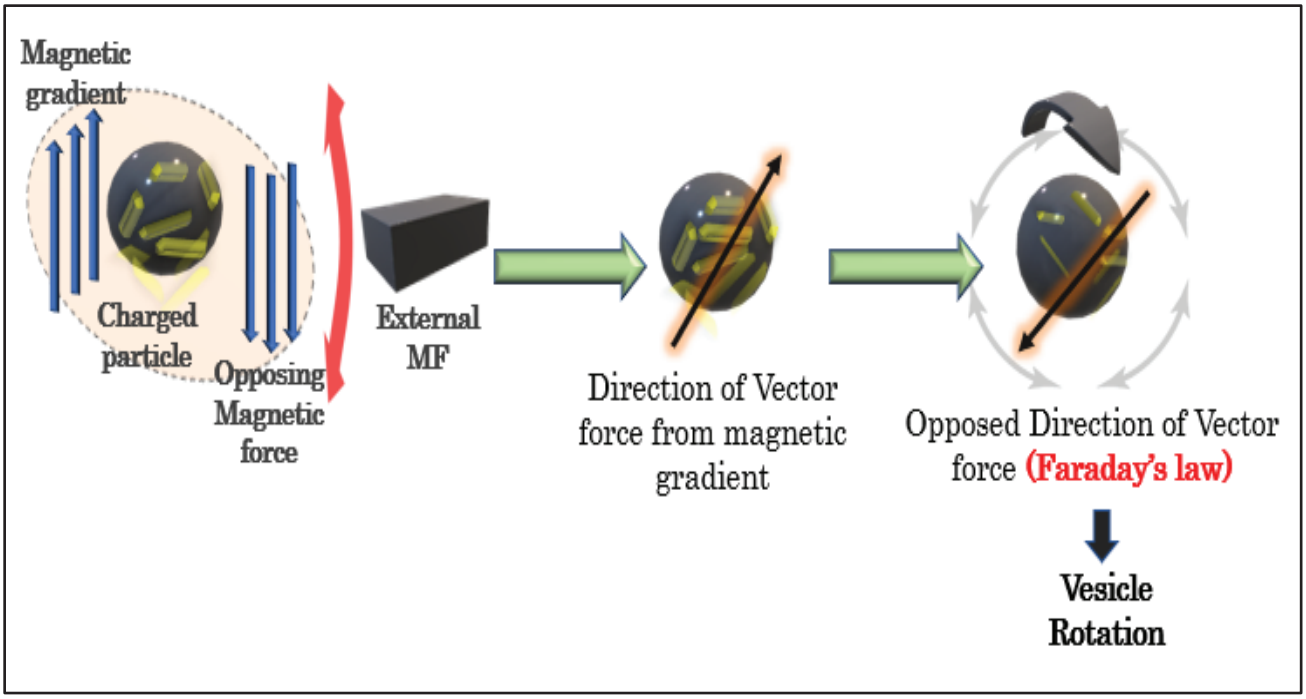

Figure 4.3.9 Hypothesis of rationale of dynamics of rotation of hybrid-vesicle with guanine crystals under magnetic field.

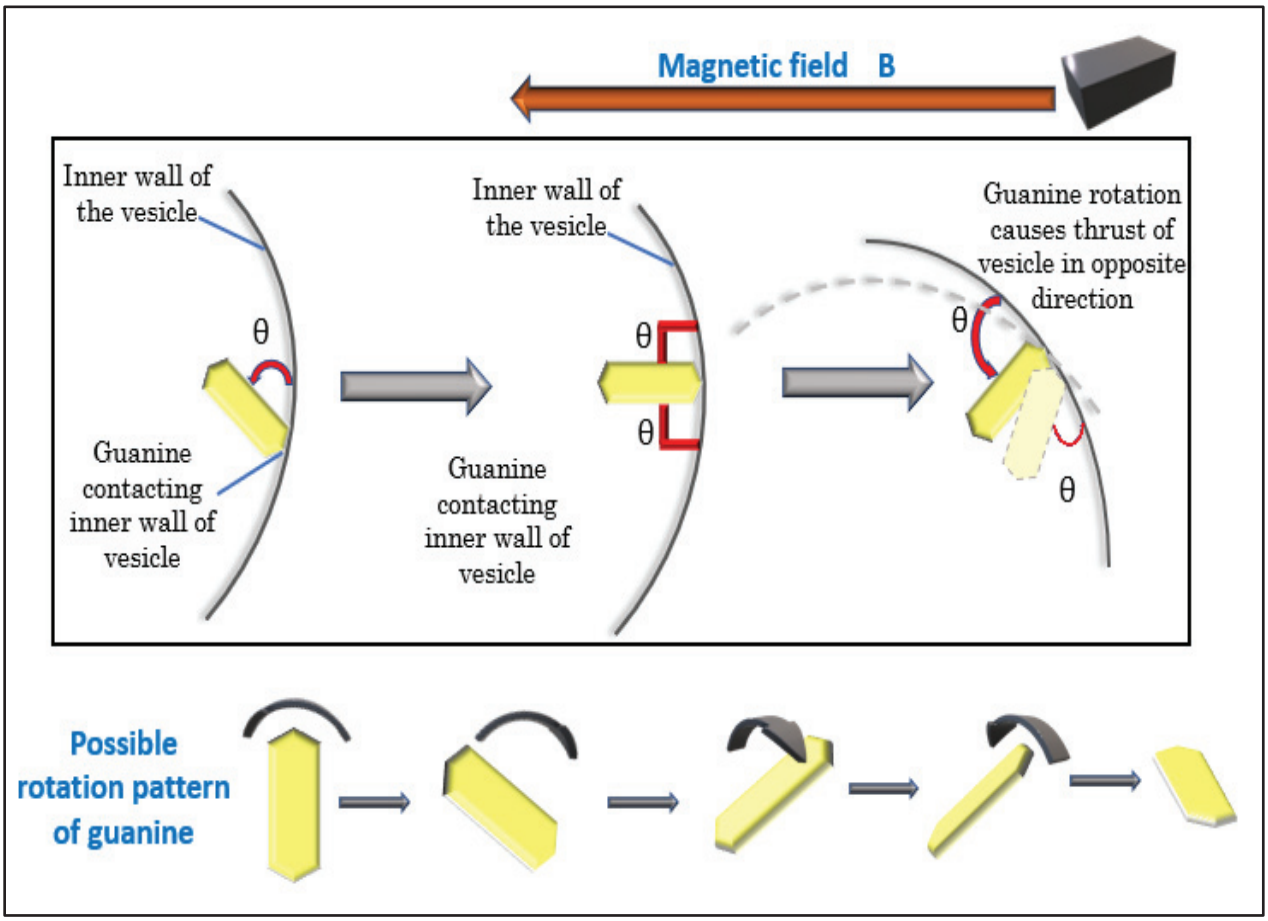

Figure 4.3.10 Hypothesis of rationale of mechanics of rotation of hybrid-vesicle with guanine crystals under magnetic field. The rotational torque acts because the edge of the crystal contacts the vesicle wall.

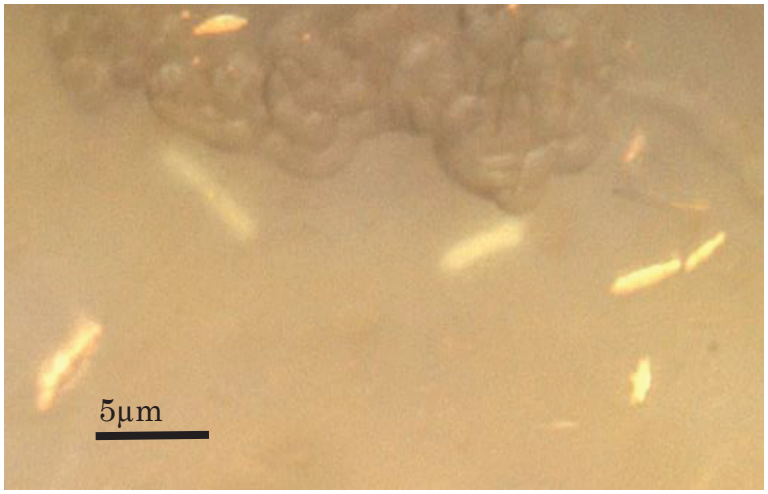

Figure 4.3.11 Interaction of Guanine crystals with lipid layer.

When the magnetic field B with magnetic torque T_M expressed with equation below is applied to a guanine crystal, the crystal rotates in the direction where the magnetic energy is minimal. That is, it rotates to the direction where the axis of rotation is easy, magnetization is parallel to the direction of the applied magnetic field.

$$T_M = V\Delta\chi \frac{B^2}{2\mu_\circ} \sin 2\theta \quad \ldots\ldots\ldots\ldots\ldots\ldots\ldots\ldots\ldots\ldots (2)$$

μ_o is the magnetic permeability in vacuum,

θ is the angle between the magnetic field and the axis of easy magnetization,

V is the volume of the crystal, and

$\Delta\chi$ is the magnetic susceptibility difference between the axis of easy magnetization and the axis of difficult magnetization.

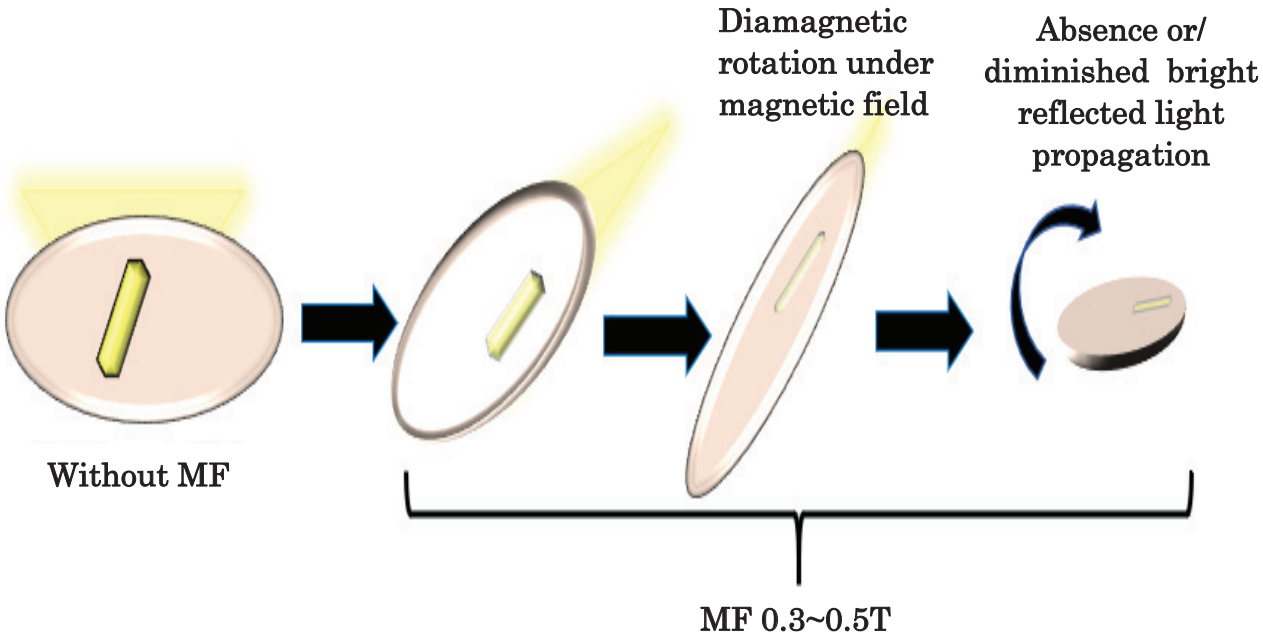

Figure 4.3.12 Proposed model of direction of vesicular rotation.

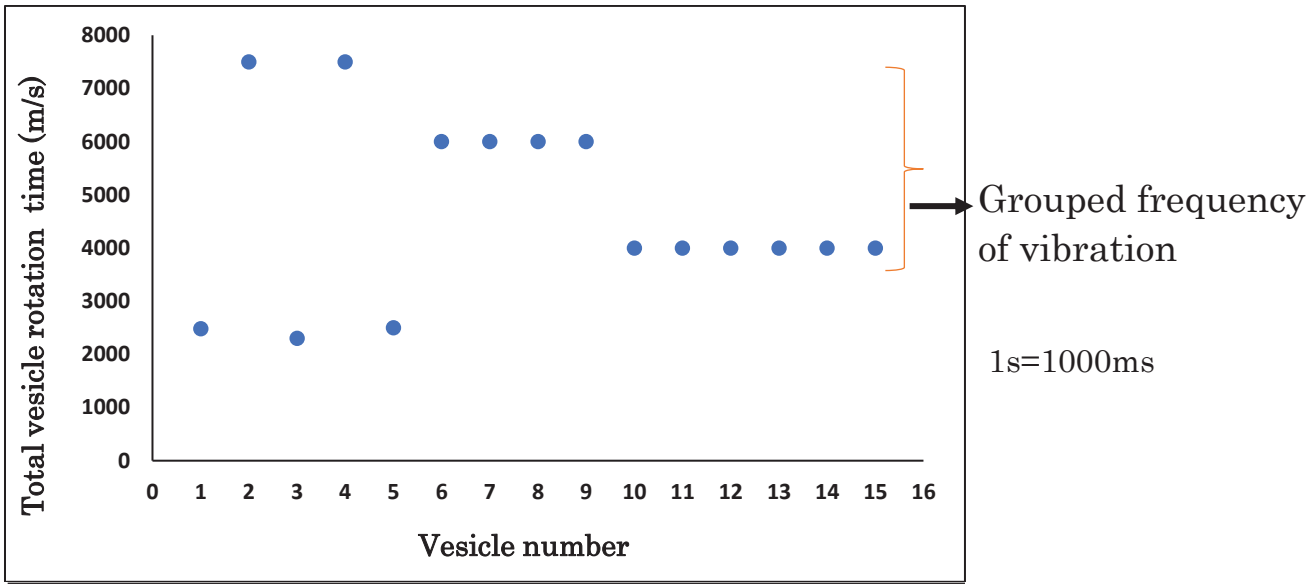

Figure 4.3.13 Total hybrid-vesicle rotation in time series.

	μ	Thickness (nm)
0	1.00	* Medium
1	1.33	400.00
2	1.47	100.00
3	1.47	100.00
4	1.33	400.00
n+1	1.49	*Base

μ = Refractive index

Detection Wavelength range :

350.0nm ~ 750.0 nm

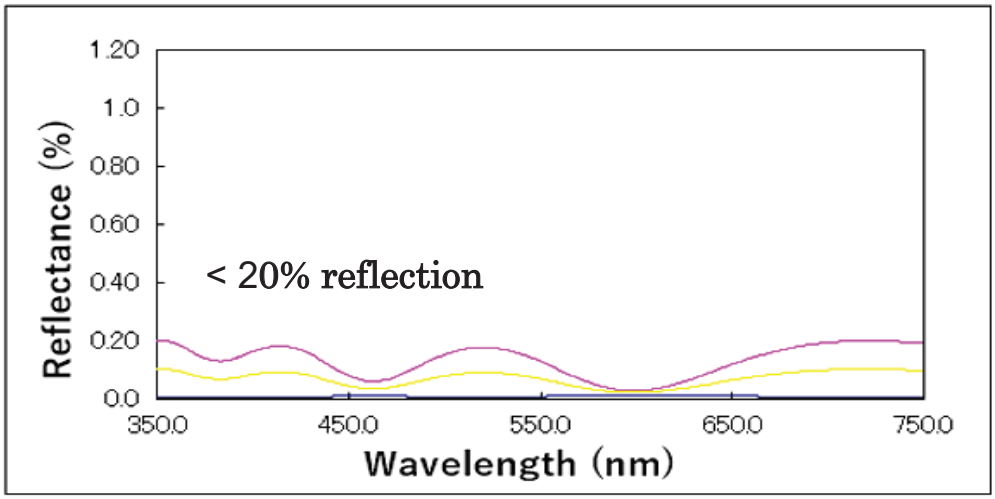

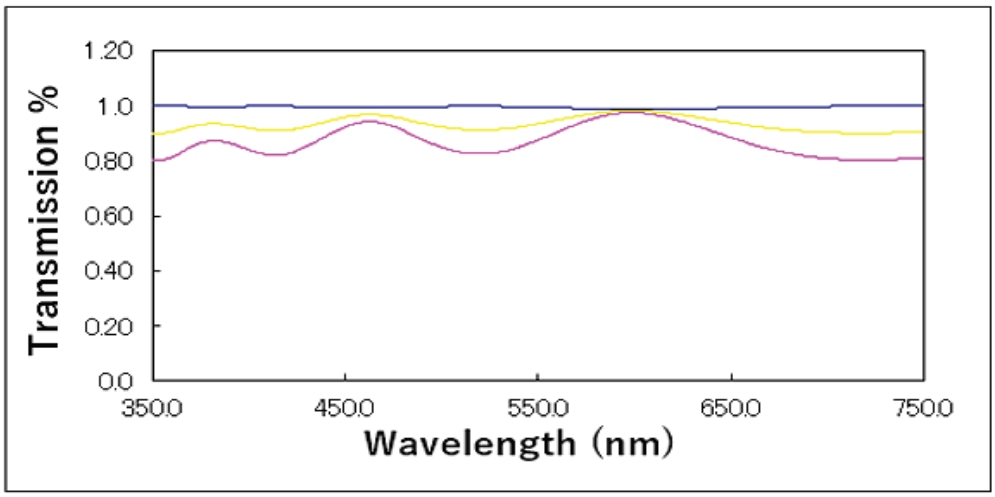

Figure 4.3.14 Simulation of light intensity reflection from water, guanine, and lipids.

	μ	Thickness (nm)	
0	1.00	* Medium
1	1.33	1000.00
2	1.47	100.00
3	1.47	100.00
4	1.33	1000.00
5	1.83	100
6	1.47	100
7	1.47	100
8	1.33	1000
n+1	1.33	*Base

μ = Refractive index

Detection Wavelength range : 350.0nm ~ 750.0 nm

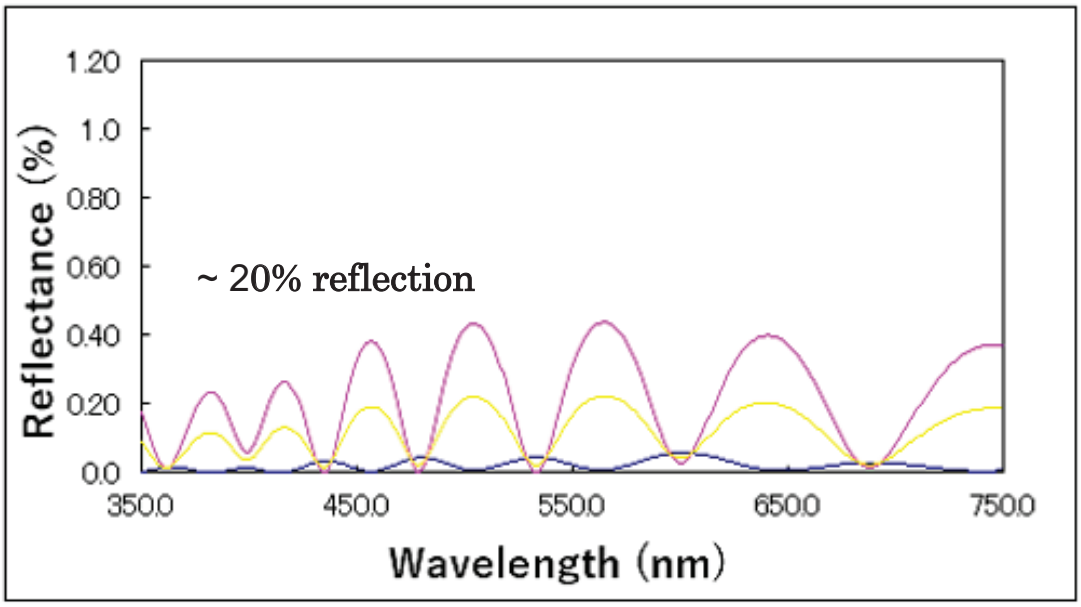

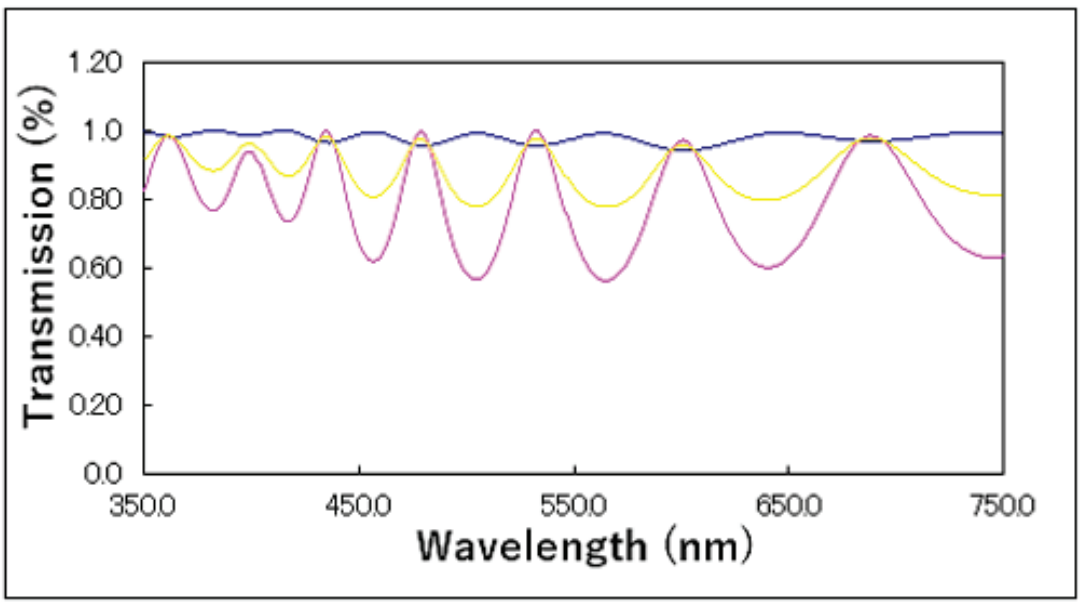

Figure 4.3.15 Simulation of light intensity reflection from water, guanine, and lipids.

	μ	Thickness (nm)	
0	1.00	* Medium
1	1.33	1000.00
2	1.83	100.00
3	1.47	100.00
4	1.47	100.00
5	1.33	1000
6	1.83	100
7	1.47	100
8	1.47	100
9	1.83	100
10	1.33	1000.0
n+1	1.33	*Base

μ = Refractive index

Detection Wavelength range :

350.0nm ~ 750.0 nm

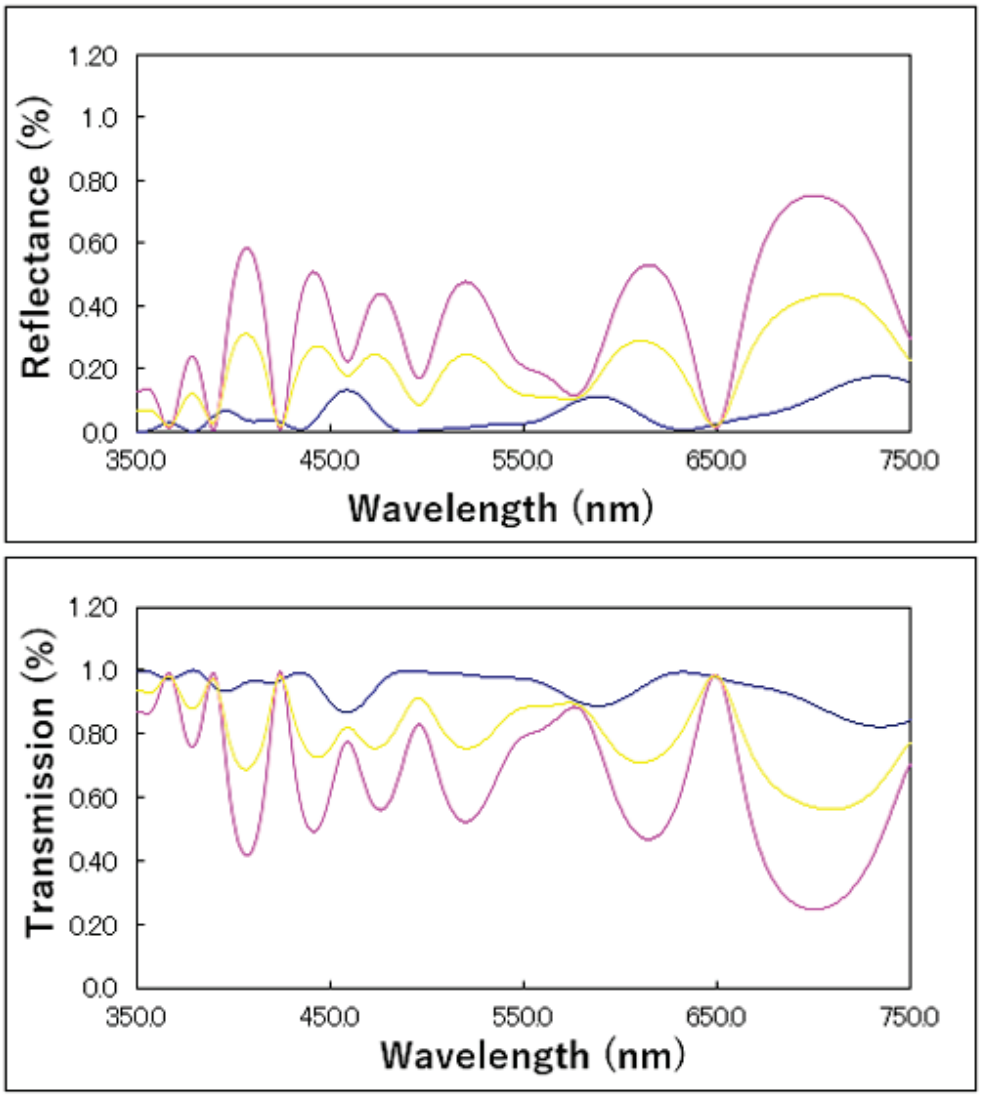

Figure 4.3.16 Simulation of light intensity reflection from a model representing guanine, bi-layered lipid membrane floating in water.

(a)

	μ	*Thickness (nm)*
0	1.00	* Medium
Water	1.33	10000.00
Guanine	1.83	100.00
Lipid	1.47	100.00
Lipid	1.47	100.00
Guanine	1.83	100
Lipid	1.47	100
Lipid	1.47	100
Guanine	1.83	100
Lipid	1.47	100
Lipid	1.47	100.0
Guanine	1.83	100
Lipid	1.47	100
Lipid	1.47	100
Guanine	1.83	100
Lipid	1.47	100
Lipid	1.47	100
Guanine	1.83	100.0
Lipid	1.47	100.0
Lipid	1.47	100.0
Water	1.33	10000
Base	1.33	*Base

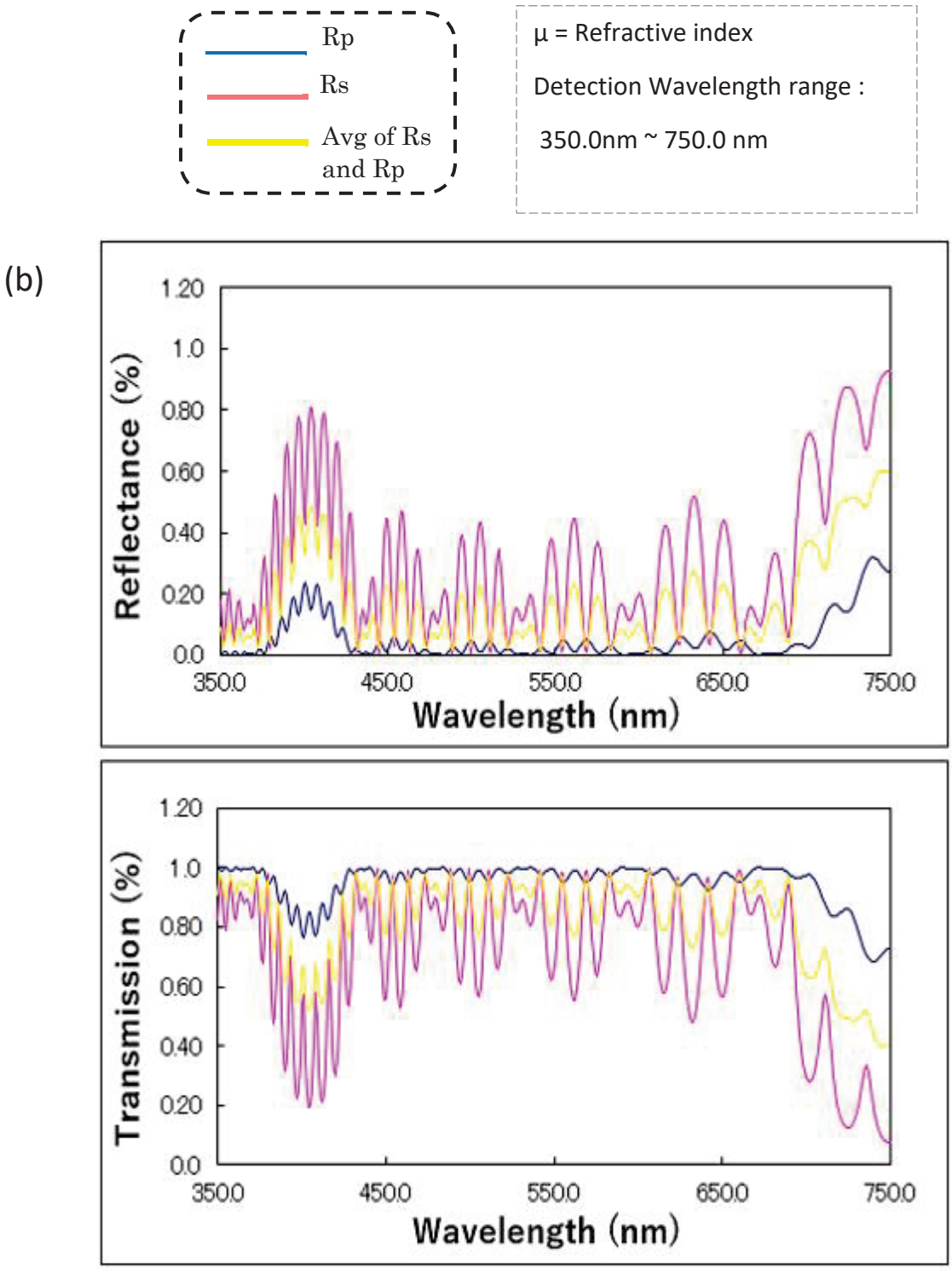

Figure 4.3.17 (a) Details of arrangement of layers with their respective thickness, (b) Simulation of reflectance and transmission of water, guanine platelets and lipid layers. The output light intensity reflected in the 20 layers of water/guanine/lipid with varying thickness is demonstrated.

4.3.2 Discussion

The observable rapid vibration or rotation of small hybrid-vesicles could possibly be explained by the following reasons:

i) The Brownian motion of small quantity of water (few microliters) inside the micro-sized hybrid-vesicle was increased under magnetic exposure, which caused increased flickering and random movement of Guanine. This was observed as a rotation of hybrid-vesicle due to physical positional-shift in distribution and flickering of Guanine particles. Figure 4.3.18 shows delta t of flickering of water particles under MF.

ii) There is a possibility that the elasticity of the lipid layer (strain on bilipid layer) was altered under magnetic exposure of a magnetic strength as low as 0.5T, which was not too high to cause disruption of bilipid layer/lipid molecules by the strain caused by MF, but was strong enough to cause a positional shift of the lipid molecules in the lipid bilayer due to diamagnetic effect of magnetic field on lipid molecules, which in turn was observable as an increased vibration/rotation of vesicles enclosing guanine using high speed CCD camera. [13]

iii) The rotation of the hybrid-vesicle could also be just an observable physical movement of the lipid bilayer which was merely just by the disrupted inner water compartment / disturbed guanine particles situated inside vesicle pushing against the wall of lipid layer under MF exposure casing mild movement of lipid layer.

Often, live cell imaging is accomplished by using complex materials for visualization. In this article, we demonstrated a simple and affordable technique

of development of hybrid-vesicle. The rationale behind prolonged diminished light intensity with a gradually rising extended period of increased intensity may be due to a complete rotation of the hybrid-vesicle in distilled water in a slow motion along with Brownian motion of distilled water, while flickering at the same time. This gives an illusion of high and low intensity of light reflected from "hybrid-vesicle". Additionally, as guanine exists in natural systems in a stacked manner, if vesicles as shown in Figure 4.3.19 are formed along with entrapped guanine inside each vesicle bulb/tube, then an in-vitro model of an iridophore can be obtained which arranges guanine crystals in a periodical fashion. This arrangement can facilitate light interference from the hybrid-vesicle which holds future potential application in optically tunable devices.

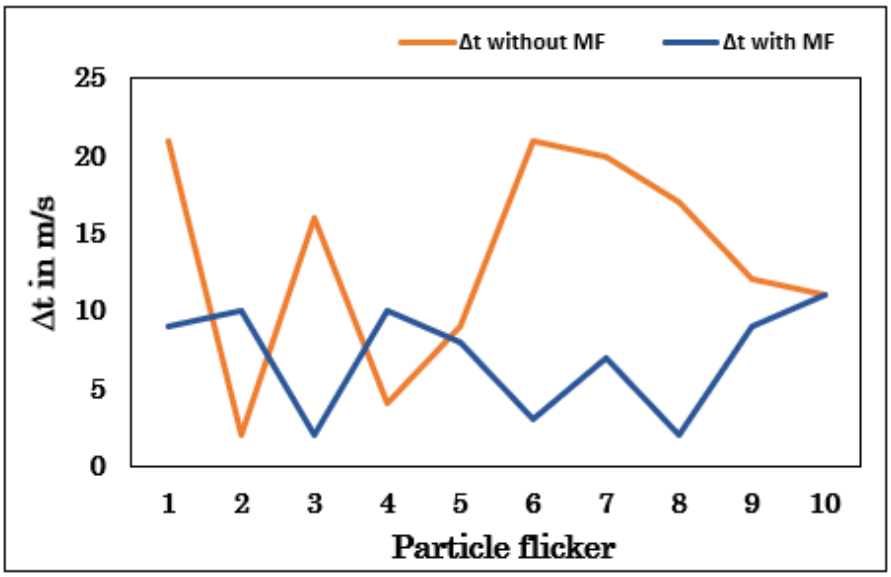

Figure 4.3.18 Flickering rate of water microparticles with and without magnetic field (MF- 0.5T).

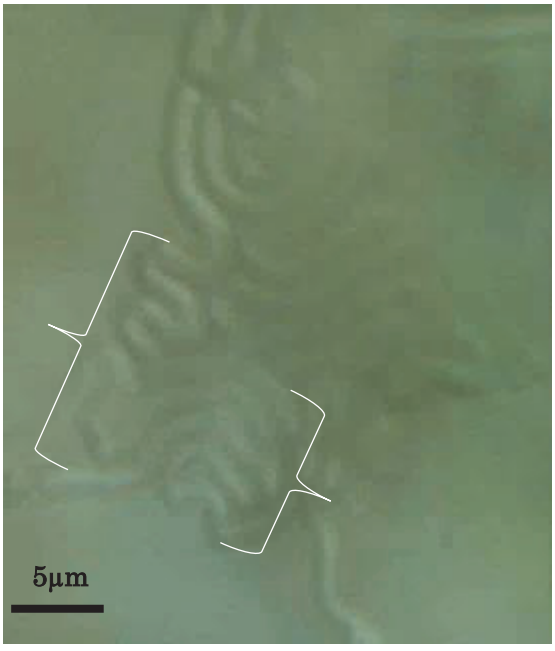

Figure 4.3.19 Lipid sacs arrangement in an aligned pattern suitable for light interference enhanced by guanine crystals.

4.4 Summary

By entrapping guanine crystals into lipid vesicles, it is possible to replicate a model of an iridosome found in fish scales as in-vitro hybrid-vesicles. In addition, the rate of vibratory motion of the hybrid-vesicle can be manipulated with an external magnetic field of a magnetic flux density of ~0.5T, which further allows manipulation of the intensity of light reflected from this hybrid-vesicle. This may serve as a tool with a simplified technique for potential application in bio-reflector based bio-imaging treating intravesicular guanine crystals as cellular micro mirrors.

References for Chapter 4

[1] C. Xu, S. Hu and X. Chen., "Artificial cells: from basic science to applications," Materials Today., vol.9, no. 9, pp. 516-532, 2016

[2] J. Li, "A review on phospholipids and their main applications in drug delivery system," Asian J. Pharm. Sci., vol.10, no.2, pp. 81-98, 2015.

[3] S. Reyhani, O. Ces and Y. Elani, "Artificial cell mimics as simplified models for the study of cell biology," Exp Biol Med (Maywood)., vol.242, no.13, pp. 1309–1317, 2017.

[4] N. Kucera, S. Tristam-Nagle and J.F. Nagle., "Structure of fully hydrated fluid phase lipid bilayers with monounsaturated chains," J. Membr. Biol., vol.203, no.3, pp.193-202, 2005.

[5] L. Vares, A.V. Koulov and B.D. Smith., "Highly impermeable vesicles composed of conformationally restricted phosphatidylethanolamine," Roy. Soc. Chem. pp. 1482-1483, 2002.

[6] D. Gur, B.A. Palmer, S. Weiner and L. Addadi., "Light Manipulation by Guanine Crystals in Organisms: Biogenic Scatterers, Mirrors, Multilayer Reflectors and Photonic Crystals," Adv. Funct. Mater., vol. 27, no.6, pp. 1-13, 2016.

[7] N. Funt, B.A. Palmer, S. Weiner and L. Addadi., "Koi Fish-Scale Iridophore Cells Orient Guanine Crystals to Maximize Light Reflection," Chem Plus Chem., vol.82, no.6, pp. 914-923, 2017.

[8] M. Iwasaka and Y. Mizukawa., "Light Reflection Control in Biogenic Micro-Mirror by Diamagnetic Orientation," Langmuir., vol.29, pp. 4328-4334, 2013.

[9] A.R. Parker., “A geological history of reflecting optics,” J. R. Soc Interface., vol. 2, no. 2, pp. 1-17, 2005

[10] M. Iwasaka, Y. Mizukawa and N.W. Roberts., “Magnetic Control of the Light Reflection Anisotropy in a Biogenic Guanine Microcrystal Platelet,” Langmuir., vol. 32, pp. 180-187, 2015.

[11] Mootha, Y. Takanezawa and M. Iwasaka., “Quenching of light flickering in synthetic guanine crystals in aqueous solutions under strong static magnetic fields,” AIP Advances., vol.8, no.5, pp. 1-6, 2018.

[12] J.P. Reeves and R.M. Dowben., “Formation and properties of thin-walled phospholipid vesicles,” J. Cell. Physiol., vol. 73, pp. 49-60, 1968.

[13] Rosenblatt C, Yager P, Schoen PE. Orientation of lipid tubules by a Magnetic field. Biophysical J; vol. 52: 295-301, 1987.

5. Refinement of synthetic guanine crystals for fast diamagnetic rotation

5.1 Introduction

Synthetic guanine crystals, with the same magnetic controllable reflection property as a biogenic guanine crystal from fish scales, were prepared using a classical Ostwald ripening method for crude crystals, from the aqueous sodium hydroxide solution of a commercially available synthesized guanine powder. The resulting synthetic guanine crystals with an average size of several tens of micrometers were in the same crystal system as the biogenic guanine crystals under measurement by X-ray diffraction (XRD). However, XRD patterns of water-floating crystals showed that the correlation between the growing direction and reflecting surface in the synthetic crystals is different from that in the biogenic crystals. Therefore, the synthetic crystals were ground by an agate mortar for refinement of its optical and magnetic-orientation characters. As a result, we realized a fast-magnetic orientation against the vertical field, which is related to the magnetic control of light reflection, the same as the biogenic guanine crystal behavior.

Guanine, which is a simple molecule with a molecular weight of only 151, is one of the most important molecules for the manipulation of light in living system. [1–8] There is a possibility that the use of guanine crystals may lead to a novel micro optical device with a higher ordered function, such as an artificial iridosome or a material exhibiting structural color. Recently, we reported that biogenic guanine crystals can be used as micro optical devices that can control the reflection characteristics by using the external magnetic field response accompanied by the

anisotropy of the diamagnetic susceptibility of guanine crystals. [5,9–11] For example, the reflection property of guanine crystal can be switched through applying or removing a magnetic field by using the perpendicular magnetic orientation character, as shown in Fig. 5.3.1 (b). [9] However, guanine crystals that can be used as magnetic switchable reflectors can only be collected from living creatures, such as fish, because the shape and size of synthetic guanine crystals prepared using an artificial method are much poorer than those of biogenic crystals. A notable reason for the difficulty in the preparation of synthetic guanine crystals by an artificial method is the low water-solubility. [12] Several groups have succeeded in recrystallizing synthetic guanine under basic aqueous solution, because the solubility can be increased by using the acid dissociation equilibrium of a guanine molecule. [12–14] The resulting synthetic guanine crystals have the same crystal structure as that of biogenic guanine crystals, but these external shapes are insufficient for use in magnetic switching optical devices, as described above. It is not necessary to make identical crystals as the biogenic crystals, but an external shape that provides reflection and perpendicular magnetic rotation is required for the creation of a magnetic switchable micro optical device. In this study, we have optimized the conditions to prepare a synthetic guanine crystal with an external shape that provides reflection and perpendicular magnetic rotation similar to the magnetic orientation in a biogenic crystal. [9] Synthetic guanine crystals were first prepared from a basic aqueous solution at pH 13 and were ripened by using a classical Ostwald ripening method. Next, the crystallographic information regarding the correlation between growing direction and reflecting surface of the ripened synthetic guanine crystal were estimated

using X-ray diffraction (XRD) measurements of the water-floating crystals. Finally, crystal grinding was applied to the synthetic guanine crystal for refinement towards our purpose.

5.2 Methodology

Crystallization from synthesized high-grade guanine (077-01692, Fujifilm Wako, Japan) was performed according to our previously reported procedure. [11] The synthesized guanine (12.6 g) was dissolved in an aqueous solution of sodium hydroxide (1 L) with a pH of 13 at the boiling point, and crude crystals were obtained after cooling to ambient temperature with a cooling rate of 10 °C/day. In slow recrystallization, there were no guanine particles left after the solvent was completely saturated. Whereas in the rapid recrystallization method, after the solvent was completely saturated, a few guanine particles were left in the solvent for serving as a seed for recrystallization and for enhancement of the process of recrystallization. (Figure 5.2.1). The temperature of the dispersion containing the crude crystals was heated again to ca. 100 °C for growth of the crystals. After ripening for several weeks, the ripened guanine crystals were collected by filtration after cooling to room temperature. (Figure 5.2.1, Figure 5.2.2) The resulting crystals were washed with water/methanol and dried in vacuo, and then were used as the “synthetic guanine crystals” for the following measurements.

Characterization of the shape of the synthetic crystal was performed by optical microscopy. Crystallographic information of the crystals, which were dried or floating in water, was obtained by using an XRD analysis.

After checking the general character of the synthetic guanine crystals without further modification, the synthetic guanine crystals were gently ground on an agate mortar in a lateral stretch manner by using an agate pestle for half-an-hour to improve its external shape of the synthetic crystal. Drastic changes were

observed from the results of XRD and magnetic orientation, as described in the next section.

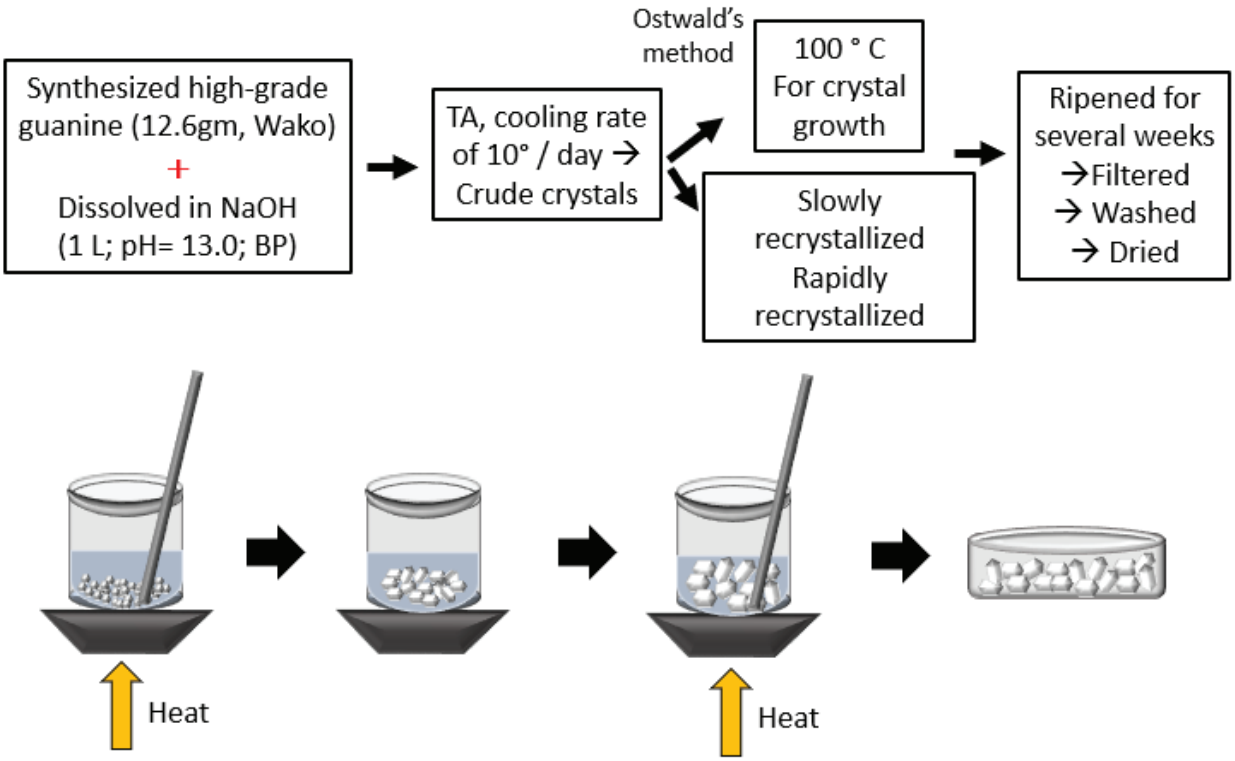

Figure 5.2.1 Recrystallization methodology.

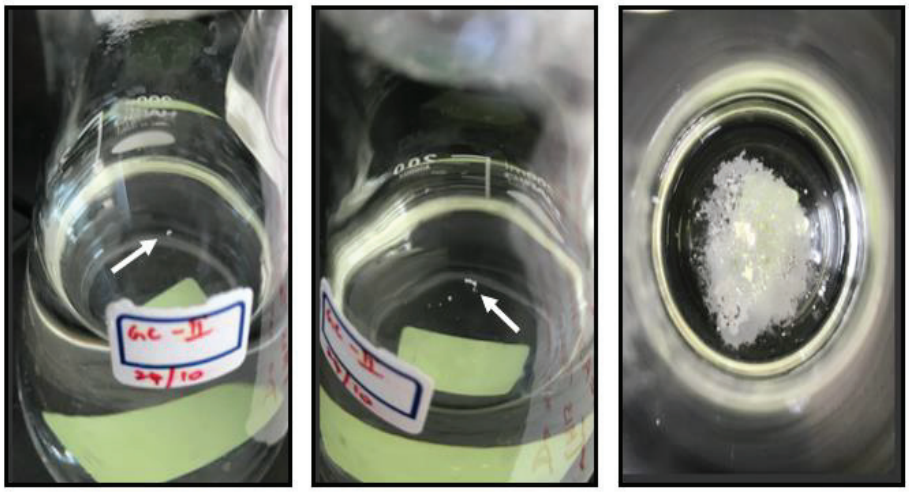

Figure 5.2.2 Gradual recrystallization growth.

5.3 Results and Discussion

The crude crystals with an average size of 10 μm were boiled at ca. 100 °C in an aqueous sodium hydroxide solution at pH 13 to increase the crystal size in a classical Ostwald ripening condition over one week. The size of the resulting guanine crystal was significantly larger than that before ripening. Although the major external

formation of the crystal was rod-like, which was the same as the previously reported synthetic crystals, plate-like crystals showing interference fringes, which are a sign of high-quality crystals without cracks, were also obtained (Fig. 5.3.1(c)). [12–14]

For XRD measurements, two types of samples were prepared for both the synthetic guanine crystal and the biogenic guanine crystal from the scales of a goldfish. Here, we defined two types of samples depending on preparation methods before the XRD measurements: The type I sample is dried crystals obtained after drying the water dispersion of crystals on the surface of a flat glass plate, and the Type II sample is floating crystals in a water droplet on the surface of the glass plate covered with a wrap film. XRD measurement of the crystals floating in water (Type II) was possible by irradiating X-rays from above the water surface. The plots of XRD patterns of the two types of samples of the synthetic and biogenic crystals are shown in Fig. 5.3.2. All clear XRD peaks could be assigned to the crystal in the anhydrous guanine-phase,3.15 which proved that the synthetic guanine crystals belonged to the same crystal structure as the biogenic crystals. This agreement was also confirmed by Fourier transform infrared spectroscopy. As a feature of the synthetic crystals, the intensity corresponding to the $(12\bar{2})$

plane became large and dominated along with the (002)/(011) plane, which could not be distinguished because their peak positions overlapped, in contrast to the biogenic crystals. [4] These results suggested that the synthesized crystals grew with a preferential orientation that resulted in flat $(12\bar{2})$
and (002)/(011) planes. The difference between the XRD patterns were observed depending on the presence of water (Fig. 5.3.2(a) and (b)) in the case of the synthetic crystals, whereas the two patterns were matched in the case of the biogenic crystals and only the peak from (102) was observed (Fig. 5.3.2(c) and (d)). The biogenic crystals exhibited an elongated hexagonal plate having a smooth broad surface of the (102) plane and the averaged size was 20 μm×5 μm×100 nm (thickness). Such a plate-formed guanine crystal was aligned so that the (102) plane was parallel to the water surface because the crystals could float in water because of its extremely thin structure. Therefore, even when the floating biogenic crystals were dried, the (102) plane was stacked parallel to the substrate surface, as was observed from XRD. However, the synthetic crystals mainly exhibited a rectangular shape with a larger thickness compared with the biogenic crystals. The dried synthetic crystals in the Type I samples should be stacked so that the plane orientation of the crystal faces adopt various directions after drying to exhibit many XRD peaks that originate from the resulting randomness (Fig. 5.3.2(a) inset). However, in the case of the floating synthetic crystal in the Type II sample, the crystals tended to float in water with a flat surface facing up (Fig. 5.3.2(b) inset). The SEM images of synthetic and biogenic crustal are shown in Figure 5.3.3 (a) and (b). The optical images of slow and rapid crystallized guanine is shown in Figure 5.3.4 (a) and (b). The condition of crystals with definite shape

of rapidly crystallized guanine (Figure 5.3.5 (a) and conditions with and without sonification are shown in Figure 5.3.4 (b). The condition of crystals with definite shape of rapidly crystallized guanine (Figure 5.3.4 (a)) and conditions with and without sonification are shown in Figure 5.3.5 (b).

The magnetic orientation experiments of the synthetic guanine crystals dispersed in water by using a permanent magnet were conducted. The optical microscopy images of the crystals under a horizontal magnetic field of 130 mT and vertical magnetic field of 150 mT are shown in Fig. 5.3.6 (b) and (c), respectively. The $(12\bar{2})$ plane and (002)/(011) plane made angles of 55.8° and 61.7° / 76.0° with the (102) plane, which meant that the (102) plane was arranged inclined to the upper surface of the crystals. When a horizontal magnetic field was applied, the synthetic crystals rotated and turned the longitudinal direction of the crystal towards 90° from the field direction, which supported the growth of the crystal planes that was discussed above. It should be noted that a quick horizontal rotation can be realized in synthetic guanine crystals. This is because that the (102) plane layered with a large thickness has a high diamagnetic anisotropy energy, and therefore a large torque is generated to make the (102) plane parallel to the magnetic field, while the biogenic guanine crystal is in a thin layer with a thickness of ca. 100 nm. However, a magnetic response is not observed in most synthetic crystals under a vertical field of 150 mT. The magnetic response of slow and rapidly recrystallized guanine is shown in Figure 5.3.7 (a, b).

The synthetic crystals exhibited the same magnetic orientation as the biogenic crystals reported previously; however, their frequency was not large. (Figure 5.3.6 and 5.3.7) It was proposed that the reason for the poor magnetic response of the

synthetic crystals to the vertical field compared with the biogenic crystals is caused by the difference in the correlation between the external shape and the molecular alignment in the crystal. [2] Such a difference should result in a different magnetic field response from the biologic crystals. The slowly recrystallized guanine crystals showed no response to a MF; however, the rapidly recrystallized guanine particles showed a magnetic response in plane (Figure 5.3.7 (a, b)).

To improve the magnetic response of the synthetic crystals through the refinement of its external shape, the synthetic guanine crystals were ground by using an agate mortar to obtain cracked crystals, because several synthetic crystals immediately after the ripening had bundled together, as shown in Fig. 5.3.1. It was surprisingly obvious that the (102) peak became dominant and no remarkable peaks of the other planes were observed in the XRD measurements (Fig. 5.3.3 (c), and also Fig. 5.3.2 (a) for a comparison). Moreover, the XRD pattern of the ground crystal did not change after floating the crystal in water (Fig. 5.3.3 (d)), which was the same trend as the biogenic guanine, as shown in Fig. 5.3.2 (c) and (d). Microscopic observation of crystals were also shown in Figure 5.3.4; along with before and after sonification of synthetic guanine crystals (Figure 5.3.5 (a) and (b)).

These results indicated that the synthetic guanine crystal could be cleaved along the (102) plane after physical grinding and its general crystal structure was maintained, even if the crystals were exposed to violent conditions such as a mechanical grinding. Through the notable toughness of the synthetic crystal, the shape of the crystal could be optimized to a flat thin plate after physical grinding, which was close to the shape of the biogenic guanine crystal. The magnetic

orientation behavior of the ground synthetic crystals is shown in Fig. 5.3.6. The longitudinal direction of the ground guanine crystal did not clearly orient along the horizontal magnetic field. Gray value intensity analysis and comparison with barium sulphate along with biogenic and synthesized guanine particles is represented in Figures 5.3.8, 5.3.9 and 5.3.10. The analysis showed that there did not appear large difference between slow and rapid recrystallized guanine. However, rapid recrystallized guanine sometimes showed slightly more or equal intensity compared to barium sulphate. Biogenic guanine has a higher intensity compared to recrystallized guanine and synthesized guanine particles.

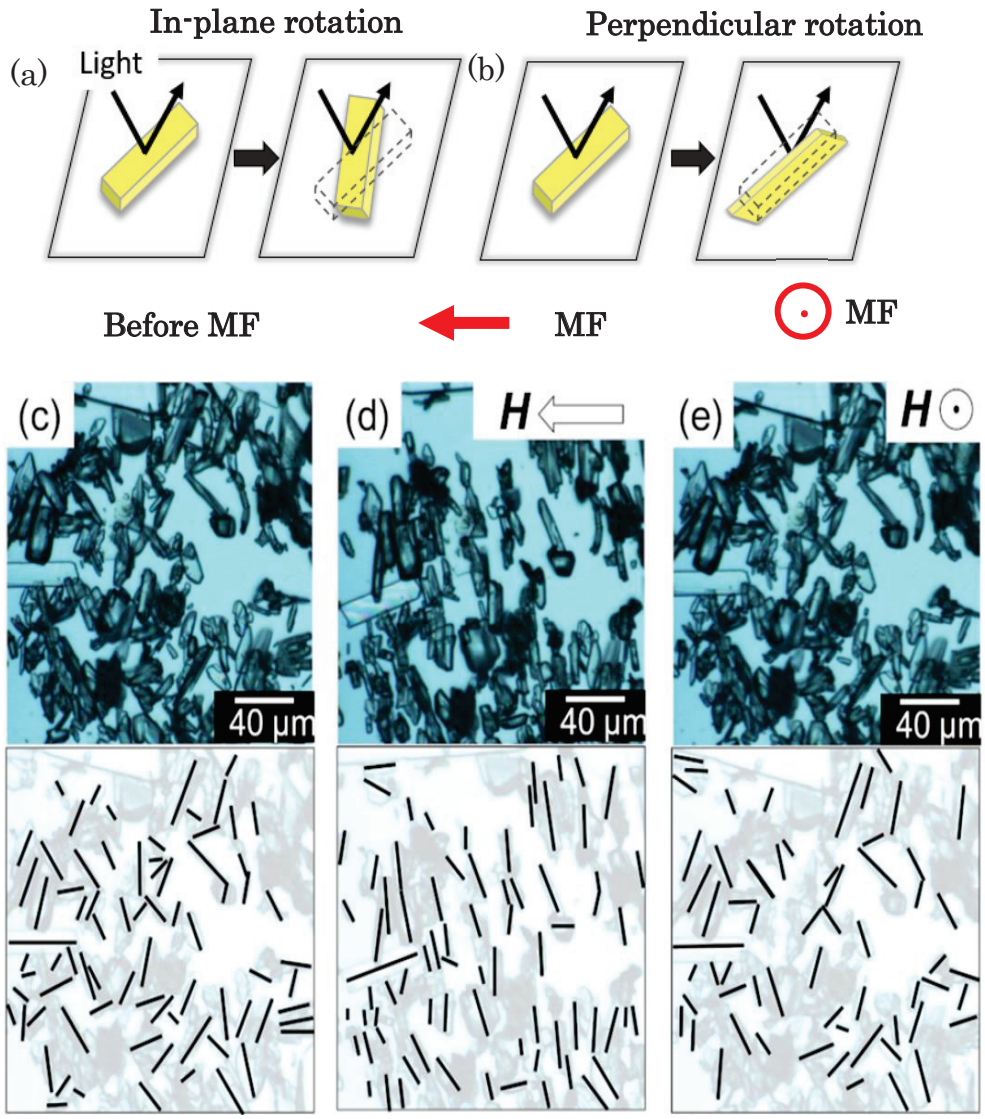

Figure 5.3.1 Schematic illustration of rotation manner of crystals under a magnetic field: (a) In-plane rotation and (b) perpendicular rotation. Rotation direction depends on the sample and direction of the external magnetic field. Optical microscopy images of synthetic guanine crystals (top) and images indicating the orienting direction of the long axis of the crystals (bottom): (c) Before applying a magnetic field, (d) after applying a horizontal magnetic field of 130 mT, and (e) after applying a vertical magnetic field of 150 mT by using permanent magnets.

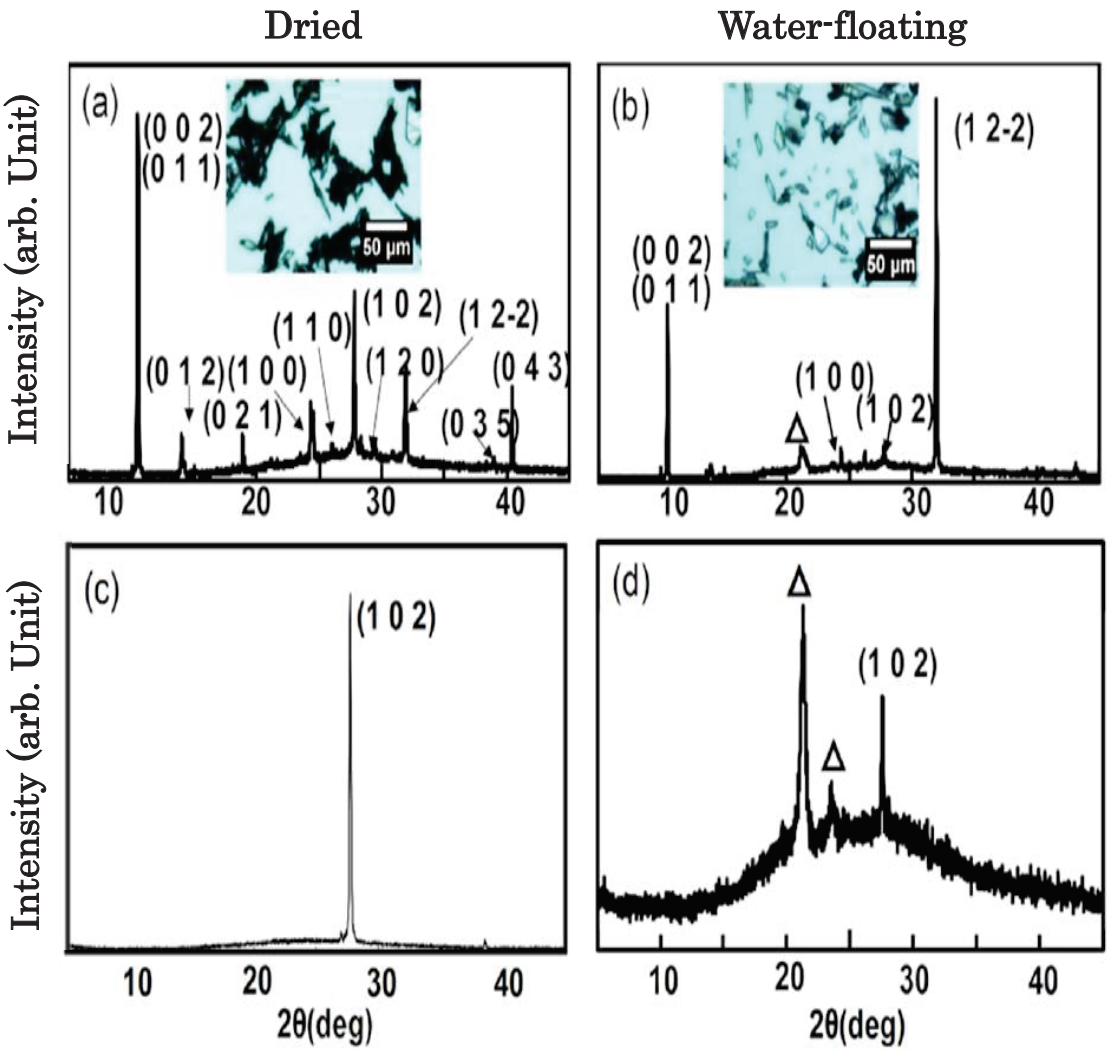

Figure 5.3.2 Diagrams of XRD patterns of (a) dried and (b) water-floating synthetic guanine crystals, and of (c) dried and (d) water-floating biogenic guanine crystals. The diffraction peaks marked by open triangles (Δ) arise from the wrap used to mount the sample. Optical microscopy images are shown as insets in (a) and (b), respectively. (a, b= Synthetic guanine, b, c= biogenic guanine).

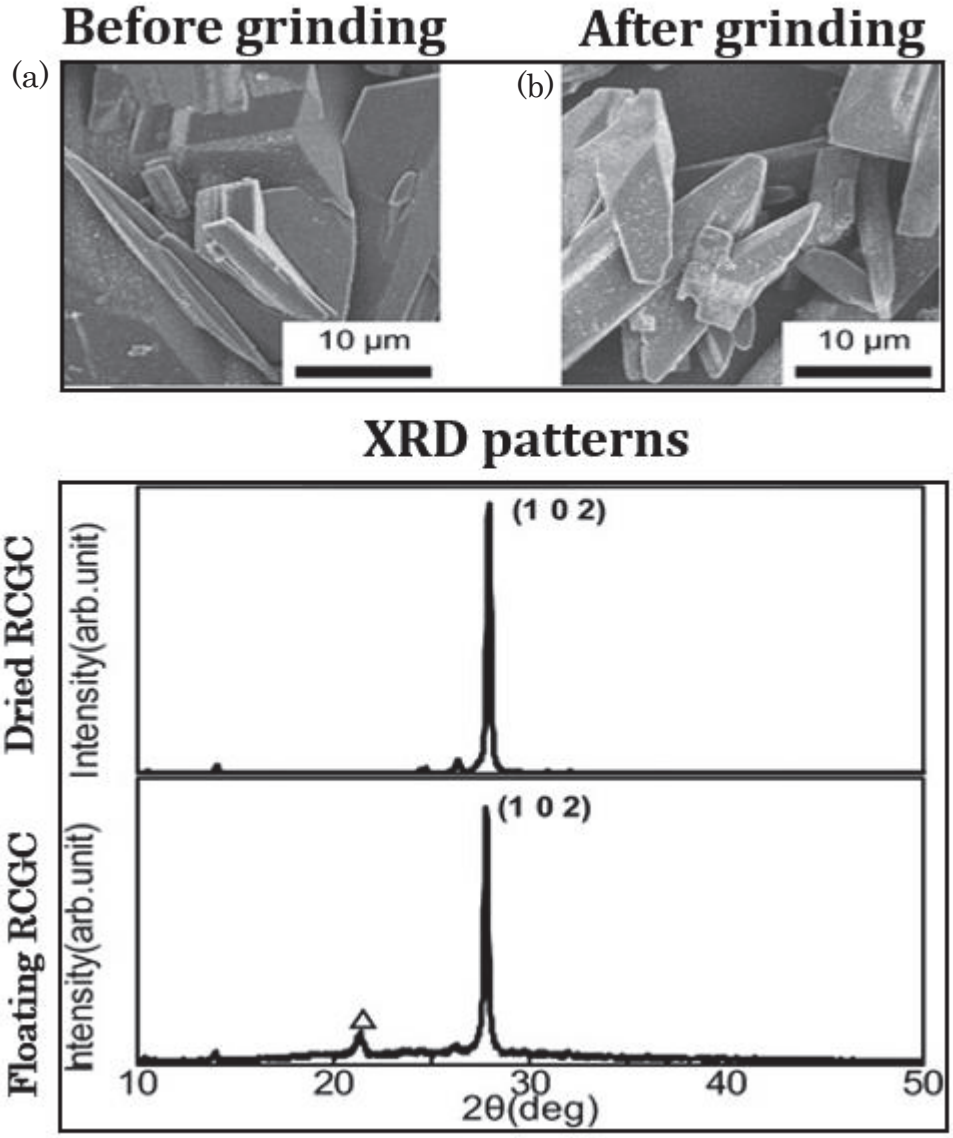

Figure 5.3.3 SEM image of crystal (a) before and (b) after mechanical grinding. XRD patterns of (c) dried ground synthetic guanine crystal, which is the same sample shown in (b), and (d) ground crystal floating in water (Type II sample). The diffraction peak marked by open triangle (Δ) arises from the wrap used to mount the sample.

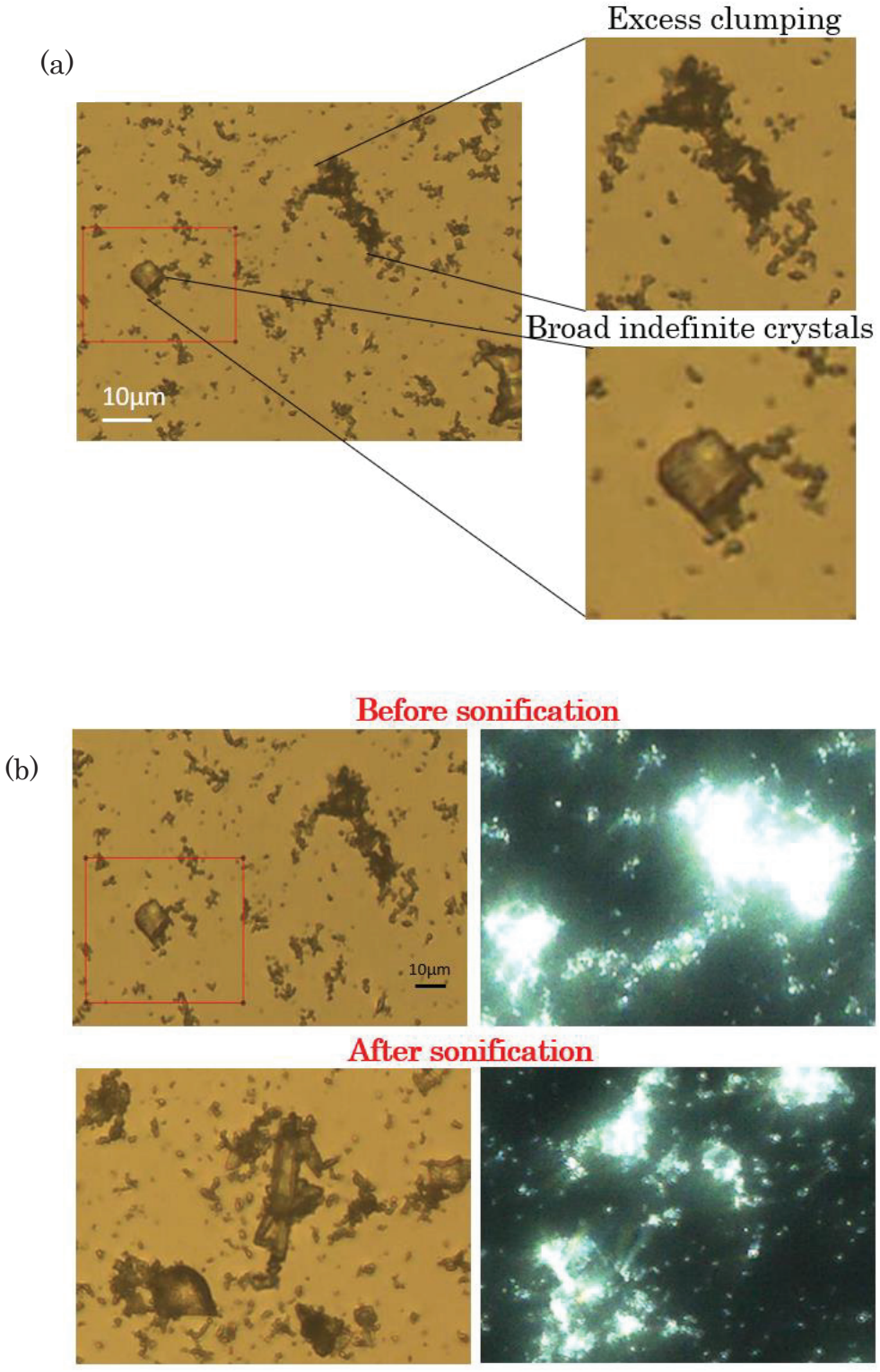

Figure 5.3.4 Light microscopic view of (a) slowly recrystallized guanine and (b) conditions with and without sonification.

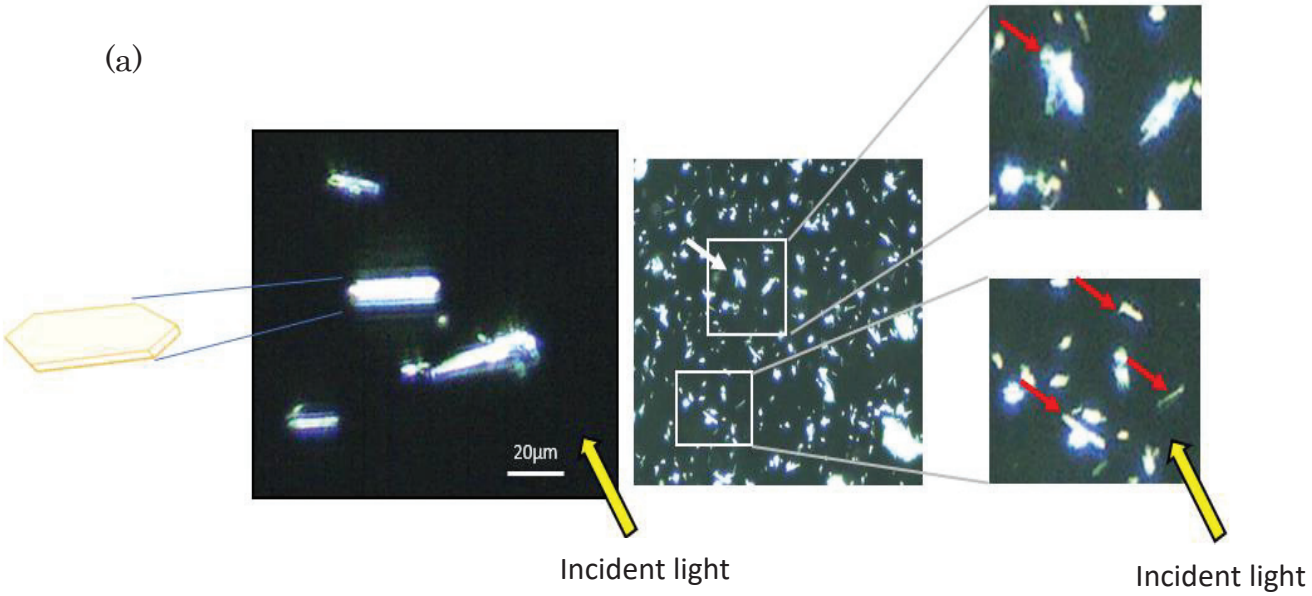

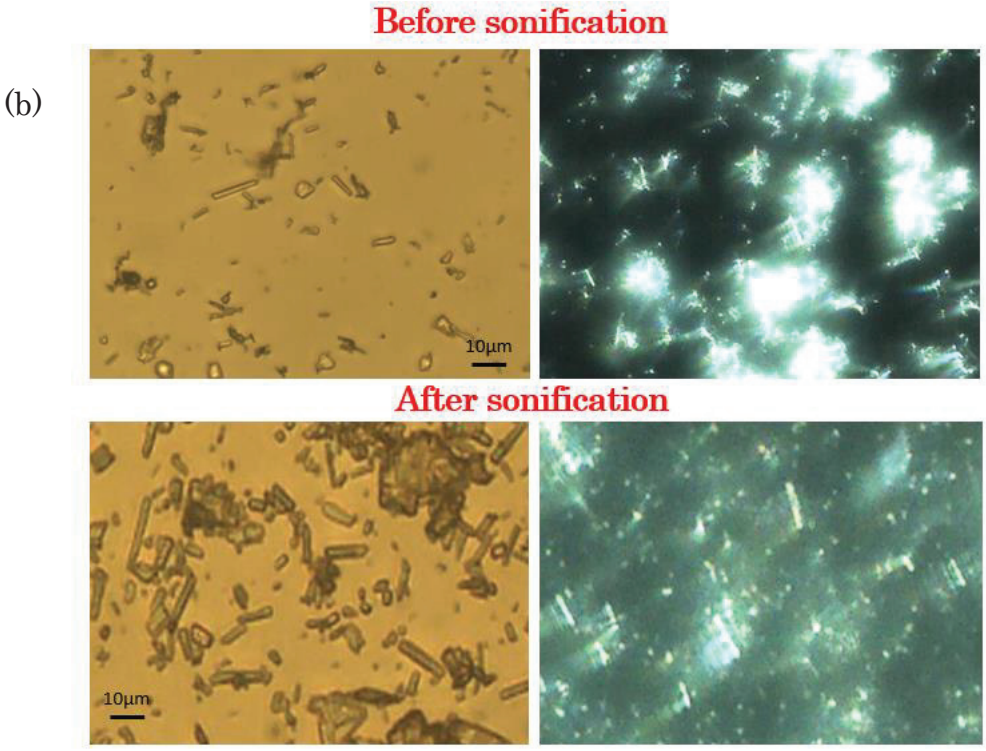

Figure 5.3.5 Light microscopic view of (a) rapidly recrystallized guanine and (b) conditions with and without sonification.

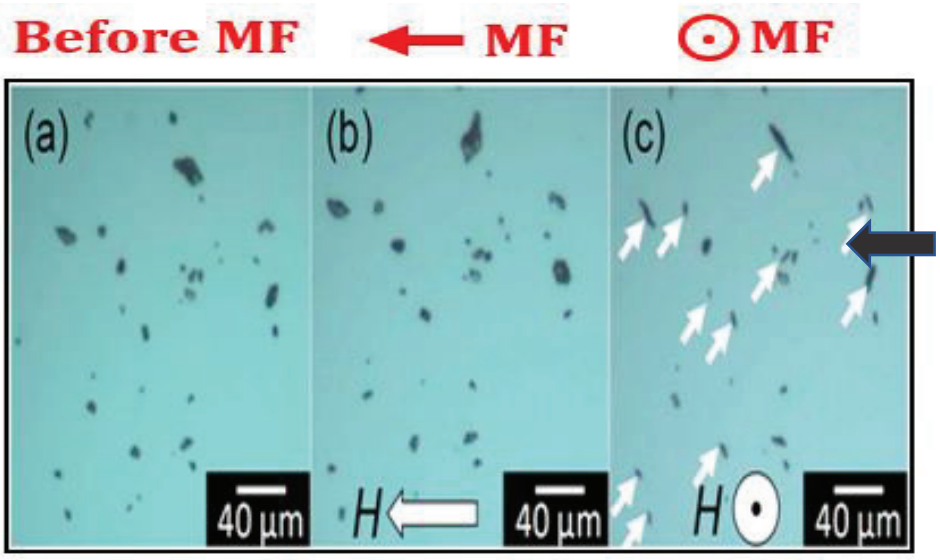

Figure 5.3.6 Optical microscopy images of a ground recrystallized guanine crystal (a) before applying a magnetic field, (b) after applying a horizontal magnetic field of 130 mT, and (c) after applying a vertical magnetic field of 150 mT by using permanent magnets. Sectional area of crystals marked by white arrows decreased under the vertical magnetic field by perpendicular rotation as shown in Fig. 5.3.1 (a).

(a)

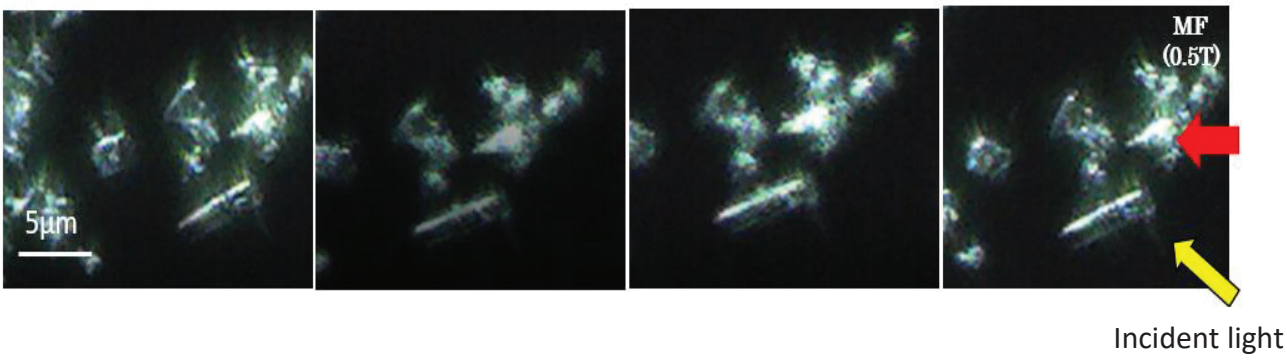

(b)

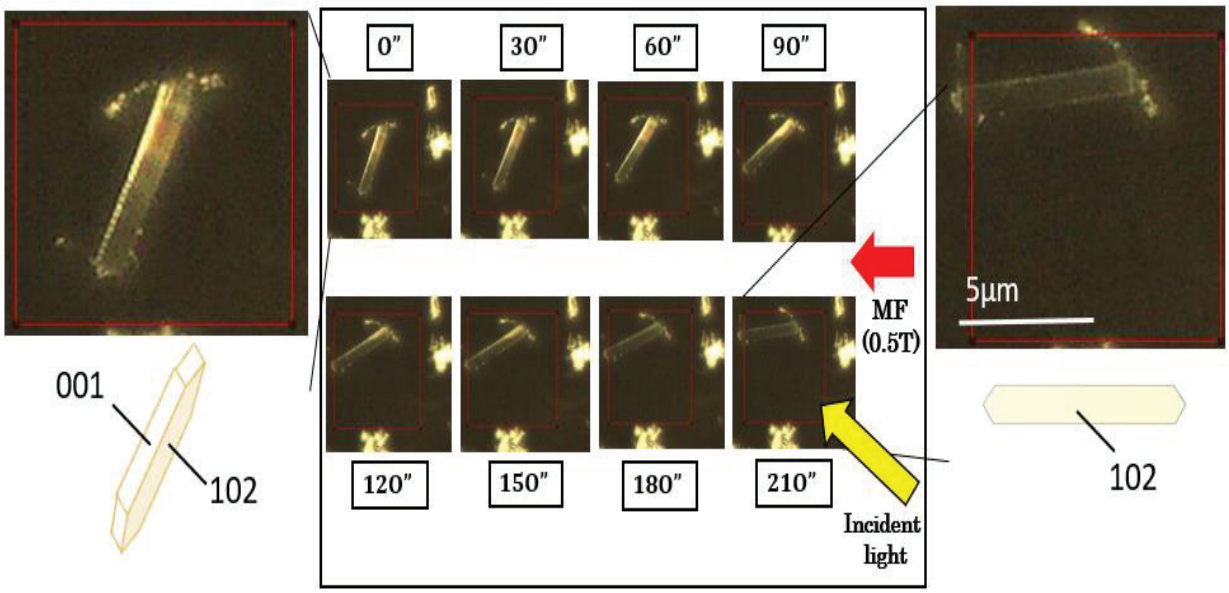

Figure 5.3.7 Magnetic response of (a) slow, (b) rapidly recrystallized synthetic guanine.

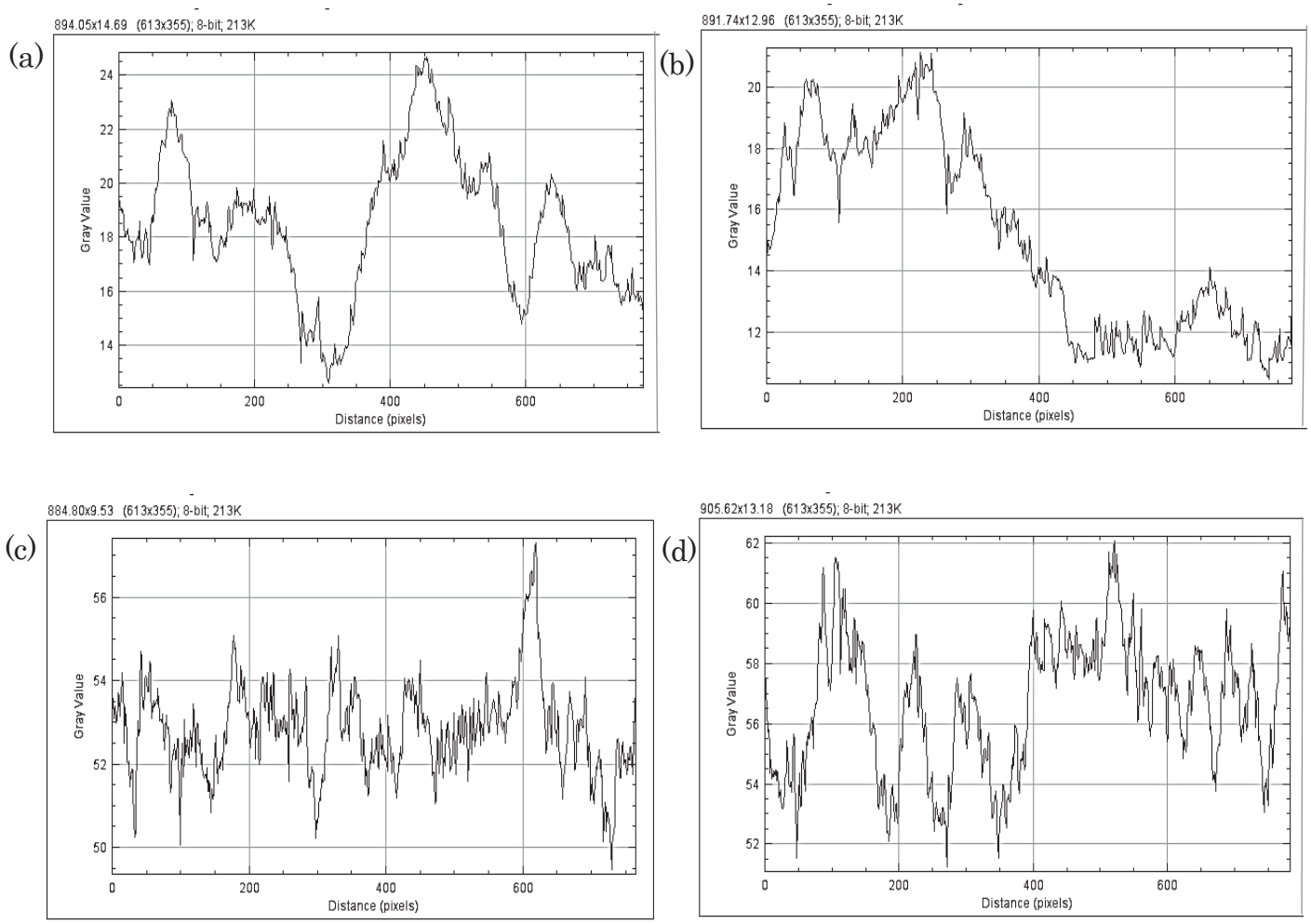

Figure 5.3.8 Gray value analysis of Barium sulphate (a, c) and mixed recrystallized guanine (b, d). Figures on top show gray value before sonification and figured below show gray value after sonification.

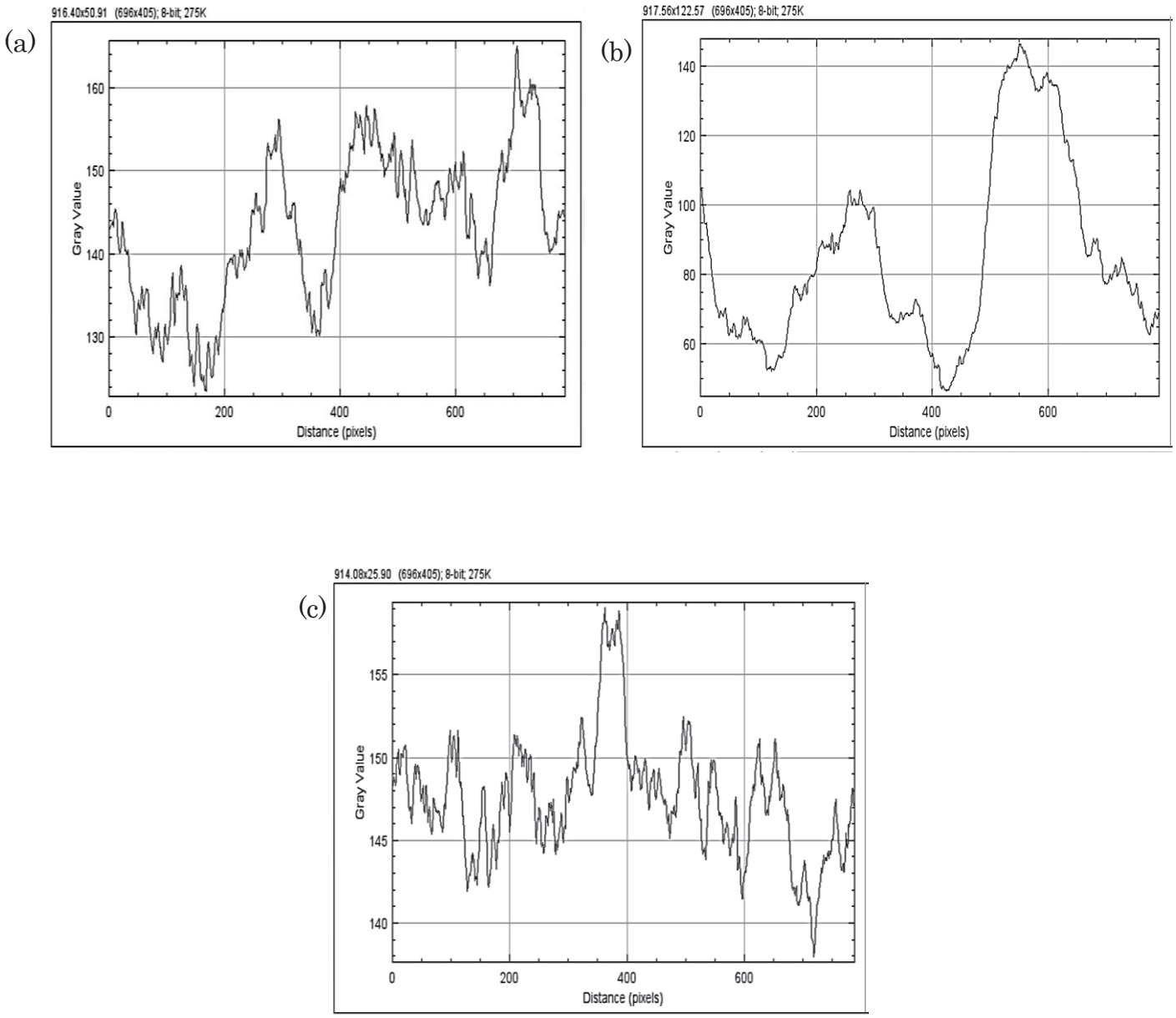

Figure 5.3.9 Gray value comparison between rapid, slow recrystallized guanine and barium sulphate (a, b and c respectively).

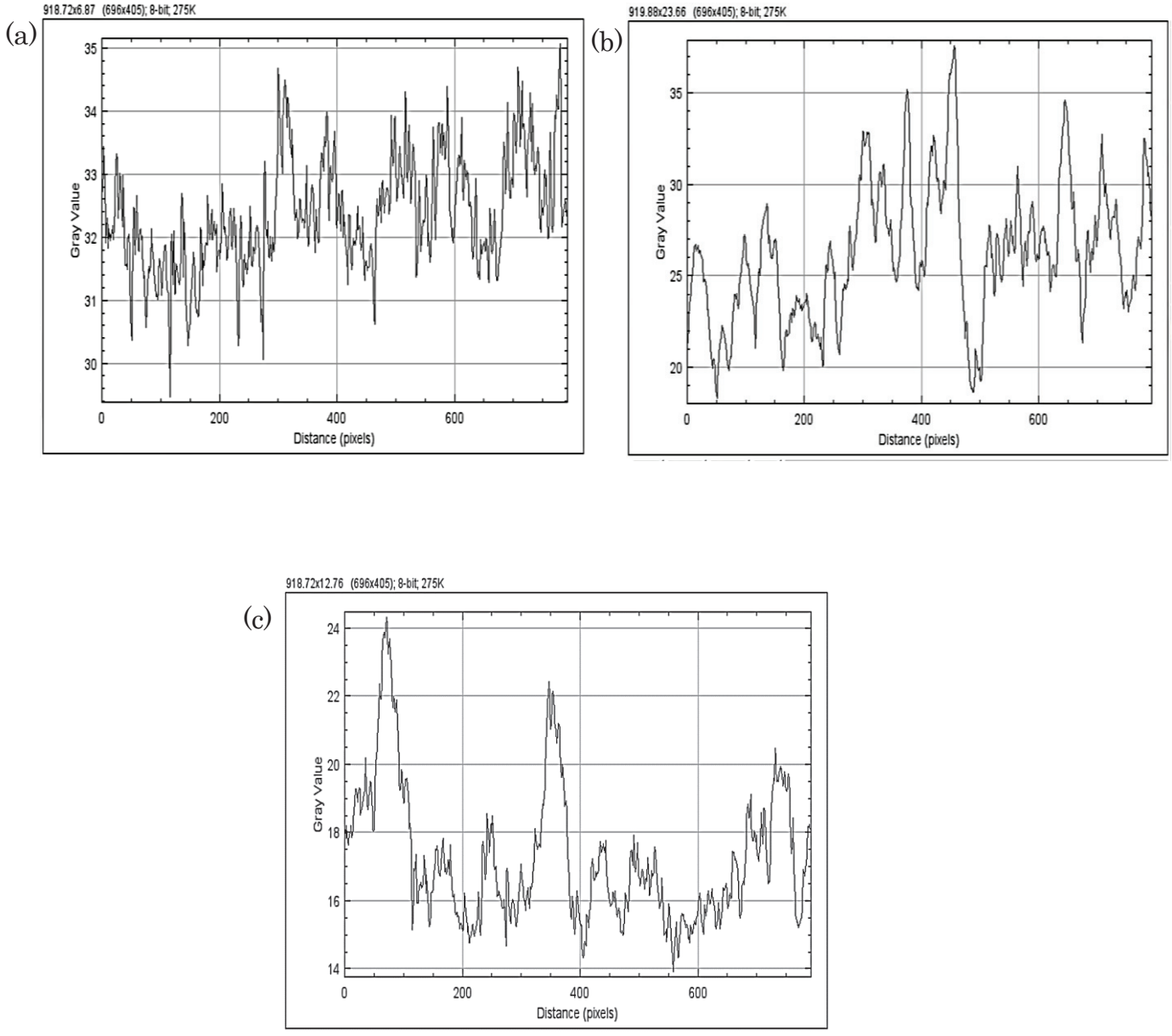

Figure 5.3.10 Gray value comparison between biogenic guanine crystals, mixed recrystallized guanine and synthesized guanine particles. (a, b and c respectively).

5.4 Summary

Here, we prepared a synthetic guanine crystal showing a magnetically controllable reflection property similar to biogenic guanine crystals. A classical Ostwald ripening for crude crystals, composed of a synthesized guanine powder, and a mechanical grinding technique were applied to refine the shapes of the resulting synthetic guanine crystal. Rapidly recrystallized guanine showed a magnetic response “in-plane”. It is surprising that the crystals with a practical property were obtained with a rough approach, which can be termed as a top-down approach. An optimization of the procedure by modifications of the recrystallization and ripening conditions is currently in progress.

References for Chapter 5

[1] D. Gur, B. A. Palmer, S. Weiner, and L. Addadi, "Light Manipulation by Guanine Crystals in Organisms: Biogenic Scatterers, Mirrors, Multilayer Reflectors and Photonic Crystals," Adv Funct Mater., vol. 27, pp. 1-13, 2017.

[2] N. Funt, B. A. Palmer, S. Weiner, and L. Adaddi, "Koi Fish-Scale Iridophore Cells Orient Guanine Crystals to maximize Light Reflection," ChemPlusChem., vol. 82, pp. 914 –923, 2017.

[3] A. L. Lior, E. Shimoni, O. Schwartz, E. G. Regev, D. Oron, G. Oxford, A. S. Weiner, and L. Addadi, "Guanine-Based Biogenic Photonic-Crystal Arrays in Fish and Spiders," Adv Funct Mater., vol. 20, pp. 320–329, 2010.

[4] L. Lior, B. Pokroy, B. L. Sivan, L. Leiserowitz, S. Weiner, and L. Addadi, "Biogenic Guanine Crystals from the Skin of Fish May Be Designed to Enhance Light Reflectance," Crystal Growth & Design., vol. 8, pp. 507-511, 2008.

[5] M. Iwasaka, K. Suzuki, and T. Sugawara, "Observations of cellular responses to diamagnetic forces acting on cell components," Science and Technology of Advanced Materials., vol. 9, pp. 1-4, 2008.

[6] N. K. Michiels, N. Anthes, N. S. Hart, J. Herler, A. J. Meixner, F. Schleifenbaum, G. Schulte, U. E. Siebeck, D. Sprenger, and M. F. Wucherer, "Red fluorescence in reef fish: A novel signaling mechanism?" BMC Ecol., vol. 8, pp. 1-14, 2008.

[7] J. Teyssier, S. Saenko, D. V. D. Marel and M.C. Milinkovitch, “Photonic crystals cause active color change in chameleons,” Nat Commun., vol. 6, pp. 1-6, 2016.

[8] D. Gur, B. A. Palmer, B. Leshem, D. Oron, P. Fratzl, S. Weiner, and L. Addadi, “The Mechanism of Color Change in the Neon Tetra Fish: a Light Induced Tunable Photonic Crystal Array,” Angew Chem., vol. 54, pp. 12426–12430, 2015.

[9] M. Iwasaka and Y. Mizukawa, “Light Reflection Control in Biogenic Micro-Mirror by Diamagnetic Orientation,” Langmuir., vol. 29, pp. 4328–4334, 2013.

[10] Y. Mizukawa, Y. Ikemoto, T. Moriwaki, T. Kinoshita, F. Kimura, T. Kimura, and M. Iwasaka, “Synchrotron Microscopic Fourier Transform Infrared Spectroscopy Analyses of Biogenic Guanine Crystals Along Axes of Easy Magnetization,” IEEE Transactions on Magnetics., vol. 50, pp. 1-4, 2014.

[11] A. Mootha, K. Suzuki, H. Asada, and M. Iwasaka, “Refinement of synthetic guanine crystals for fast diamagnetic rotation,” IEEE Trans. Magn., vol. 54, pp. 1-4, 2018.

[12] T. Darvishzad, T. Lubera, and S. S. Kurek, “Puzzling aqueous solubility of guanine obscured by the formation of nanoparticles,” J Phys Chem B., vol. 122, pp. 7497–7502, 2012.

[13] Y. Oaki, S. Kaneko, and H. Imai, “Morphology and orientation control of guanine crystals: a biogenic architecture and its structure mimetics,” J Mat Chem., vol. 22, pp. 22686-22691, 2012.

[14] D. Gur, M. Pierantoni, N. E. Dov, A. Hirsh, Y. Feldman, S. Weiner, and l. Addadi, “Guanine Crystallization in Aqueous Solutions Enables Control over Crystal Size and Polymorphism,” Crystal Growth & Design., vol. 16, pp. 4975-4980, 2016.

[15] K. Guille, and W. Clegg, “Anhydrous guanine: a synchrotron study,” Acta Cryst C., vol. 62. pp. 515–517, 2006.

6. General discussion of chapters

The optical principles of natural photonic systems serves as guiding pathways for making improved synthetic optical devices. The properties of biogenic guanine has been explored relatively. However, fewer studies are available on the concepts of synthesized guanine powder, artificial guanine crystals, and interaction of guanine with biological molecules.

In this study it was shown that it is possible to use synthetic guanine crystals in the same manner as biogenic crystals to act as efficient fluidic tracers by obtaining their flickering/quenching signals with and without magnetic field exposure. In addition, guanine crystal platelet is a promising material as a new tracer for dynamics of objects floating in aqueous solution, although the technique for tracing is yet to be established. As a preliminary step towards biological tracing (imaging), we hypothesize that dental tooth and surrounding structures can be a model where guanine crystal platelets can be used as "biological tracers" for sensing bacteria on tooth surfaces.

In addition, by entrapping guanine crystals into lipid vesicles, it was possible to make a hybrid-vesicle similar to iridosome found in fish scales. The rate of vibratory motion of the hybrid-vesicle can be manipulated with a magnetic field as low as ~0.5T, which further allows us to alter the intensity of light reflected from this artificial iridosome due to change in Brownian motion and diamagnetic susceptibility of guanine crystals and lipids. This is a simple model for potential application of guanine for bio-reflector based bio-imaging treating intravesicular guanine crystals as cellular micro mirrors.

To limit the extraction of guanine from fish-scales, artificial recrystallization of synthetic guanine particles was carried out. Artificial crystals were obtained using the classical Ostwald ripening method for obtaining crude crystals and the crystals were further refined by mechanical grinding to improve physical characteristics such as shape, light reflective properties of the resultant artificial guanine crystal. Artificial crystals which showed light reflective properties almost similar to biogenic crystals were obtained with a preliminary approach. Further optimization of the fabrication steps and recrystallization procedure by modifications of the recrystallization and ripening conditions will assist in improving its physical characteristics and diamagnetic susceptibility similar to biogenic guanine crystals.

Biogenic guanine crystals have been used for several decades in the cosmetic industry. It has been under effective use because of its luminous appearance, brilliant silvery mirror-like shine. It was thought to me harmless when applied superficially to skin. However, as procurement of guanine was time consuming, and the amount that was obtained was uncertain, it was replaced in several products with other synthetic materials zinc oxide and metals like mica, aluminum and bronze [1].

As observed previously it was possible to combine biogenic guanine along with biological components like artificial lipids. Guanine crystals were also combined and dispersed in dental organic solvents to check its dispersibility and ability to maintain its inherent flickering and light reflective property in organic solvents.

Briefly, after biogenic guanine was washed and cleaned as described in Chapter 4, the final residue collected in plastic vials was mixed with 100µl of Methyl methacrylate (MMA), or alternatively mixed with 100µl ethanol (70 %) and the plastic vials were frozen for 24 hours. On the next day, the samples were allowed to thaw at room temperature to evaporate the residual alcohol/water from the sedimented guanine. Then, the sedimented dried guanine pellet was dispersed in 2 ml of MMA solution, shaken well and exposed to short cycles of sonification to disperse the guanine freely in the solvent and observed under the light microscope. Microscopic evaluation showed that biogenic guanine crystals dispersed freely in MMA solution and no visible large clumps were observed. Dark field observation revealed freely floating guanine crystals, with minute clumps and strong light reflection seen from the flickering of the crystals in the solvent as shown in Figure 6.1.

MMA solvent is the most used solution for combining dental acrylic powder to the solvent and then make a highly viscous paste or as required depending on the area of application in the oral cavity. Several simulation experiments were carried out with the aim of utilizing biogenic guanine crystals for the esthetic enhancement of tooth colored dental resin fillings. The purpose of this simulation was to assess the effectiveness of guanine in increasing the light reflective property when combined with water and dental acrylic resin. Layers of several materials were added to the simulation model as shown in Figure 6.2. Results of light reflection and light transmission values were reported while altering arrangement and the thickness of layers of materials in the simulation model.

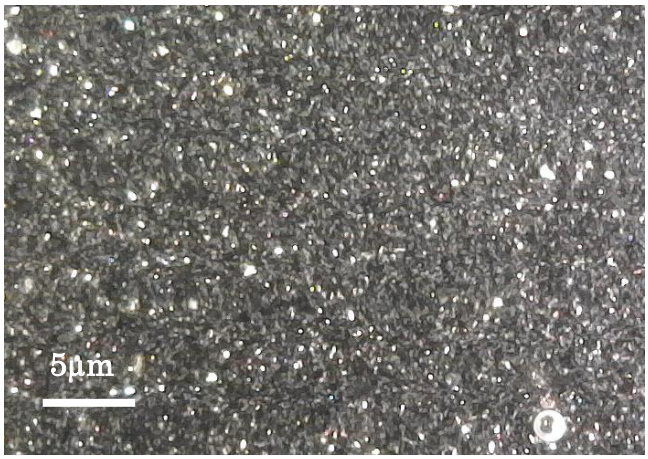

Figure 6.1 Biogenic guanine dispersed in methyl methacrylate solution (MMA).

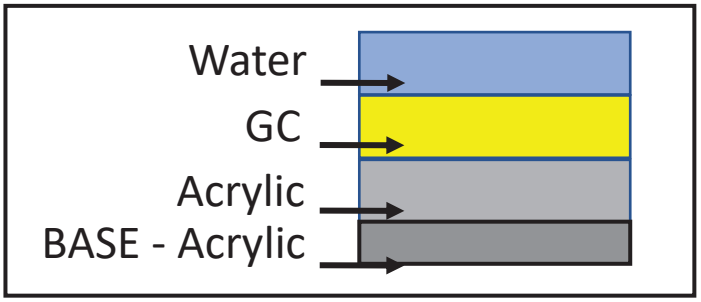

Figure 6.2 Layer model used for analysis of reflection light intensity of guanine and dental acrylic.

S.No	Refractive index	Thickness (nm)
Air	1.00	* Medium (Air)
Water	1.33	400.00
GC	1.83	500
Acrylic	1.49	1000
n+1	1.49	Base

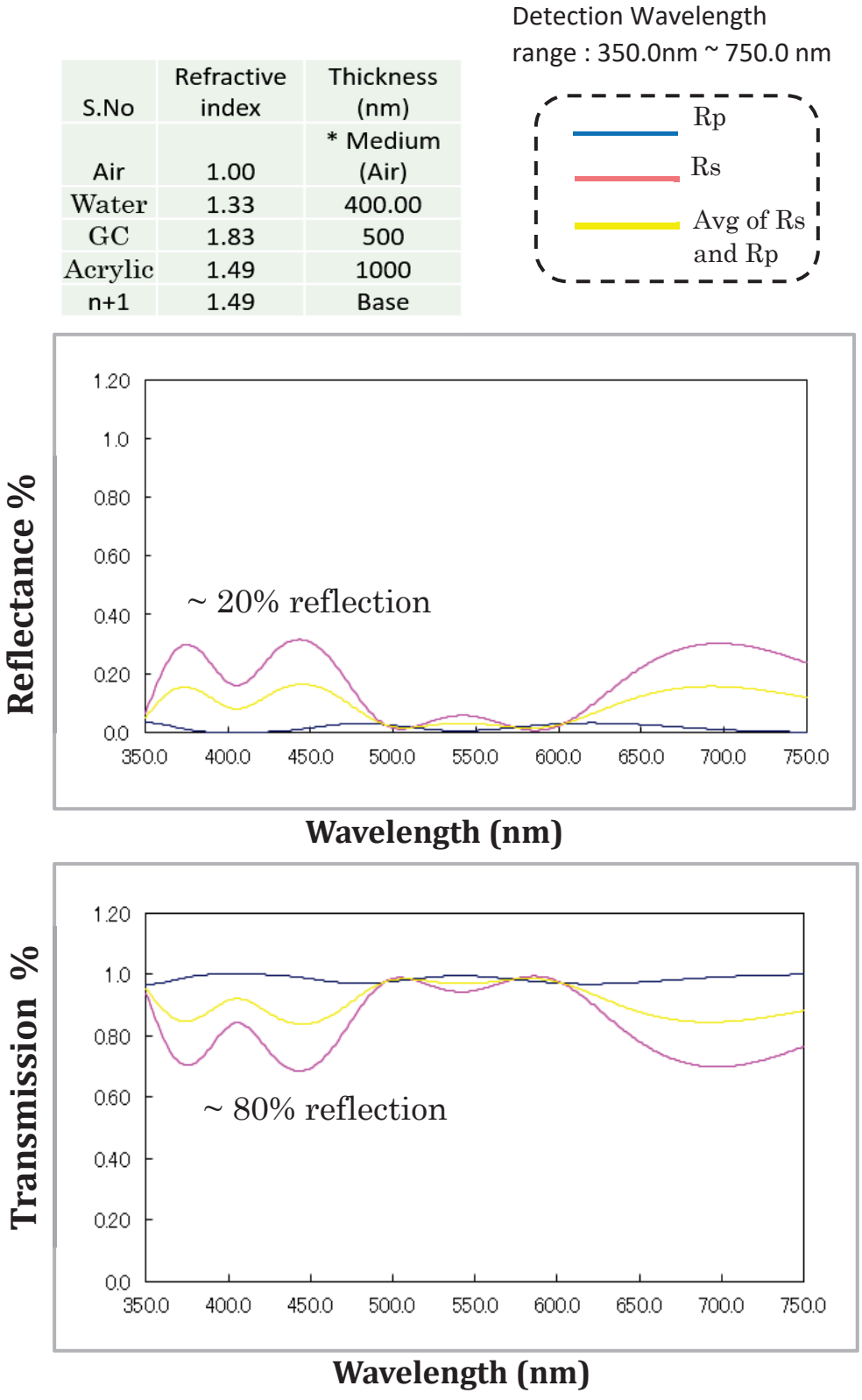

Figure 6.3 Simulation of light intensity reflected from guanine and acrylic particles with varying thickness.

Thickness of GC and water layer was increased

S.No	Refractive index	Thickness (nm)
Air	1.00	* Medium (Air)
Water	**1.33**	**500.00**
GC	**1.83**	**700**
Acrylic	1.49	1000
n+1	1.49	Base

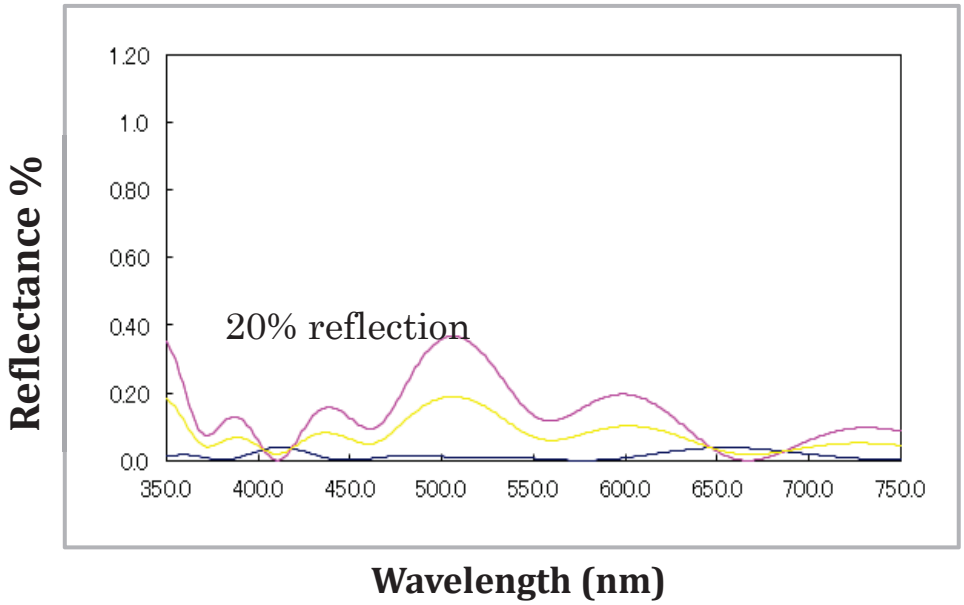

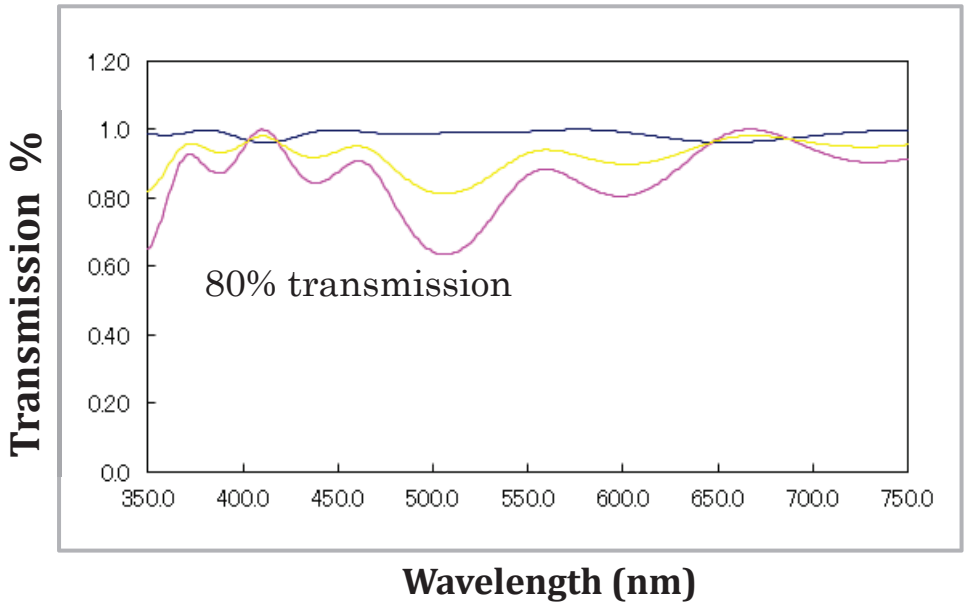

Detection Wavelength
range : 350.0nm ~ 750.0 nm

Figure 6.4 Simulation of light intensity reflected from guanine and acrylic particles with varying thickness.

Results after an additional layer of GC was added

S.No	Refractive index	Thickness (nm)
Air	1.00	* Medium (Air)
water	1.33	400.00
GC	1.83	500
GC	1.83	500
Acrylic	1.49	1000
n+1	1.49	Base

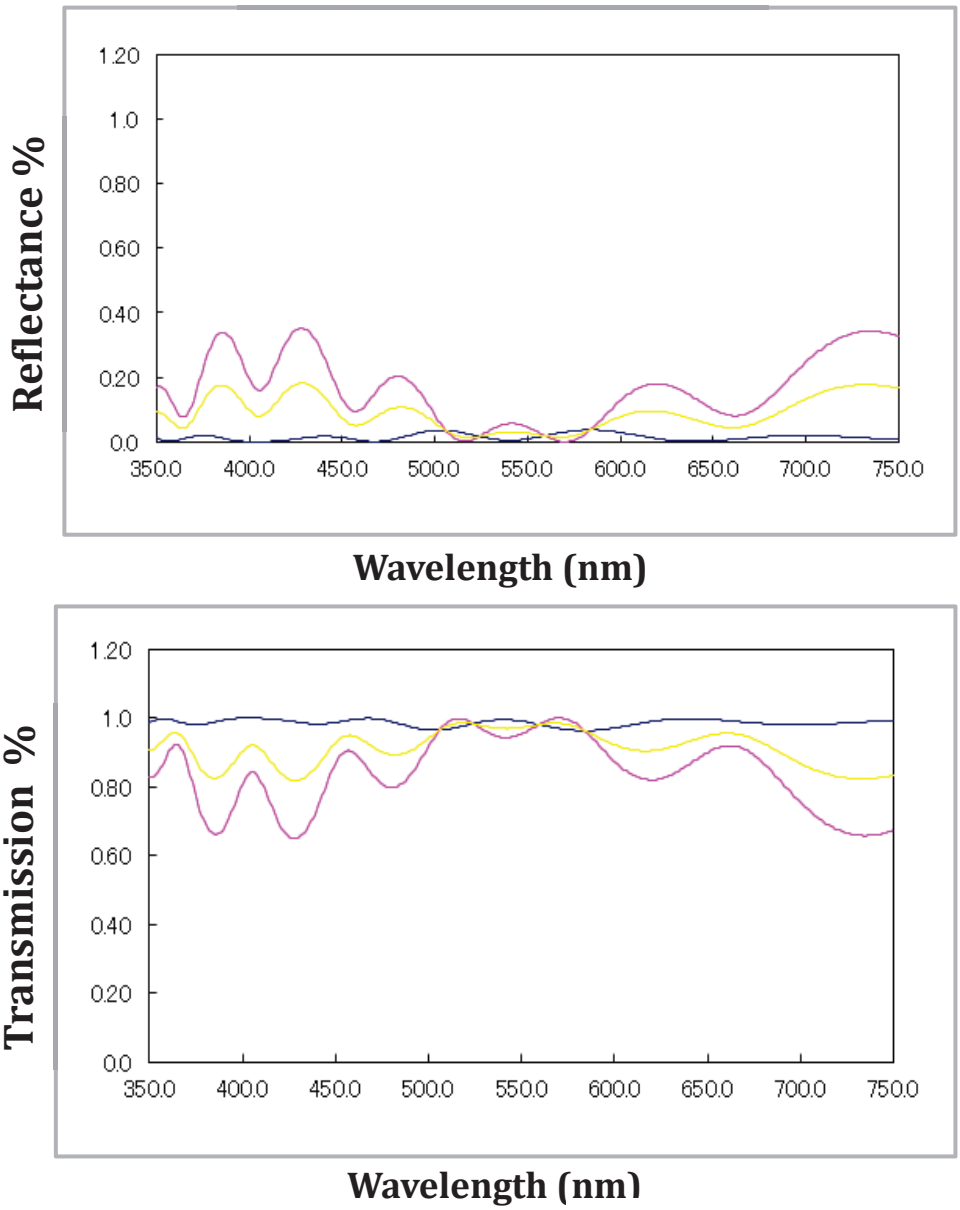

Detection Wavelength
range : 350.0nm ~ 750.0 nm

Figure 6.5 Simulation of light intensity reflected from guanine with acrylic particles with varying thickness and combinations.

1) GC layer mixed with water layer

2) Additional GC layer added

S.No	Refractive index	Thickness (nm)
0	1.00	* Medium (Air)
Water + GC	**3.16**	**400.00**
Acrylic	**1.83**	**500**
n+1	1.49	Base

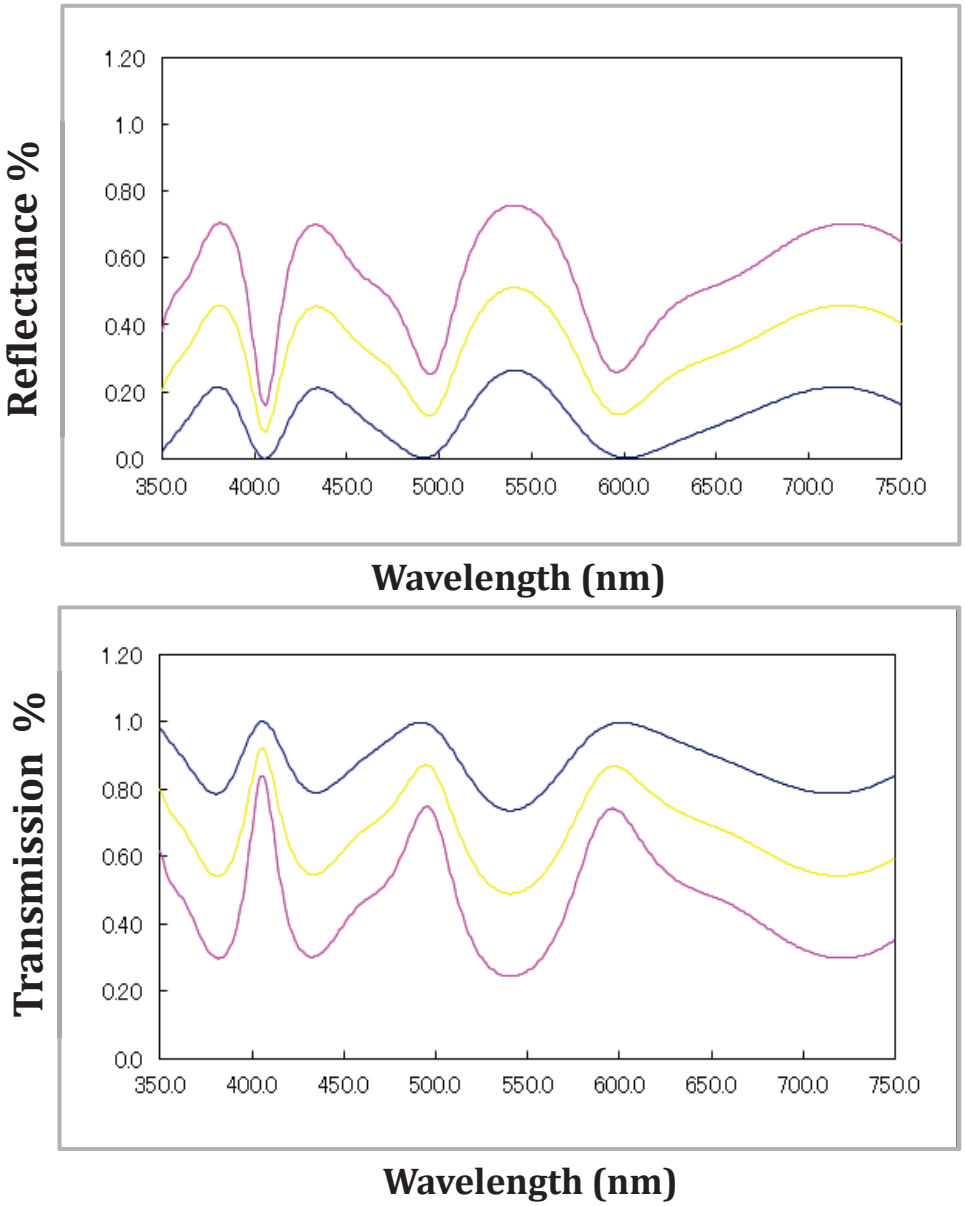

Detection Wavelength
range : 350.0nm ~ 750.0 nm

Figure 6.6 Simulation of light intensity reflected from guanine with acrylic particles with varying thickness and combinations.

Results of the simulation experiments are shown in Figure 6.3 up to Figure 6.6. It was observed that when the thickness of guanine layer was altered, the reflection and transmission patterns also changed accordingly. Whereas, when the number of guanine and water layers were increased, corresponding to these changes, the intensity of reflection and transmission increased up to 4-fold. The water film added above the guanine layer was hypothesized to be saliva covering the tooth surface with the resin filling. Although, in the practical scenario guanine will not be floating in the saliva but incorporated into the acrylic resin filling, further analysis regarding light reflective and light transmission properties of incorporated guanine in solid state layers like acrylic resin in this scenario, will guide to throw light on the applicability of guanine crystals for esthetic enhancement of tooth colored dental acrylic resin fillings.

References

[1] S. K. Singh, "Handbook on Cosmetics (Processes, Formulae with Testing Methods)," Asia pacific business press Inc., pp. 1-646, 2010.

7. Conclusion

Analysis of utilization of bio-crystals such as guanine crystals for bio-sensing and biological applications was carried out. A static magnetic field at ~5 T inhibited the flickering light intensities in synthetic guanine crystal particles. Analysis of the individual particle motion and flickering rate (Δt) revealed a change in the flickering frequency with magnetic field exposures at 300-500 mT. These analyses revealed that it was possible to manipulate the flickering of synthetic guanine particles using a weak external magnetic field.

The interaction of biogenic guanine crystals with lipid molecules were studied. Artificial lipids were used to make lipid sacs and assess the entrapment of guanine crystals inside the sacs to mimic the design or an iridophore. Guanine crystals interacted with lipid sacs / vesicles by either adhering to outer wall of vesicles or floating freely within the intravesicular fluid of the vesicle. At rare occasions, guanine was found to float within close proximity to the inner vesicle wall. This investigation of interaction of guanine with biological molecules was a preliminary step for utilization of guanine as cellular micro mirrors for biological imaging as microfluidic devices for bacterial detection.

Synthetic guanine particles were recrystallized artificially with the aim to make artificial light tunable micro-mirrors which respond to magnetic field. Crystals with light reflective properties almost similar to biogenic guanine crystals were obtained. Further refinement of the technique will provide more structured crystals which mimic biogenic crystals exactly. Guanine crystal platelet is a promising material for a new tracer for dynamics of any objects in aqueous solution.

The technique for the tracing is not established at this point. Possible future utilization of guanine can serve as "biological tracers" for detecting bacterial occurrence in the nearby vicinity.

8. Future development and applications

Guanine crystal platelet is a promising material as a new tracer for micro-particle dynamics in an aqueous solution. The technique for molecular tracing remains to be well-established at this moment. Research is promising in this direction and prompts further possible application of guanine crystals for biological tracing (imaging) as "biological tracers" for bacterial localization or bacterial detection.

Further optimization of recrystallized guanine will help to improve physical characteristics of guanine pertaining to size of crystal and weight of crystal, to enhance its physical characteristics such as shape, size, thickness and weight, along with other optical and light-reflective characteristics, will assist in future utilization of guanine crystals as an optical sensor or micro-mirror manipulated under MF.

Possible investigation on interaction and affinity of Guanine with other biological molecules will assist in development of a bio-reflector based optical system for biological use and use along with other biological specimens like cells or micro-organisms. Additionally, interaction and compatibility of guanine crystals with biological molecules and successfully studying these interactions will lead to a direction of research involving application of guanine to areas where it can serve as an optical bio-sensor. Additionally, due to its inherent property of iridescence, its utilization to serve as aesthetic enhancer for tooth colored acrylic resins in dentistry by enhancing light interference, tooth translucency and light reflective properties of dental filling materials is an exciting path yet to be explored.

Acknowledgements

Firstly, I would like to express my sincere gratitude to my supervisor, Professor. Masakazu Iwasaka (Research Institute for Nanodevice and Bio Systems (RNBS)) for providing me with the opportunity to enroll Ph.D. under his supervision and guiding me through every step with fruitful discussions regarding research activity and research progress. I would also like to thank him for constantly motivating me to do better and bringing clarity with his valuable comments in pursuit of my doctoral dissertation. I thank my thesis advisors Professor. Takahiro Onimaru and Professor. Yoshiko Okamura for their valuable suggestions and guidance to add more value to this dissertation.

Next, I express my deepest appreciation to my collaborators Professor Kentaro Suzuki (Faculty of Science Department of Chemistry, Kanagawa University) for guiding me to develop the hybrid-vesicle technique and other skill sets; Professor Hironori Asada (Graduate School of Sciences and Technology for Innovation, Yamaguchi University) for assisting me to develop understanding about guanine recrystallization and data regarding recrystallized guanine; and Professor Taro Toyota (Department of Organic Chemistry, Tokyo Institute of Technology) for his thoughtful consideration to invite me to his laboratory in Tokyo and demonstrating his technique for fabrication of lipid vesicles with fluorescent staining techniques. I greatly benefitted from their guidance and meaningful insights along with helpful discussions with them during my doctoral course, which I will be able to apply throughout my academic career.

I gratefully acknowledge the support of past and present members of Iwasaka laboratory. I truly appreciate the technical assistance given by Mr. Hiroharu Kashiwagi, along with several discussions about challenges in experiments using goldfish. I am particularly grateful for cooperation of Mr. Yudai Takanezawa, Mr. Takaki Chikashige and Mr. Yuta Fukagawa with daily academic activities. I would like to express my gratitude to the Graduate School of Advanced Sciences of Matter for their financial support during my doctoral course and the student-support office staff for their ever-welcoming nature and friendly support.

Finally, I would like to thank my husband, Mr. Deepak Kumar for his constant support and motivation to achieve more throughout my doctoral course and stay in Japan. I could not have been able to achieve this degree without his presence.

March 2021, Archana Mootha.

公表論文

(1) Quenching of light flickering in synthetic guanine crystals in aqueous solutions under strong static magnetic fields.

Mootha A, Takanezawa Y, Iwasaka M.

AIP Advances 8(5), 1-6(2018).

(2) Guanine Vesicle Hybrid Particles for Bio-Reflector-Based Bio-Imaging.

Mootha A, Suzuki K, Asada H, Iwasaka M.

IEEE Transactions on Magnetics (99),1-4(2018).

(3) Refinement of synthetic guanine crystals for fast diamagnetic rotation.

Mootha A, Suzuki K, Kimura T, Kurahashi M, Muneyama E, Iwasaka M, Asada H.

AIP Advances 9, 1-4(2019).